2015

Investigation of Potentially Hazardous Particulate Matter in Homes: Designing a Particle Filtration System

John Scott Young
Louisiana State University and Agricultural and Mechanical College

INVESTIGATION OF POTENTIALLY HAZARDOUS PARTICULATE MATTER IN HOMES: DESIGNING A PARTICLE FILTRATION SYSTEM

A Thesis

Submitted to the Graduate Faculty of the
Louisiana State University and
Agricultural and Mechanical College
in partial fulfillment of the
requirements for the degree of
Master of Science

in

School of Plant, Environmental and Soil Science

by
John S. Young
B.A. Biology, B.A. English, College of Charleston, 2008
December 2015

ACKNOWLEDGMENTS

I would like to thank and acknowledge the support from these schools and programs at Louisiana State University: the School of Plant, Environmental, and Soil Sciences, the LSU Superfund Research Center, the School of the Coast and Environment, and all the staff and students therein. I would especially like to acknowledge the guidance and assistance of my advisor, Dr. Maud Walsh, and of my thesis committee: Dr. Maud Walsh, Dr. Jim Wang, and Dr. Slawo Lomnicki. This research was completed in part with the assistance of funding from the Louisiana Environmental Education Commission and funding from the Superfund Research Program.

Special assistance in this research in collecting samples and running instruments was provided by Ajit Ghimire, Albert Dela Cruz, William Gehling, Elisabeth Feld, Balamurugan Subramanian, Buffy Meyer, Greg Olson, Kelli Palmer, Brittany Dupre, Grace LeBlanc, Ugwumsinachi Nwosu, Cholena Ren, Chuqi Quo, Xia Guan, Hunter Ryland, and Lydia Corie. Thank you all very much. Also, thank you to SPESS staff Sheila Rowher and Jere Townsend. Finally, thank you to all my friends and family during my course of study and research.

TABLE OF CONTENTS

ABSTRACT

This research documents the process of designing a technique, materials, and method to filter particulate matter (PM) deposited on surfaces in homes. PM collected from homes in a known industrial corridor, Baton Rouge, was tested for key pollutants sorbed to their surface in an investigation of household air depositions. This research successfully designed a collection method for bulk samples and a filtration apparatus and method for collecting sized laboratory testable samples using porous membrane filtration technology. This research found relatively high concentrations of polycyclic aromatic hydrocarbons (PAHs), and the presence of some metals. This research also found the presence of persistent, organic radicals in homes which may be environmentally persistent free radicals (EPFRs). EPFRs are formed in industrial processes and are an emerging pollutant of importance described by the Louisiana State University Superfund Research Center. The manner in which organics, metals, and EPFRs exist as particle-pollutant systems in real environmental conditions will require more study. Further research can also be undertaken to draw spatial relations between sources of particle pollution and particle abundance and chemical composition on surfaces in homes in Baton Rouge and other urban areas.

1. INTRODUCTION

1.1: General

Particulate matter (PM) is a pollutant of critical importance worldwide. The U.S. Environmental Protection agency identifies particulate matter as one of the six criteria pollutants addressed by the National Ambient Air Quality Standards (NAAQS). The NAAQS sets levels of acceptable aerosols which are measurements given in micrograms per cubic meter and leveled to protect the public in primary and secondary standards. Primary standards are a level for sensitive populations such as asthmatics, the young and the elderly, secondary standards provide protection against decreased visibility, and damage to crops, animals, vegetation and buildings (US EPA 2015).

Combustion at industrial sites and on roadways releases particulate matter into the atmosphere. Biomass burning and other mechanisms are important sources of particulate matter pollution. Indoor air pollution is also a significant source of particulate matter, specifically during cooking (Kearney et al. 2011). Particulate matter can be dangerous by itself and is of increased importance from a health perspective because of specific compounds that may be associated with it.

This research develops and tests a model sampler for simple and effective use in collecting particulates of specific sizes from surfaces in homes for subsequent laboratory testing for the chemical makeup and particle-pollutant systems. The compounds associated with particulate matter that this research focuses on include metals, polycyclic aromatic hydrocarbons (PAHs) and environmentally persistent free radicals (EPFRs), all of which have been shown to have serious potential health effects (Brauer et al. 2012; Umbuzeiro et al. 2008). These pollutant-particle systems are an emerging topic of importance in environmental science. Pollutant-particle

systems refers to the manner in which certain pollutants associate with PM and the relationship they may have to each other in the pollutant-particle formation. The goal of this project is to enhance scientific knowledge of efficient collection and separation practices and identify the prevalence of potentially dangerous compounds in households.

There is a paucity of documentation on the presence of EPFRs in homes as well as on the combination of EPFRS, PAHs, and metals in PM in homes. This research will provide data on pollutants found in households that may be associated with PM in pollutant-particle systems. PM samples will be taken from sediments in the home that have settled out of suspension as ambient PM.

1.2: Sampling Design

This thesis research focuses on proof of concept for a sampling device that provides an appropriate sample for our laboratory analysis to determine potential toxicity of collected particle-pollutant systems taken from home surfaces. The filtration device segregates particles of various sizes after a bulk collection has been completed. Research focuses locally on sampling in Baton Rouge, Louisiana, a known industrial corridor. In future research, it may be possible to draw spatial relations from roadway and industrial sites to levels of pollutant deposition. It is also possible that LSU researchers could be allowed to collect samples in the home of volunteer participants. Future work could also serve as a method of community outreach and seek citizen participation in sampling by eventually engaging others to collect sample in their own homes and return sample to LSU for analysis. This future research would serve to educate the community on air quality and public health issues, and to translate the importance of air quality and air quality research to a larger audience.

Collection and characterization of particles gathered from deposited airborne particulate matter from homes would enrich the body of literature about environmental pollutants and provide valuable guidance to future research and to regulators in assessing air quality standards by correlating ambient pollution to deposited levels of pollutants in homes. It may be possible in the course of this, or future research, to document relationships between organics, metals and EPFRs sorbed to the surface of PM.

Ambient sample times can take weeks to months to collect a large enough sample for analysis, while the technique described by this research can collect an appropriate bulk sample in minutes. Bulk collections of deposited PM are simple and inexpensive enough to utilize multiple collections and sample a large number of areas.

1.3: Overview of Analytical Approach

This research tested collected samples using a number of analyses: gas chromatography-mass spectrometry for PAHs, scanning electron microscopy for particle sizing and scanning electron microscopy energy dispersive x-ray spectroscopy for metals. Electron paramagnetic resonance (EPR) was used to test samples for free radicals. In this case EPR was used to study environmentally persistent free radicals, a pollutant associated with PM which can persist in the environment for extended periods.

2. BACKGROUND

2.1: Particle Types and Importance

Particulates are categorized by their diameter into various groups. PM10, or inhalable coarse particule matter, has a diameter smaller than 10 micrometers. PM2.5, or fine particulate matter, particles have a diameter of less than 2.5 micrometers and are frequently a combustion byproduct that may include organic compounds or inorganic compounds like metals (US EPA 2015). Ultrafine particules are anything smaller than 0.1 micrometer and largely are produced by combustion processes. The contribution of ultrafine particulate matter to total mass of particulate matter is small, but this class represents the dominant size of particle in urban aerosols (Yinon et al. 2010).It has been shown that the smaller the particulate matter, the higher its relative toxicity because of its higher surface area to volume ratio (Lu et al. 2014). The shapes of aerosol particles are not often spherical and are porous, meaning a higher surface area. Also, most airborne aerosol particles are aggregates consisting of many smaller particles (Okuda 2013).

As the chemistry and composition of PM is studied in this research to a greater extent, it is important to note current allowable standards for PM concentration in ambient air. Table 2.1 provides some current standards for fine particulate air quality in the United States, worldwide and proposed standards in China that are to be implemented in 2016. China currently has no such standards in place.

Table 2.1: Air Quality Standards for Fine Particulates

Fine Particulate	US EPA	WHO	China (standards for 2016)
Annual arithmetic mean standard	12, 15 ug/m3 (primary, secondary standards)	10 ug/m^3	35 ug/m^3
24 Hour standard	35 ug/m3 (standard for primary and secondary)	24 ug/m^3	75 ug/m^3

*None of these organizations/countries have standards for ultrafine particulate matter (Source: United States Environmental Protection Agency 2014; World Health Organization 2015)

The guiding directive of research for this thesis was to establish improved sampling techniques to more accurately depict PM potential toxicity from particles that were originally suspended in air. Also, this research seeks to determine potential risks in our environment as suitable air quality is an important part of public health. This research has striven to make these sampling techniques simple and cost effective. Regarding the importance of air quality to health, one study notes that ambient air pollution is associated with a considerable burden of global disease (Brauer et al. 2012). The study also reports that the World Health Organization (WHO) estimates that exposure to fine particulate air pollution caused 800,000 deaths and 6.4 million lost years of healthy life in the world's cities in the year 2000 (Brauer et al. 2012). Most of these effects were experienced in Southeast Asia where population density is extremely high. However, largely industrialized areas of the United States, like Baton Rouge, Louisiana, may have similar health concerns. Brauer's synthesis of the data demonstrated that as of 2005, 89% of the world's population live in areas where the WHO air quality guidelines were exceeded for PM2.5 (2012).

Air quality is a concern for outdoor air as well as indoor air, with many studies focusing on particulate matter in indoor air. Studies of particulate matter of indoor air found that particles in indoor air are removed from aerosols by air exchange (open windows) and deposited on duct surfaces, fans, or air filters. Ultrafine particles can also coagulate and precipitate out of suspension. This occurs when ultrafine particles combine with larger particles and are removed from the aerosol mixture (Wallace et al. 2013). This research lends credence to the plausibility of our research collecting deposited particles in homes, where deposited dust should contain a fraction of various PM sizes. One of the goals of this thesis is to use surfaces as a source for collected particulate matter.

There are various sources of indoor particulate pollution, like cooking, but it is noted by many studies that outdoor particulates can infiltrate homes and subsequently deposit on surfaces in the home (Kearney et al. 2011). The rate of infiltration by particulates into homes is largely dependent on building characteristics of the structure, and age is often a large factor. Particulates can transport indoors by small leaks in the house (Stephens and Siegel 2012). Therefore in our test area, Baton Rouge, it is reasonable to assume various particulate sizes from outdoor sources infiltrate homes and deposit, available for collection. One tenet of this research is that we will be able to test an area of the house that has direct air exchange with the outside ambient air, for example, the attic. The attic will most likely be a location for a high concentration of settled, undisturbed PM. Previous research has noted attic dust to be a “museums” of contamination of hazard, specifically for toxic metals (Davis and Gulson 2005).

One study notably found that particulates from indoor sources were less harmful than particulates from outdoor sources (Ebelt et al. 2005). With this information in mind, this research looked for compounds associated with particulate matter from outdoor sources which are known

to be deleterious to health. There will be an expected background of indoor particulates but these are not expected to contribute as significantly to PAHs, metals or EPFRs which are the particle-pollutant combinations tested for because indoor levels of metals and PAHs have been found to be most influenced by outdoor PM sources (Hasheminassab et al. 2014).

2.2: Pollutants of Concern Associated With Particulate Matter

Polycyclic aromatic hydrocarbons (PAHs), environmentally persistent free radicals (EPFRs) and metals are the pollutants that are associated with particulate matter and will be tested for in laboratory analysis.

Polycyclic aromatic hydrocarbons can have deleterious effects on health. PAHs are a class of over 100 chemicals composed of up to six benzene rings fused together so that two adjacent benzene rings share two carbon bonds. PAHs result from combustion processes both natural and artificial, from any process that burns carbon containing compounds. Vehicle emissions, industrial processes, and biomass burning are all examples of processes which release PAHs into the atmosphere (Kim et al. 2013).

The Agency for Toxic Substances and Disease Registry (ATSDR) lists PAHs as ninth on their 2013 Substances Priority List. The Comprehensive Environmental Response, Compensation, and Liability Act (CERCLA) requires ATSDR and the Environmental Protection Agency to prepare the list of substances that are most commonly found at facilities on the National Priorities List (NPL) and which are determined to pose the most significant potential threat to human health due to their known or suspected toxicity and potential for human exposure at NPL sites. Note, this priority list is not a list of "most toxic" substances, but rather a prioritization of substances based on a combination of their frequency, toxicity, and potential for human exposure at NPL sites (Agency for Toxic Substances and Disease Registry 2014).

Studies of PAHs in house dust have shown evidence of PAHs present in the past. One study in North Carolina indicated that PAHs associate with PM from homes and that PAH concentration increased with decreasing particle size across various size fractions (Lewis et al. 1999). Another study found that three specific PAHs tested for were found in all residences in a study of over 500 residences tested in Denmark (Langer et al. 2010). The research referenced above shows that PAHs are nearly ubiquitous.

Another pollutant that can associate with particulate matter in a complex manner is environmentally persistent free radicals (EPFRs). EPFRs are relatively new to the literature of air quality but are thought to have important health impacts (Burn & Varner 2015). As its name indicates, an EPFR is a free radical, meaning that it is an atom or compound which is unstable due to an unpaired electron. Unlike typical free radicals, these atoms or compounds possess a free radical that associates by chemisorption to the surface of metal oxides like iron and copper. An electron is transferred from the adsorbate to the metal center, reducing the metal cation and resulting in a stable radical species (Vejerano et al. 2012). This allows the free radical to persist in the environment for days or weeks, giving a much larger potential for the radical to enter biological systems and cause oxidative chain reactions because of its highly electrophilic nature. The genesis of the EPFR is thought to arise through industrial processes, where chemisorption of the radical to a metal oxide occurs at high temperatures in the post flame cool-zone of combustion processes (Fahmy et al. 2010). More specifically, an organic pre-cursor like a substituted benzene ring or other aromatic will become physisorbed to a metal oxide which allows for elimination of H_20 and subsequent chemisorption and electron transfer from the pre-cursor to the metal oxide which results in the metal being reduced (gaining an electron) and

creating an EPFR. This is thought to take place in high temperature areas 100-500 degrees Celsius (Patterson et al. 2013).

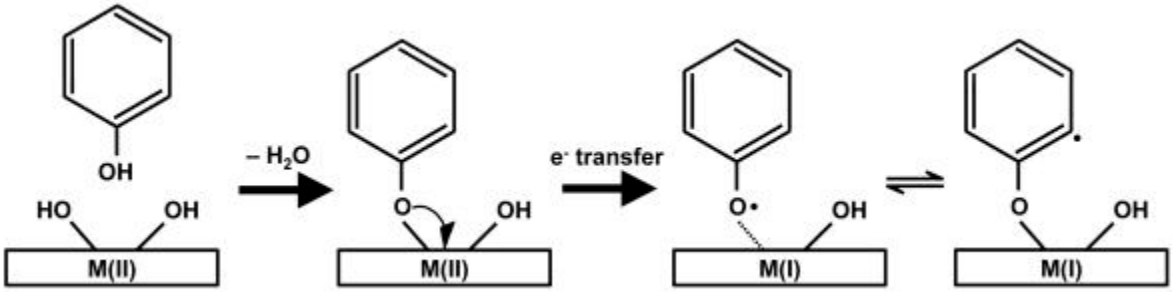

Figure 2.2: Radical formation from phenol adsorbed to metal oxide (Patterson et al. 2013)

Reactive oxygen species are generated from the redox cycling of EPFRs in models and in tested particulate matter. Samples of particulate matter showed that decay of radicals took place but many of the radicals were persistent for days to weeks to months to even years (Gehling and Dellinger 2013).

One study examining the levels of persistent free radicals even found that abundant free radicals in a biochar sample inhibited germination, caused root and shoot retardation and plasma membrane damage in corn, rice, and wheat seedlings. This shows the deleterious effects of persistent free radicals across a wide range of biological systems including plants, not just mammals (Liao et al. 2014).

Researchers studying EPFRs in the Baton Rouge area have found relatively high levels on the stable unpaired electron compounds in fractions of fine PM collected from ambient air samplers. Radical concentration was measured and calculated using electron paramagnetic resonance. Samples from the Baton Rouge industrial corridor were found to contain fine PM that most commonly contained10^16-10^17 spins per gram (Gehling and Dellinger 2013) ; (Dellinger et al. 2008).

Inhalation of EPFRs associated with PM has been shown to cause sustained radical generation by redox cycling. These chain reactions are often caused by semiquinone radicals which have a g-factor of 2.0031-2.0044. The g-factor is the measure of the magnetic moment of a free radical and is used to characterize whether a radical is oxygen centered or carbon centered (Squadrito et al. 2001). It has also been found that oxygen centered radicals are more reactive than carbon centered radicals. Semiquinone radicals are more oxygen centered than phenyl and phenoxyl radicals (Dellinger 2007).

The final pollutant associated with PM that is tested in this research is metals. Copper and iron are the elements in the highest concentration for metals in fine particulate.Nickel is also known to associate with particulate matter, often from the combustion of petroleum additives. These transition metals may play a key role in the generation of reactive oxygen species (Vejerano et al. 2012). One study found that metals bound with particulate matter posed an increased health risk to landfill workers who were exposed to the particulate matter. Arsenite, lead and cadmium associated with particulate matter were found to accumulate in various tissues of the body and posed a health risk (Chalvatzaki et al. 2014).

2.3: Health Concerns Associated With Particulate Matter Exposure

Health effects related to PM inhalation are diverse and are being studied closely as an emerging topic of importance in public health.

One health effect study noted that the concentration-response relationship was linear without any threshold for PM2.5, even at exposure levels below the EPA annual standard (Lepuele et al. 2012). This demonstrates that there is no baseline for safe fine particle exposure. The paper noted evidence for a strong association between chronic PM2.5 exposure and early mortality.

The Lepeule study was a follow-up to long term health studies of particulate matter and found significant associations between PM2.5 exposure and all-cause, cardiovascular, and lung cancer mortality (Lepeule et al. 2012). While there are documented cardiovascular effects, this study points out that the most significant and obviously affected organ from particulate exposure is the lungs. All PM smaller than 10 micron in diameter is inhalable, which means it can enter the respiratory bronchioles and alveolar ducts. Fine and ultrafine particles will deposit deeper in the lungs, with some particles small enough to reach the alveoli, the site of gas exchange with blood in the lungs where these particles are not easily cleared out, resulting in potential local and systemic pulmonary inflammation (Lepeule et al. 2012). Non-soluble pollutants may be able to enter the bloodstream at the alveolar-capillary area by passing through the thin cellular membrane of the alveoli. The exact mechanisms of PM transport in biological systems are unknown, but the above scenario is possible. It may also be possible that water soluble metals and fly ash components like vanadium and cadmium enter the system and translocate by extra-pulmonary circulation (Kim et al. 2013).

Particulate matter is a complex and heterogeneous mixture that can vary highly depending on source and location. Therefore, the toxicity of particulate matter has been difficult to quantify. One study called it one of the most challenging areas of environmental health research (Kelly and Fussell, 2012). In this field of emerging importance in air quality, one study was able to narrow down the particulates of importance in terms of effects on health. They found that ambient exposures from outdoor sources were associated with decreased lung function (Ebelt et al. 2005). The Ebelt study emphasized the importance in categorizing the source and size of the particles as key to their toxicity and stated that particles need to be more closely evaluated in terms of toxicity and health effects.

The mechanism by which particulate matter actually decreases lung function, causes cancer, or induces/exacerbates asthma is being looked at more closely, but is still not well understood. When particulate exposure was tested on cells in laboratory experiments, one study noted that an increase in the observed effects was always associated with a decrease in particle size (Mueller et al. 2006). This confirms other studies' reports that toxicity increases inversely to particle size. This is most likely due to an increased surface area to volume ratio. Smaller particles are associated and bind with more chemicals than larger particles. The Muller study further explained that cell dysfunction in exposed cells caused symptoms they attributed to oxidative stress (Mueller et al. 2006). Oxidative stress is a key mechanism of cellular damage associated with particulate matter. Oxidative stress in biological systems results from reactive oxygen species (ROS) initiating reactions in the body. ROS can damage key cellular components including proteins, DNA, and lipids. Lipids are a key component of cell walls (Klaassen and Watkins 2010). Numerous studies aiming to gauge the levels of oxidative stress in a system use markers of lipid peroxidation like isoprostanes to measure oxidative stress. Isoprostanes are products formed from free radical peroxidation of fatty acids or lipids (Klaassen and Watkins 2010). When biological systems show elevated levels of isoprostanes, this is indicative of systemic oxidative stress.

Ultrafine (or nanoparticles) are a health concern when inhaled as PM or as an agglomerated constituent of PM. Research has shown that nanoparticles when inhaled translocate rapidly from the lung to lymph nodes (Choi et al. 2010). Additionally, research has indicated that solid ultrafine particles that deposit in the nose can travel to the central nervous system, in this case, the olfactory bulb, and the striatum, frontal cortex, and cerebellum of the brain. Translocation to extrapulmonary areas of the body can have systemic affects and is related to

many factors including particle size, solubility, deposition site, and integrity of the epithelial lining (Elder et al. 2006). One study found that nanoparticles in solution could de-aggregate in aqueous solution in the presence of blood protein albumin (Tantra et al. 2010). This may indicate the possibility that agglomerated particles, containing nano-scale particles, if re-suspended can be inhaled and subsequently break up and then translocate en-vivo.

2.3.1: Environmentally Persistent Free Radicals

The research group at the LSU Superfund Research Center has been able to demonstrate that EPFR containing particulate matter produces ROS and that this produces a redox cycle which was maintained in biological environments (Kelley et al. 2012). They have also shown that PM containing EPFRs directly correlated to the quantity of hydroxyl radicals in the lab (Gehling et al. 2013). In the Kelley experiment neonatal rats were exposed to inhalation of EPFRs, and they caused an oxidant injury within the lung lining fluid, and that the body responded by increasing antioxidant levels in the lung. The researchers concluded that ROS may govern toxic responses of particulate matter in biological tissues like the lung (Kelley et al. 2012).

Many studies gauge antioxidant levels such as glutathione and oxidized glutathione in order to measure the level of oxidation injury (Fahmy et al. 2010). The body will often compensate with increased glutathione production to account for oxidant injury from ROS (Balakrishna et al. 2011). The Fahmy study was able to determine that epithelial cells exposed to EPFR particles showed a higher proportion of oxidized glutathione (GSH) to total GSH. The epithelial cells were dosed in vitro with mixtures containing EPFRs. This experiment simulates inhalation of suspended PM and potential systemic effects on the cellular level. The elevated presence of oxidized GSH, or depleted GSH, is indicative of oxidative stress. Ultimately, the

EPFRs are associated with causing oxidative stress by means of ROS (Balakrishna et al. 2011). Oxidative stress can also be caused by semiquinone radicals. Semiquinone radical redox cycling is thought to be a contributing factor to the toxicity of cigarette smoke and diesel exhaust (Squadrito et al. 2001).

Another study sought to identify the effect of EPFRs on developing neonatal rat lungs. This study was undertaken because young populations, including humans, are thought to be more susceptible to the harmful effects of particulate matter pollution due to more air per pound of body weight breathed and immature immune systems. EPFR exposure is hypothesized to be the cause of significant deficits in respiratory growth, leading to important deficits in lung function in children (Balakrishna et al. 2011). The study ultimately found that particulate matter-EPFR pollutant particle systems induced acute airway dysfunction, enhanced oxidative stress in the lungs, and induced distinct changes in pulmonary architecture among other effects. In terms of altering the lungs fundamental structure, the study indicated that alveolar thickness was decreased, while smooth muscle in the peribronchial region was increased, narrowing the space for airflow and causing constriction. On the whole, particulate matter air pollutants exacerbates asthma, chronic obstructive pulmonary disease, and will make respiratory tract infections more serious, especially in the most vulnerable: young, sick or old populations (Balakrishna et al. 2011). This susceptibility of sensitive populations is the reason that the EPA has primary and secondary standards, primary standards exist for the most sensitive populations (US EPA 2015).

Similarly to the above study, other studies have found that inhalation of EPFR particle systems can cause hypertrophy of small pulmonary arteries. This increased arterial thickness raises blood pressure in the lungs. This artery thickening and increased blood pressure has been

seen in epidemiological studies by dosing particles with EPFRs and allowing the particles to be inhaled by rats (Mahne et al. 2012).

More studies seek to identify the exact mechanisms to explain the induction and exacerbation of asthma by xenobiotics like particle-pollutant systems. Currently, these mechanisms are not well understood. A study by Wang indicated that exposure to EPFR particulate matter was partly responsible for altering the pulmonary immune profile (levels of T-cells) and exacerbating allergen-induced asthma development (Wang et al. 2013). More specifically, the study examined pregnant mice and dosed them by inhalation with EPFR particulate matter and gauged the effect on offspring. The study found that the offspring of dosed mice demonstrated altered proportions of helper T-cells in their pulmonary systems. It is assumed that oxidative stress induced on pregnant mice was significant enough on the systemic level to fundamentally alter the immune system of the offspring. This results in airway hyper-responsiveness on the mice that may be permanent. The amounts of certain critical T-cells, which can play crucial roles in asthma, continued to be diminished even at six weeks of age (Wang et al. 2013). Therefore, the inhalation of particulate matter in the environment is significant not only to sensitive young populations, but also to pregnant populations where systemic dysfunction may result from particulate matter exposure.

The immune levels in biological systems can further be disrupted by an EPFR-particulate matter pollutant system, as evidenced by a study that dosed infant rats with this pollutant system by inhalation. This study found that epithelial cells in the rat's airways could actually be changed in phenotype to mesenchymal cells. This change involves a radical reformation of cell morphology. When cells were exposed for 24 hours they lost their cobblestone morphology and adopted an elongated spindle-shaped morphology characteristic of mesenchymal cells. This

transition is thought to be part of the key to smooth muscle changes in airway structure. Also, these cellular alterations are a key reason for airway hyper-responsiveness (Thevenot et al. 2013).

2.3.2: Polycyclic Aromatic Hydrocarbons

PAHs are also a pollutant of critical health importance associated with PM. Southeast Asia is an area where PAHs and air pollution are an important topic due to high air pollution. A study in China collected particulate matter samples in areas where electronic waste processing and recycling was conducted. This study tested the PM samples for polycyclic aromatic hydrocarbons. This research was conducted to estimate the inhalation risk associated with breathing particulate matter and compounds that are frequently associated with the particulate matter like PAHs. PAHs are produced from incomplete combustion and are being produced at extremely high levels in China. PAHs are dangerous because they can be inhaled into a biological system and bind covalently with DNA to form PAH-DNA adducts, a cause of DNA damage that has been linked to cancer (Wang et al. 2013). Lung cancer is the leading cause of cancer deaths in China and ambient air pollution plays a significant role in causing lung cancer. This is very significant to public health because cancer is the leading cause of death in Chinese cities. Cities like Beijing have a high PAH concentration that is exacerbated by activities like burning coal for heat. Other primary sources for PAH pollution in urban areas in China are combustion of fossil fuels for industrial processes, vehicle exhaust and biomass burning (Wang et al. 2013).

One study by Souza et al. examining atmospheric PAHs found that local biomass burning of sugarcane in Brazil contributed a significant amount of particulate matter to the atmosphere. The study found that the organic fraction from sugar cane burning was especially large and

complex. Some species of PAH that they study examined are known to be carcinogenic or mutagenic, specifically the nitro and oxy containing PAHs are thought to be most harmful in terms of mutagenicity and carcinogenicity. Various species of PAHs may have different lifetimes in the atmosphere, depending on sunlight and photolysis (Souza et al. 2014).

In a similar study (Pavagadhi 2012), a research team in Singapore found that biomass burning as part of the annual agricultural cycle caused smoke-haze episodes. This group found that 90% of soot originating from biomass burning episodes was particles less than 2.5 micron in size, fine particles. This fine particulate soot can remain suspended for a week and travel long distances throughout the region. During burning episodes fine particulate levels were four times higher than normal. Also, particulate collected during the burning episodes was analyzed for PAHs and it was discovered that various PAHs thought to be carcinogenic were present in significantly higher levels than in background air. Concentration of metals was also found to be at higher than background level concentration (Pavagadhi 2013).

As in the Fahmy (2010) study, the Pavagadhi study used GSH as an indicator of oxidative stress, as it sequesters ROS but can become depleted. Pavagadhi and his group believe that oxidative stress from ROS plays a direct part in pulmonary inflammation that can occur after PM exposure. They found that the antioxidant GSH levels were significantly depressed when epithelial cells were exposed to smoke haze aerosols compared to controls. They determined that the chemical components of the smoke haze are toxic and hazardous to epithelial cells (Pavagadhi 2013).

Particulate bound PAHs and water soluble metals may be responsible for oxidative stress experienced by the cells in the Pavagadhi study (Pavagadhi 2013). Samples from the smoke haze were tested for 16 priority PAHs and 10 transition metals. The study found 5 of the 7 PAHs

known to be potential or suspected carcinogens in the smoke haze sample. Almost all of the PAHs tested for were significantly higher during smoke haze events. Particularly high amounts of naphthalene were detected and significantly a high differential of benzo(b)fluoranthene, benzo(k)fluoranthene, benzo(a)pyrene and dibenz(a,h)antracene in smoke haze events was detected compared to periods with no smoke haze events (Pavagadhi 2013).

2.3.3: Metals

The analysis of airborne metals in the Pavagadhi study is significant because the main exposure pathway for PM to humans is in the lungs (Pavagadhi 2013). Inhaled PM can get deep into the lungs, depending upon its size (LePeule et al. 2012). During smoke haze events, collected particulate matter had higher concentration of aluminum, chromium, manganese, iron, cobalt, nickel, copper, zinc, cadmium and lead than background air. Zinc was found in particularly high concentrations; it was found to account for 59% of the particulate bound metals. It has been shown that metals passing through the air and lung interface can cause inflammation and tissue damage. This can occur at sites associated with biologically accessible metal ions (Pavagadhi 2013).

Zinc was the focus of a study on metals in the home by Beauchemin et al. (2014). Zinc is generally a low risk metal from oral or dermal exposure, but can be harmful if inhaled; especially when associated with repeated exposure from urban air pollution (Beauchemin et al. 2014). The study found that zinc in the samples, and potentially other metals, became more bio-accessible when stored in humid and oxygenated conditions. Zinc is known to be more prevalent in industrial areas (Beauchemin et al. 2014). It is plausible that metals may store in areas of the home with high outdoor PM exchange and become more bio-accessible in a humid climate.

The Chalvatzaki (2014) study estimated tissue concentrations of metals from inhalation of particulate matter bound metals. Decomposition of landfill deposited materials contributed to inhalation doses for workers on site as did truck exhaust, brake dust and re-suspended road dust. This is a common problem at landfills (2013). Inhalation is the primary route of exposure to these particulates; therefore, the smaller the particles, the more likely they have of causing systemic disruption. The Chalvatzaki (2014) study focused on arsenic, cadmium and lead and found that these metals were stored in the lungs, blood, bone, muscle kidney and liver. Because of these deposits, average landfill workers were more likely than other members of the general public to experience inflammatory effects, respiratory-related hospital admissions, cardiovascular problems, lung cancer and damage to other organs depending on the source of the PM and its composition (Chalvatzaki 2014).

In addition to metals in PM being potentially dangerous in their own right, research by the LSU Superfund Research Center has indicated that metal oxide nanoparticles such as copper and iron have been identified as active sites for the formation and stabilization of EPFRs (Herring et al. 2015). Also, enhanced molecular growth in the presence of iron oxide nanoparticles resulted in increased formation of PAHs in high temperature industrial processes (Herring et al. 2012). This is significant in positing that there may be a correlation between metals, PAHs and EPFRs, all of which will be examined in this research. Additionally, metal cations associated with nano-scale particles of metal oxides have demonstrated higher surface reactivity and adsorption at the particle surface. (Herring et al. 2012).

These studies show the large number of effects that particulate matter pollutant systems like metals, PAHs and EPFRs can have on health, and hence the importance of studying and

regulating particulate matter emission levels. It is also worthwhile to collect deposited PM to discover where pollutants end up after their production, emission, and transport.

2.4: Collection and Measurement of Particles

To study PM and associated pollutants like metals, PAHs, EPFRs, an understanding must be gained of how particles behave once released and how size influences behavior. It is also important to examine the activities that make up the amounts of ambient particulate and some of the methods that are used to measure these levels.

A study by Rim et al. (2013) found that there were many variables to determining entry levels of particulates into homes and noted the difficulty of measuring airborne particle transport into buildings. Variables affecting particulate entrance into homes include: building construction and operation (HVAC systems and window position), weather conditions, deposition rate and outdoor particle concentrations. Given all of these variables it is difficult to provide a model for outdoor particle inflow rate and deposition, but it can be confidently stated that outdoor particles come indoors and settle onto surfaces. Outdoor ultrafine particulates originating from vehicle emissions and other sources can penetrate the building envelope, particularly in urban environments. This has a significant impact on ultrafine particulate (UFP) levels in buildings (Rim et al. 2013). Studies of high particulate matter aerosol density areas in China suggest that vehicles contribute significantly to ambient PM levels. PM contributions from road transport equaled about a quarter of ambient PM in source (Cheng 2013).

Another study in Los Angeles found that vehicular traffic accounted for 39% and 46% of indoor and outdoor total particulate matter respectively. This study utilized a 24 hour sampling period with a personal cascade impactor sampler (Hasheminassab et al. 2014). The price of this apparatus can be in the high hundreds to thousands of dollars range. The Hasheminassab study

found that even those who spend most of their time inside are exposed to considerable PM of outdoor and indoor origin. Further, the researchers found that indoor levels of metals and PAHs were most affected by outdoor sources (2014).

Measurement of particulate matter levels and collection of particulate matter can be achieved many ways. Various devices utilize lasers to merely detect particle levels in aerosols rather than collect PM (Wallace et al. 2013), while other methods physically collect the particles for analysis rather than sensing them. One example is a high volume sampler that transfers suspended fine and ultrafine particles into a liquid suspension that can then be analyzed and its relative toxicity measured (Wang et al. 2013). The sampler in the Wang study is a complex and specialized impactor. Other methods for segregating particles based on size include the use of a fluidized bed aerosol generator to re-suspend particles and a cyclone to segregate them based on size (Lewis et al. 1999). This research project lays out the design and implementation of a much simpler and inexpensive collection method and filtration apparatus to collect a size-resolved sample.

While other studies have collected house dust in bulk and placed the dust in solution with phosphate buffered saline (PBS) and then filtered through glass wool filters, it is the goal of my research to re-suspend particles and filter them in their dry state (Boasen et al. 2005). The Boasen method yielded enough sample to test in the laboratory without potential interactions with PBS.

In using membrane filtration technology, it is noted that there are two types of filter in common use: a porous membrane filter, which is made by creating holes on a solid surface, and or a fibrous air filter which collects PM by multiple layers of thick fibers. The second type of filter can be thick and bulky (Liu et al. 2015). This research will examine both of these filters types mentioned in the Liu article.

The Liu study noted that particles trapped on a filter were able to move along the filter and aggregate with other particles while leaving behind some empty space for later PM to be caught. The study also found that smoke captured on filters in their analysis often contained organic carbon including alkanes and aldehydes and criteria pollutants CO, NO2, SO2, as well as benzene, toluene, xylene and PAHs. The PM they analyzed showed more agglomeration in high humidity and the filters had better capture efficiency when the filter surface had strong dipole-dipole and induced-dipole intermolecular forces (2015).

2.5: Particle Dynamics

An important factor to consider in particle collection is the way that particles behave. During the course of this research it became necessary to investigate the behavior of particles because collection of bulk samples was followed by sub-sequent particle re-suspension for size determined filtration.

The most important characteristic in determining the behavior of aerosols or particulate matter is the particle size. Most individual aerosols cover a very wide range of size distribution within them (Hinds 1999). Particle shape will also determine particle behavior. Many models of aerosols and particles assume that they are spherical, but this is often not the case in real scenarios (Lieberman and Scott 1973). Liquid aerosols are usually spherical, but solid particles generally have complex or irregular shapes. Assumption of a regular, spherical shape is sometimes necessary to give an approximate particle size, which is expressed in diameter (Hinds 1999). For irregular particle sizes aerodynamic diameter is defined as the diameter that has the same settling velocity as a spherical particle given a specific density (Hinds 1999).

Many aerosol filtration systems use a standard aerosol particle to test filtration efficiency. A particle that is frequently used is a 0.3 micron dioctyl phthalate (DOP) liquid aerosol. DOP is

often chosen because of its characteristics including: stable, non-volatile, and high boiling point. The 0.3 micron size was chosen because filtration efficiency varies with particle size and 0.3 micron was a historically convenient size for filters of the time period of initial development. DOP efficiency is commonly expressed as a percentage of DOP concentration. A 99.9% efficiency means that 99.9% of particles larger than 0.3 micron are retained by a filter (Japuntich 1995).

Particle density is also a factor which influences particle behavior. For modeling purposes, particles are assumed to have a standard density of 1 gram/cubic centimeter. However, smoke and fume particles may have densities significantly lower than expected. This is because there may be areas of voids within their structure, due to the agglomerated nature of some particles (Hinds 1999). Many smoke aerosols have an average particle diameter of 0.1 to 0.5 micron (Japuntich 1995).

When a particle is released in still air it begins to undergo gravitational settling, which will ultimately draw the particle to a surface. All of the above factors: size, shape and density, will affect settling. When a particle is released it reaches its terminal settling velocity quickly. Settling velocity is much faster for larger particles (Hinds 1999). This statement is supported by research by Lee et al. which finds that particle deposition rate is highly size-dependent (2014). However, particles are rarely settling in completely still air. Lee et al. and other have noted that particle deposition indoors is also influenced by mixing of air by ventilation and air exchange. The Lee study also found that particle collisions and subsequent coagulation were a mechanism for particle removal from suspension (2014). Smaller particles have lower settling velocities and increased mobilities (Hinds 1999).

When aerosol particles come into contact with any surface they adhere to it. They will also adhere to one another and form agglomerates. Particle adhesion is poorly understood and highly complicated. The main adhesive forces are van der Waals, electrostatic and the surface tension of adsorbed liquid films. The strength of these forces depends on the material, size and shape of the particle. It also depends on the material, smoothness, and potential contamination of the surface. In addition, temperature, duration of contact, and initial contact velocity all determine adhesive forces. Van der Waals forces are attractive long range forces that can draw molecules together by way of dipoles (Hinds 1999).

Because surfaces may be irregular where particles contact one another, or they contact surfaces, the exact attractive force is difficult to measure. However, after initial particle contact van der Waals and electrostatic forces will cause deformation of the particle to increase surface area in contact and reduce separation distance. The extent of this deformation, and hence the adhesive force, depends on the hardness of the particle. Because most particles have adsorbed liquid particles on their surface, the attractive force occurs here because of surface tension of the liquid drawn into the capillary space at the point of contact (Hinds 1999).

Centrifugal force, vibration and air currents can all remove particles from surfaces. There is a diminishing return in energy spent to detach all particles from a surface. Nearly ten times as much force is required to remove 98% of particles from a surface than 50% of particles, centrifugally. Also, the detachment of particles from a surface (which is a key part of the goal of this research) is complicated by unknown variables like particle-surface adhesive characteristics and by unknowns like the geometry of the air flow and the boundary layer velocity profile (Hinds 1999). Therefore, re-suspending particles (as this research does) would be a simplification towards effective size-based particle collection.

Hinds notes that as particle size decreases it becomes increasingly difficult to remove them from surfaces, which makes it difficult to re-suspend and filter small particles. Also, particles adhere tightly together once agglomerated from collisions that remove them from suspension, the large agglomerate they form can be easily blown or shaken from the surfaces (Hinds 1999). But it is unknown if vibration or agitation is sufficient enough to break these agglomerates apart. It may be possible that these agglomerates could break apart with vibration releasing them from their deposition point or upon impact onto the filter surface. Samples in this research are shaken by a Fisher Scientific vortex mixer and sucked into a filtration apparatus.

It has been shown that at low velocities a particle contacting a surface can deform and attach itself to a surface, losing its kinetic energy. At a higher velocity, part of the particle's kinetic energy is lost in deformation but some is retained and the particle may rebound elastically. This is called particle bounce (Hinds 1999). It may be possible that the impact of these collisions at higher velocity may dislodge agglomerated particles from one another. The deformation or the particle impact may be significant enough to break apart agglomerates. Success in collecting small size particles from deposited particulate matter samples would potentially indicate that breaking apart agglomerated particles is possible, this research will investigate that possibility.

Three particle characterizations that would impact re-suspended particles include Brownian motion, diffusion, and flux. Brownian motion is the irregular motion of a particulate in suspension caused by the constant bombardment of the particle with gas molecules. Diffusion is the transport of particulate in a concentration gradient, this always occurs from a higher concentration to a lower concentration. Flux is the movement of particles through 1 cm2 of air each second. The overall flux rate of an aerosol is a product of the particle concentration gradient

and the diffusion coefficient. A higher diffusion coefficient indicates more rapid movement because of more frequent contact from gas molecules due to higher concentration (Hinds 1999).

The table below from Hinds shows that smaller diameter particles have greater mobility and a higher diffusion coefficient. They are more easily moved by collisions with gas molecules. There may be billions of collisions between particles and gas molecules in a meandering path. In this scenario a .01 micron particle will be transported by diffusion 20,000 times as fast as a 10 micron particle (Hinds 1999).

Table 2.2: Particle mobility and diffusion coefficient based on their diameter (Hinds 1999).

Particle Diameter (micron)	Mobility (cm/s x dyn)	Diffusion coefficient (cm2/s)
.01	1.3 x 10^10	5.2 x 10^-4
.1	1.7 x 10^8	6.7 x 10^-6
1.0	6.8 x 10^6	2.7 x 10^-7
10	6.0 x 10^5	2.4 x 10^-8

Particle dynamics and Table 2.2 indicate that particle mobilities and diffusion differ vastly depending on particle size. When particles are re-suspended, the fine and ultrafine particles will be transported much more quickly through the air than larger particles. It is possible with air currents in a room that smaller particles in suspension could be moved more easily and be more sensitive to ambient air conditions and can be potentially transported longer distances.

In terms of this research: the agitation of the bulk sample jar by a vortex mixer should be strong enough to influence particle rise, but as controlled as possible to be effective. Jar agitation

should not be wild enough to spew particles, especially smaller particles, outside of the path of the suction from the filtration apparatus. Re-suspended smaller particles would theoretically be drawn to the path of suction and filtration than large particles due to their higher mobility. The filtration apparatus should maintain a constant and consistent suction. For this to be true, filter integrity must be maintained where the filter meets the apparatus and also on the surface area of the filter. A tear in the filter, even of a very small diameter, can result in significant pressure and suction changes, including uneven suction. More significantly a torn filter allows particles of a larger size to pass through the filter (Mouret et al. 2009).

Another point of importance for filtration and particle dynamics is that penetration through filters increases when the flow velocity increases because of reduced diffusional deposition (Mouret et al. 2009). Therefore, the higher the flow rate, the more particles that are likely to pass through the filter onto a collection surface.

The examined literature does not mention whether fine and ultrafine particles can exist by themselves once re-suspended, or if they are irrevocably agglomerated to other particles that would fall into the coarse fraction. It will be important to this research to minimize the surfaces that re-suspended and filtered PM comes into contact with to minimize particle loss via adhesion to surfaces, particles adhere to any surface they contact. As noted above the smaller fraction of particles are especially difficult to remove from surfaces (Hinds 1999).

2.6: Citizen Science

Giving citizens the ability to experience scientific collection processes for themselves is part of the experiential theory where information gained through experience provides a contextual base for organizing and remembering information more effectively. In addition, it provides participants with a more positive view on science (Broussard et al. 2005).

The importance of keeping the non-scientifically oriented public informed about science and research is crucial as scientific discoveries continue to be made. One study notes that three out of four American adults are scientifically illiterate (Cronin and Messemer 2013). If the American public does not keep abreast with scientific discoveries, they run the risk of falling behind in knowledge and information that affects everyday life through governmental policy and public health.

In the future the results of this study may be used to engage the public in collecting scientific information from home PM samples from home surfaces or their attics for analysis. Bulk sample locations could be selected strategically throughout the Baton Rouge area and the collected samples could be provided to the LSU Superfund Research Center to analyze and plot spatially.

The benefits of citizen science are many. As a social benefit, the engagement of the public educates and informs many on important environmental and scientific issues. Also, as a technical benefit to this study, citizen science can cover large spatial areas, can collect data from private households and collect a large amount of data that would otherwise be labor intensive to obtain (Freitag and Pfeffer 2013).

Freitag and Pfeffer (2013) make a key point about “democratizing” science. This is applicable in our study as hazardous pollutants collected from the home draw attention to an important and potentially overlooked air quality issue. Data and knowledge collected through this study could empower communities to affect political decision making (Freitag, Pfeffer 2013). Our study would be a crucial first step in establishing baseline data of hazardous pollutant systems in homes that originate from nearby combustion sources.

Participants would be provided with with appropriate instructions for collecting deposited particulate, thereby making them citizen scientists. These instructions would ensure quality control of data and include simple and key points from the literature to highlight the nature and importance of the research. This would serve to crystalize new scientific knowledge and terminology passed from researchers to citizen scientists.

3. MATERIALS AND METHODS

3.1: Materials and Methods Introduction

This study was conducted during the years 2014 and 2015. Samples of household dust were collected for filtration and laboratory analysis from numerous locations using a variety of methods for collection, filtration and extraction. The original aim of the study was to design a "citizen sampler" that would collectively use a vacuum cleaner and a filtration apparatus to simultaneously collect and filter a sample of size resolved particulate matter from dust collected on an undisturbed substrate in a home. As originally conceived, the citizen sampler would segregate a size specific sample of deposited particulate matter for laboratory analysis, namely, fine particulate matter, or particles smaller than 2.5 micron. Collecting and filtering a sufficient sample *in situ* proved difficult using membrane filtration and alternate methods were designed.

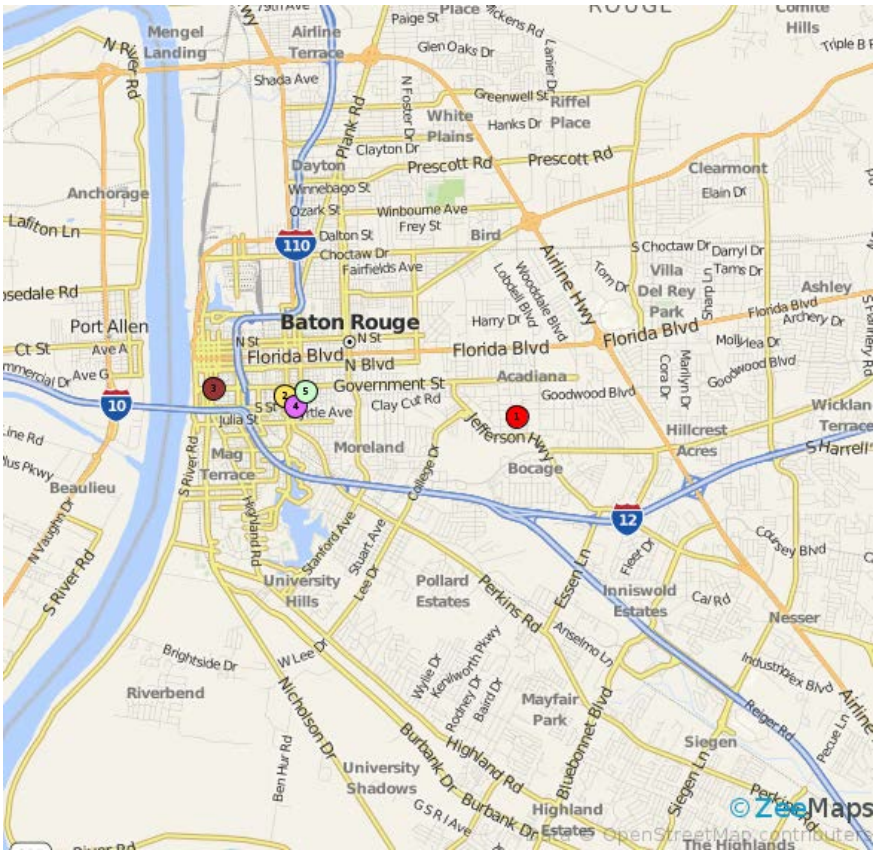

Figure 3.1: Approximate sampling locations in Baton Rouge.

Table 3.1: Sampling locations and their corresponding sources for all samples.

Sample #	Source Location	Location #	Sample #	Source Location	Location #
1	Attic	1	16	Home surfaces	Not on map
2	Outdoor Porch	2	17	Home surfaces	1
3	Attic	5	17b	Home surfaces	1
4	Attic	5	18	Attic	1
5	Outdoor Porch	2	19	Attic	1
6	Window Unit Filter	5	20	Attic	1
7	Home interior	1	21	Attic	4
8	Home interior	1	21b	Attic	4
9	Home interior	1	22	Outdoor Porch	2
10	Attic	Not on map	23	HVAC Filter	4
11	Home interior	1	24	Attic	4
12	Home interior	1	25	Attic	4
13	Home interior	5	26	Attic	4
14	Home interior	Not on map	27	Attic	3
15	Home interior	Not on map	28	Attic	3
			29	Attic	3

Sampling locations, and collection details can be viewed in Table 3.1 and Figure 3.1 to demonstrate spatial details of sampling around Baton Rouge.

In situ sampling and simultaneous filtration involved using the vacuum and collecting deposited particulate matter that had come out of suspension and settled onto surfaces in attics. While doing this it was found to be most effective not to hold the filtration apparatus nozzle flush with the surface, but rather, to hold it an angle to collect smaller particles and avoid larger clumps of agglomerated particles that would cause clogging of the membrane filtration system. Even while attempting to avoid clogs to the pre-filter membrane, multiple filter changes and cleanings with a brush were required to clear excess debris. Another method attempted to exclude heavy from the pre-filter was a fiberglass screen cover to protect the pre-filter. This was effective to an extent, yet not effective enough to allow for simultaneous collection and filtration.

Dust was either filtered *in situ*, or later in the development process, collected as a bulk sample for subsequent filtration in the laboratory. The methods for dust collection and filtration both *in situ* and in the laboratory were extensive. These methods included: direct sampling of deposited particulate matter from surfaces, re-suspending deposited particulate matter from surfaces using a brush, re-suspending collected particulate matter from air conditioning window unit filters using a brush, collection of bulk sample from a concentrated dust source like a vacuum cleaner filter or canister, and collection of a bulk sample from an attic, either manually or with a vacuum. Once bulk samples of dust were collected for later laboratory filtration, these samples were agitated by hand for re-suspension and filtration. This process evolved into using a Fisher Scientific vortex mixer to agitate a jar of bulk sample to re-suspend particles, thereby making filtration more successful because the lighter PM rose to be filtered, while the heavier debris stayed in the jar.

Ultimately the method for particle filtration that proved to be the most effective is the collection of bulk samples with a Dirt Devil™ hand vacuum and removing the sample in a clean laboratory setting. The bulk sample was then re-suspended by placing a jar of the bulk sample on a vortex mixer, thereby causing the particles to rise. The rising particles are then filtered by the vacuum and filtration apparatus. The nozzle of the filtration apparatus is held over the jar with the vacuum running to draw rising particles across the filtration membrane at a high velocity to catch and filter rising particles effectively.

Filtration of either bulk samples in the laboratory or samples *in si*tu in homes was accomplished by attaching a filtration apparatus onto a Stinger™ 2.5 gallon wet/dry vacuum with a 1.75 horsepower, 4 amp motor. The specifications for the vacuum list it as having an air volume capacity of 48 cubic feet per minute (CFM). The measured value for the vacuum's filtration volume was actually slightly higher at 54 CFM. The anemometer for measuring airflow was a DAF800 digital anemometer manufactured by General Tools and purchased through Global Industries.

The filtration apparatus setup and design was changed and developed concurrently with the adaptation of sampling methods. Filtration apparatuses had three constructions: A, B and C. The vacuum hose was permanently modified by affixing a 1'' PVC coupling to the end of the hose and securing it with black duct tape for an airtight seal.

3.2: Bulk Sample Collection Methods

There were numerous methods and substrates used to collect bulk samples for filtration. These methods include:

1. A brush and dustpan in attic
2. A brush and dustpan on covered outdoor porch windowsills

3. A brush and dustpan on window air conditioning unit filter
4. A brush and dustpan on HVAC intake filter
5. Stinger vacuum cleaner in attic
6. Stinger vacuum cleaner with modified filter collection bag in attic
7. Bulk dust collected directly from vacuum canister
8. Bulk dust collected directly from secondary vacuum foam filter
9. Dirt Devil™ hand-held vacuum cleaner in attic

Collecting sample from HVAC systems filters, window air conditioning unit filters and from vacuum canisters and filters within the vacuum is a convenient and easy way to collect bulk samples. However, these are not discrete collections and have taken place over an indeterminate amount of time or an indeterminate sampling area. For discrete, location-specific sampling of deposited particulate matter in the home the most successful method has been the utilization of hand held vacuum to collect bulk sample. These bulk samples can then be removed from the hand held vacuum and sub-sampled in the laboratory. The Dirt Devil 9.6 volt "Gator™" hand-held vacuum has easy to change filters and the surfaces of the inside of the vacuum are easy to clean between uses with wipes and solvents to ensure cross contamination does not occur. Also, extra vacuum filters may be purchased to use for each collection.

3.3: Filtration Apparatus Setup

The filtration apparatuses that were designed and tested consist of the same general setup: a pre-filter and a collection surface housed by the fittings of the filtration apparatus. Polyurethane Foam (PUF) is used as a collection surface for filtered particulates. The PUF foam pieces used in this experiment are also used in the BGI 900 High Volume Sampler, which is now discontinued. The BGI product line is now owned by Mesa Labs and specifications on older

products are no longer available. The PUF can also be purchased in a roll from McMaster-Carr as antistatic polyurethane foam, product number 87035K52. The PUF collections substrate is preceded by a pre-filter that is also held in place by the apparatus. The pre-filter is often fragile or delicate and therefore requires the backing of fiberglass vinyl coated mesh screen, purchased in a roll from Home Depot. All PVC fittings can be made airtight by the insertion of filtration and collection materials into the apparatus, and if not, by the use of PTFE Teflon tape. Teflon tape was purchased from Home Depot. PVC couplings and reducer bushings (used in filtration apparatus C) were purchased from Home Depot.

Pre-filters include a variety of pore sizes and materials. Filtration apparatuses A and C both use 47 mm disk filters. Apparatus B uses a 40 micron nylon mesh cartridge filter. For the 47 mm disk filters, all filters were manufactured by EMD Millipore. Filters used include a 2.7 micron glass-fiber filter, an 8 micron nitrocellulose filter, an 11 micron nylon net filter and a 20 micron nylon net filter. The glass fiber and the nitrocellulose were extremely delicate and subject to tearing and perforating, while the nylon net filters were much more durable. Nylon net filters could be brushed clean and kept within the filtration apparatus during a course of sub-sampling, while the nitrocellulose and glass microfiber filters could not. Changing nitrocellulose and glass microfiber filters constantly throughout the course of a sub sampling would prove prohibitive to the research.

3.3.1: Apparatus A

Filtration apparatus A was constructed from two 3/4’’ PVC couplings and one 1’’ PVC coupling purchased from Home Depot. The 3/4’’ PVC coupling fits into the permanent 1’’ PVC coupling on the end of the vacuum hose loosely enough to also accommodate the presence of the PUF collection substrate. The presence of the collection surface makes the seal airtight. The pre-

filter and fiberglass vinyl mesh are held in place in the junction of 3/4'' PVC and 1'' PVC. Figures 3.2 and 3.3 show the disassembled and assembled construction of filtration apparatus A.

A later design of filtration apparatus A also included the presence of fiberglass mesh vinyl coated screen over the end of the filtration apparatus to exclude the largest particles from suction and filtration. Large particles often cause clogging and the use of a fiberglass screen was an attempt at preventing large particles from reaching the pre-filter. It is desirable to keep the pre-filter as clean as possible to avoid particulate agglomeration on the pre-filter surface that would exclude smaller particles from reaching the collection surface.

In testing, apparatus A was damaged the pre-filter by stressing the ring edges and cutting the pre-filter in a circle where the edges of the 3/4'' PVC coupling fit into the 1''PVC coupling. Particles larger than the pre-filter pore size are thought to have passed the pre-filter and been retained on the collection surfaces through tears in the filter.

Figure 3.2

Figure 3.3

Figures 3.2 and 3.3: The disassembled (left) and assembled (right) construction of filtration apparatus A.

3.3.2: Apparatus B

Filtration apparatus B is a Dustream® Collector (DU-ST-1) purchased from Indoor Biotechnologies. The Dustream® has an end fitting that attaches to the 1'' PVC coupling on the

vacuum hose and a nozzle that houses a 40 micron nylon mesh cartridge filter. The filter can be easily removed for cleaning. The Dustream® end nozzle that attaches to the permanently affixed 1'' PVC coupling houses the PUF collection surface between itself and the PVC coupling. Particulate matter gathered into the airflow of the Dustream® enters the nozzle where particles larger than 40 micron are captured, while particles smaller than 40 micron progress to the PUF collection surface where they are captured. Detail of the assembled and disassembled construction of apparatus B can be seen in figures 3.4 and 3.5.

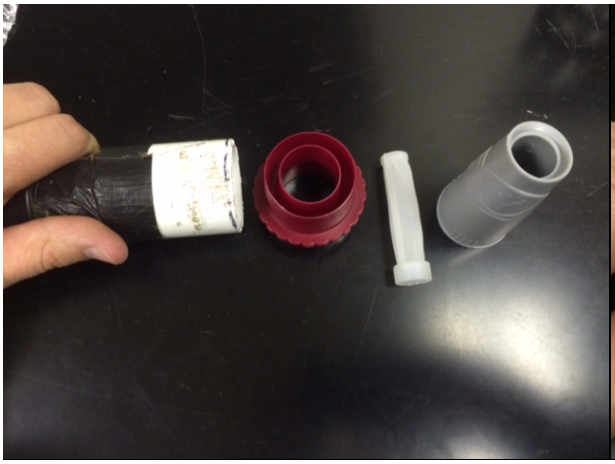

Figure 3.4

Figure 3.5

Figures 3.4 and 3.5: The disassembled (left) and assembled (right) setup for the filtrations apparatus B.

3.3.3: Apparatus C

Filtration apparatus C is similar to A, but this design was implemented to avoid the damaging effects of tearing the pre-filter that were experienced with filtration apparatus A. The difference in construction is that the final piece of 1'' PVC coupling is replaced with a 1 ½'' x 1 ¼'' PVC reducer bushing. The reducer bushing fits over the 1'' PVC like a sleeve and has an inside lip that holds the pre-filter and fiberglass screen backing in place firmly, but gently enough to avoid tearing of the pre-filter. This design also utilizes a larger surface area of the pre-filter compared to filtration apparatus A. Another difference is that the pre-filter is exposed on

the tip of the suction nozzle of the filtration apparatus instead of being housed inside of the PVC. This allows for less surface contact with PM on the PVC pieces and prevents particle loss, as PM will agglomerate on any surface it touches. Figures 3.6 and 3.7 show the disassembled and assembled construction of filtration apparatus C.

Figures 3.6 and 3.7 below illustrate the construction of the filtration apparatus in disassembled and assembled form. Figure 3.8 illustrates the general setup of the apparatus.

Figures 3.6

Figure 3.7

Figures 3.6 and 3.7: The disassembled and assembled setup for filtration apparatus C.

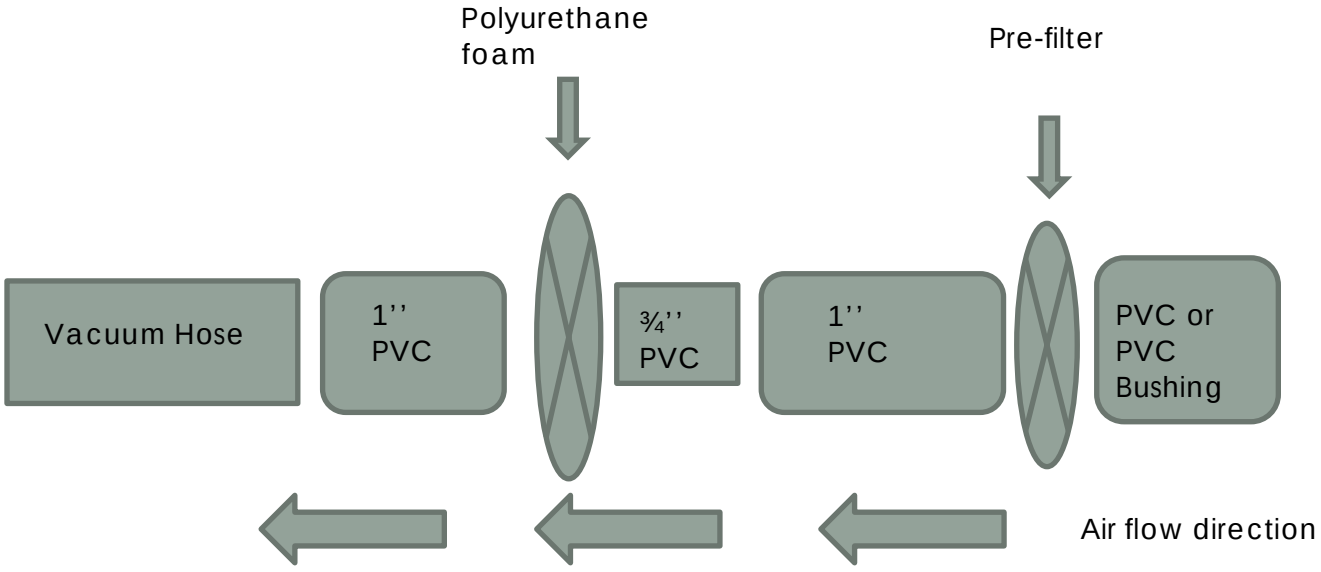

Figure 3.8: Illustration of hose and filtration apparatus setup with filter and collection surface placement, for filtration apparatuses A and C.

3.4: Particle Re-Suspension

During the time of the experiment in designing the best collection and filtration method it was found that re-suspension of the collected particles before they entered the filtration apparatus was most effective. This was initially accomplished by re-suspending particles with a brush *in situ* in an attic, brushing dusty surfaces in the direction of the filtration apparatus. This technique was slightly more effective than suctioning deposited PM directly from surfaces. As the research progressed it was found that re-suspension and filtration of a more concentrated particle sample was more effective than sampling directly from dusty PM coated surfaces. A jar with a bulk sample was manually agitated and this caused particles to rise. The filtration apparatus attached to the vacuum was held over the mouth of the jar to collect and filter rising particles. This method was eventually replaced by agitation of a jar with the bulk sample on a Fisher-Scientific Vortex Genie™ which caused the particles to rise in a more consistent manner and dissipate in manner similar to smoke.

3.5: Particle Removal from PUF

After collection and filtration, if a sample was collected on the PUF collection surface, it was taken to the laboratory for removal. Early filtration experiments produced little to no particulate on the collection surfaces. In these situations the material from the pre-filter was manually sorted and the largest particles taken out and the remaining PM was tested.

As collections progressed the collection surface showed that more collected particulates were embedded in the foam. Early attempts to remove these particles included manual shaking by hand, vibration on a Fisher Scientific Vortex Genie, and sonication. The above techniques were all done dry, and were successful in removing the particulates embedded in the PUF collection surface.

The inability to remove embedded particles from the PUF collection surface in a dry fashion necessitated the adoption of a wet removal method. This method involved placing the PUF into a vial with Milli-Q water and manually shaking the vial. The vial was also placed onto a vortex genie to dislodge more of the particles from the PUF. The PUF was rinsed 3-5 times or until totally clean, on the final rinse the PUF was sonicated in the milli-Q water for 15 minutes to dislodge any remaining particles. After each rinse the water was placed into a single jar. After rinsing the PUF, the liquid in the jar was quickly frozen. This was accomplished by placing dry ice into a bowl of acetone, this cooling bath will freeze the water with the particles in suspension when placed in the bath for 5-10 minutes, depending on the volume of liquid in the jar.

To isolate the particles, the sample with particles frozen in suspension was placed into the lyophilizer, or freeze dryer. The lyophilizer used was a Labonco Model 7740020, 1 Liter -50 degrees Celsius, 115 volt unit. The frozen sample remained in the lyophilizer for approximately two to three days to remove the ice and leave behind a filtered particulate sample that was samller than a given pre-filter pore size. The sample can then be analyzed. Laboratory analyses include electron paramagnetic resonance, scanning electron microscopy imaging and quantitative elemental analysis, and polycyclic aromatic hydrocarbon (PAH) analysis by PAH extraction, followed by gas chromatography-mass spectrometry (GC-MS).

3.6: Scanning Electron Microscopy Method

SEM images were taken in the LSU Shared Instrumentation Facility with the FEI Quanta 3D FEG FIB/SEM. The Quanta™ 3D DualBeam™ FEG FIB-SEM combines a Focused Ion Beam (FIB) with a high-resolution Field Emission Gun Scanning Electron Microscope (FEG-SEM). This combination provides enhanced 2D and 3D materials characterization and analysis for samples. In SEM use, an electron beam is projected onto a sample and an image is formed

from secondary electrons and back-scattered electrons. For metal analysis of tested samples, the energy dispersive X-ray spectroscopy function was used, SEM-EDS. SEM-EDS can typically analyze a sample to a depth of several microns.

SEM was used to view and analyze particle constituency. SEM-EDS analysis functions by interaction of the sample with the electron beam of the microscope, which ultimately causes the emission of an x-ray that is characteristic of the element in the sample. X-rays can be used to form elemental maps showing the elemental distribution of a specific portion of a sample. The element overlay map provides a tool for visualizing the elemental makeup of a given sample. It provides an elemental percentage based on the uncorrected net intensity of a given element within the sample. The quantification is corrected by normalizing the measured intensity based on the characterisitic X-ray each element emits. This emission occurs because of inner shell electron ejections caused by the electron beam. Therefore both the intensity and the elemental quantification are included later in the results (University of Buffalo).

3.7: Electron Paramagnetic Resonance Method

Filtered particulate matter samples were tested with electron paramagnetic resonance. Each sample was typically tested in a long range scan of 5000 gauss to view all of the sample's paramagnetic species as well as a short range scan of 100 gauss to observe the organic radical. The samples were also tested for their g-factor. The g-factor is a quantity that describes the magnetic moment of the electron. The g-factor can be used to characterize and identify the type of radical present in a sample. Carbon centered radicals have a g-factor close to the free electron value, which is 2.0023. Other compounds may have a value closer to 2.004, like benzosemiquinones which have electron spin density focused on oxygen atoms (Eaton et al. 2010).

Isolated particulate matter samples were placed into Wilmad-LabGlass Suprasil EPR tubes and measured for radical signal. It was found that the particulate sample may be fluffy and clumpy, therefore an EPR tube with a wider opening is preferable, in this case the 5mm wall EPR tube. Also, the shorter tubes were preferable to longer tubes because particles may stick to the sides of the tube via electrostatic charge. The tube length that was easiest to work with was the 100 mm length tube. Electrostatic charge was exacerbated by latex gloves on glassware and the charge was attempted to be removed using an electrostatic reducing ionizing gate. A Haug EN8 LC was the power pack that supplied voltage to the electrostatic reducing ionizing gate.

All electron paramagnetic resonance (EPR) spectra for particulate matter were measured using a Bruker EMX 10/2.7 EPR spectrometer (X-band) equipped with a dual cavity utilizing modulation and microwave frequencies of 100 kHz and 9.516 GHz, respectively. Parameters for radical signal measurement were as follows: 2.05 mW power; modulation amplitude of 4.0 G; scan range of 100 G for organic radical and 5000-6000G for qualitative metal measurement; time constant of 40.96 ms corresponding to a conversion of 163.84 ms; sweep time of 167.77 s; receiver gain 3.56 × 10^4; and three scans. All samples were run at 20 dB attenuation unless otherwise noted. Radical concentrations for particulate matter were calculated by comparing the signal peak area of its first derivative spectra, as calculated from the (ΔHp‑p)^2 multiplied by the relative intensity, to a 2,2-diphenyl-1- picrylhydrazyl (DPPH) standard. The g-factors were determined by the WinEPR program. This method was based on work by Gehling and Dellinger (2013).

EPR spins per gram calculation for free radical concentration measurement:

--[Sample signal peak area of the first derivative spectra (spins) - y-intercept from the standard calibration curve] x (1/slope from standard calibration curve (spins/ug)) x (1g/ 1000 ug) x (1/molar mass of DPPH (g/mol)) x (6.02 x10^23 spins/mol) = uncalibrated spins

--Uncalibrated spins x (receiver gain of sample/ receiver gain of DPPH) x (√ number of scans per sample/ √ number of scans of DPPH) = calibrated spins in sample

--Calibrated spins in sample (spins/ grams of sample measures = spins/gram (spins per gram) (Wertz and Bolton 1986).

In electron paramagnetic resonance spectroscopy, the interaction of an unpaired electron with the magnetic field produces an energy difference, this effect is called the Zeeman effect, which is what is measured in EPR spectroscopy. An electron has only two allowed energy states, it can interact with the magnetic field and be aligned with it or against it. The electron is said to have a lower energy when the magnetic moment is aligned with the magnetic field and a higher energy when the magnetic moment is against the magnetic field. The two states are designated by the electron's spin number. The electron interaction's with the magnetic field causes two energy states. The difference in the two energy states is what is measured by the spectrometer. This is determined by how much energy the spins absorb from the magnetic field to account for the energy differential between the two states. This absorption is called resonance. In EPR the electromagnetic frequency is held constant while the magnetic field is scanned (Eaton 2010).

3.8: PAH Analysis Extraction Method

To extract polycyclic aromatic hydrocarbons a method was used which was developed in the LSU Department of Environmental Sciences as their standard operating procedure. This method is in line with EPA Method 3500C for organic extraction and sample preparation (US

EPA 2007). Samples were extracted with dichloromethane as a solvent using a Buchi E-916 speed extractor. Samples were placed into tubes in the speed extractor with the following method, extraction tube is filled with:

1. One teaspoon of sand
2. One tablespoon of sodium sulfate (NA2SO4)
3. Sample to be extracted
4. 10 grams of sand
5. Two microliters of internal standard (chloronaphthalene)
6. One half teaspoon of sodium sulfate
7. Capped with a cover filter

Tubes are placed into the extractor for a forty minute run. After the pressurized solvent extraction is complete, the liquid samples are placed in the speed evaporator to reduce sample volume to approximately one milliliter. The evaporator is a vacuum controlled Buchi Syncore evaporator. After the solvent and sample are reduced, they are placed into injection vials and capped.

EPA's method 3500C, specifically method part 3545, recommends pressurized fluid extraction (PFE) for solid, semi-volatile and non-volatile organics. The EPA method, similar to this research method, utilized an extraction cell for PFE with anhydrous sodium sulfate. EPA's method recommends extraction using a solvent compatible with further analysis, in this case dichloromethane was used (US EPA 2007).

3.9: Gas Chromatography Mass Spectrometry Method

The samples from the PAH extraction were then tested with gas chromatography mass spectrometry to obtain their composition. One microliter of sample was injected into a gas

chromatograph and the spectral peaks were used to identify constituents of the samples. The gas chromatograph used was an Agilent Technologies 7890A GC system paired with a 5975C inert XL MSD in the LSU Department of Environmental Sciences.

The Agilent Technologies gas chromatograph interfaced to a mass spectrometer with a 70 eV electron impact ionization source. The system also includes a computer to control the instrumentation and auto-sampler for consistent injection of samples into the instrument system. The column used was a capillary GC column, low bleed, fused silica, 5% diphenyl/95% dimethyl polysiloxane, 30 meters long, 0.25 inner diameter and 0.25 micron film thickness.

In GC-MS, a sample and its compounds are injected and heated, causing them to volatilize, the compounds will separate through the column as they are heated and carried by inert gas. The compounds that are more volatile will pass through the column and elute first, before the less volatile compounds. After passing through the column, compounds travel to the mass spectrometer. When in the mass spectrometer they are first ionized. After being ionized, the ions go to the mass analyzer and subsequently the mass detector. Based upon the mass of the ions analyzed, ultimately a mass spectrum is created to identify what compounds are present in a sample.

The concentrations of target PAHs are determined by response factors that are calculated from commercially available internal calibration standards. The internal standards used in all analyses are naphthalene-d8, acenaphthalene-d10, chrysene-d12, and perylene-d12. The calibration standards are prepared at five different concentrations (5-point calibration curve). The calibration curve is used to generate response factors that are used to calculate the individual analyte concentrations on the sample.

In this thesis research, compounds were injected and run in scan mode as well as selective ion monitoring (SIM) mode. Scan mode will find a wider variety of organics, yet SIM mode will allow the detection of specific compounds the detector is calibrated to find based on molecular weights of specific ions.

4. RESULTS

4.1: Sampler and Collection Results

The original goal of this research, producing a sampler that would simultaneously collect and filter a size resolved PM sample for laboratory analysis, was not successful. Pre-filters became too easily clogged and required too many changes. Also, using small diameter membrane filtration system for a small particle size like fine PM may not be feasible compared to other methods such as cyclonic exclusion and electrostatic precipitation. Although the original aim of the research was unsuccessful, the research was successful in producing a method for a cost effective and simple collection of bulk sample PM from homes that can be filtered using membrane technology. This method can be used to study various PM sizes from homes in analyzing pollutant-particle systems associated with the PM . This project was successful in collecting bulk settled particulate and dust from undisturbed areas like attics, and bulk dusts from filters and vacuum cleaners. These bulk samples were then re-suspended and filtered with varying degrees of success based on materials and methods used.

The most simple and effective method for collection of a bulk sample was the use of a hand held vacuum. The model used was a Dirt Devil™ Gator 9.6 volt hand held vacuum. This vacuum's collection surfaces could easily be cleaned in between sample collections and a new filter installed. The most successful filtration apparatus design was design C, that is described above in the materials and methods. This apparatus was most successful with a nylon net filter from Millipore, either the 11 micron pore size or the 20 micron pore size. These nylon filters were more durable and therefore more effective than 8 micron nitrocellulose filters or 2.7 micron glass microfiber filters. Also, this slightly larger pore size allowed the passage of a range of particles including coarse, fine, and ultrafine. This was ascertained from sample viewing with

scanning electron microscopy and will be discussed in more depth later in this thesis. Fine and ultrafine particles were often agglomerated in these samples and it was impossible to tell from this research at what point the particles became agglomerated: in suspension, deposition, collection, extraction or freeze drying. It is also possible that agglomerated particles became unbound from one another at some point in the collection, re-suspension or filtration process.

The various flow rate efficiencies of the filtration apparatuses were measured with the previously mentioned anemometer. A higher flow rate is desired for the filtration because penetration through filters increases when the flow velocity increases (Mouret et al. 2009). Table 4.1 shows the flow rate results for various filtration apparatus setups

Table 4.1: Various apparatus and pre-filter setups with corresponding flow rate.

Apparatus	Pre-Filter	Opening Radius (inches)	Opening Diameter (inches)	Flow rate (FPM)	Flow rate (m/s)	Flow rate (L/min)	Flow rate (CFM)	flow rate as a % of max flow
none	none	0.625	1.25	6400	32.5	1543.8	54.52	100%
B	40 micron mesh cartridge	0.25	0.5	860	4.37	33	1.17	2.15%
C	8 micron nitrocellulose	0.625	1.25	355	1.803	85.8	3.02	5.50%
C	2.7 micron glass microfiber	0.625	1.25	500	2.54	120.6	4.26	7.80%
C	20 micron nylon net	0.625	1.25	1460	7.4168	352.2	12.44	22.80%
C	11 micron nylon net	0.625	1.25	1200	6.096	289.8	10.23	18.80%

The rates in Table 4.1 were calculated by multiplying measured air velocity in meters per second by the radius of a circular duct to determine the air volume flowing past a point in the duct for a given unit of time. In Table 4.1 meters per second is transferred to liters per minute and cubic feet per minute. Meters per second is directly transferrable to linear feet per minute.

One linear foot per minute is 0.00508 meters per second. Finally, the flow rates for each apparatus are expressed as a percentage of unencumbered flow rate.

These data show that the nylon net filters allow the best flow rate at 22.8% of maximum flow rate for 20 micron pore size and 18.8 percent of maximum flow rate for 11 micron pore size. Apparatus B has a larger pore size which should allow for a larger volume of filtered air, but a much smaller radius which inhibits flow rate significantly. From this data it is apparent that the higher flow rates found using apparatus C and the nylon net filters will allow for greater success in obtaining a filtered sample sample due to higher flow rate.

Apparatus A was not tested for flow rate because its design was not tenable for effective particle filtration. The design of apparatus A caused cutting and tearing of the filter around the apparatus edges that allowed larger particulate through the pre-filter onto the collection surface. Below in Figure 4.2 all of the sample filtrations can be seen, along with collection location and collection source, date and the amount the filtration yielded in milligrams. Some of these collections were *in situ* and some were in the lab. For more complete sample data refer to appendix.

Table 4.2: The progression of sample times, filtration apparatuses used, filter types and amounts of filtered particulate yielded.

Sample Number	Source	Collection Time	Apparatus	Re-suspension	Pre-filter	Sample Yield (mg)
1	Attic	20 mins	A	None	8 micron	0.0
2	Porch	6 mins	A	None	8 micron	0.0
3	Attic	10 mins	A	None	8 micron	0.0
4	Attic	10 mins	A	Brush	8 micron	0.0
5	Porch	5 mins	B	Brush	40 micron	1.1
6	AC window filter	15 mins	B	Brush	40 micron	2.7
7	Home Surfaces	21 mins	B	Jar agitation	40 micron	8.1
8	Home interior	27 mins	A	Jar agitation	8 micron	17.0
9	Home interior	30 mins	A	Jar agitation	2.7 micron	8.0
10	Attic	30 mins	A	Jar agitation	2.7 micron	0.0
11	Home interior	36 mins	C	Jar agitation	8 micron	1.3
12	Home interior	40 mins	C	Jar agitation	2.7 Micron	0.0
13	Home interior	24 mins	B	Jar agitation	40 Micron	23.5
14	Home interior	30 mins	C	Jar agitation-with vortex	20 micron	6.0
15	Home interior	30 mins	C	Jar agitation-with vortex	11 micron	1.4
17	Home interior	35 mins	C	Jar agitation-with vortex	20 micron	3.9
18	Attic	40 mins	C	Jar agitation-with vortex	11 micron	9.0
19	Attic	40 mins	C	Jar agitation-with vortex	20 micron	16.5
21	Attic	40 mins	C	Jar agitation-with vortex	20 micron	13.8
22	Porch	40 mins	C	Jar agitation-with vortex	20 micron	6.0
24	Attic	40 mins	C	Jar agitation-with vortex	20 micron	1.5
25	Attic	40 mins	C	Jar agitation-with vortex	20 micron	13.2
26	Attic	40 mins	B	Jar agitation-with vortex	40 micron	143.1
27	Attic	40 mins	C	Jar agitation-with vortex	11 Micron	49.0
28	Attic	25 mins	B	Jar agitation-with vortex	40 Micron	175.6

From Table 4.2 it can be seen that success of obtaining a testable filtered sample varied. Sometimes sample yield was low due to unforeseen events in the process. For example, sample 24 only yielded 1.5 mg of particulate. This was due to the vacuum in the freeze dryer being released too rapidly, resulting in a rapid displacement of particles inside the jar. This displacement caused the filtered particles to disperse and stick to the sides of the jar containing them. Recovering the particles was impossible, as they adhere to surfaces very effectively and were highly diffused across the entire surface of the interior of the jar. Also, some bulk samples are "richer" than others as previously mentioned. The bulk sample that produced filtrations 27 and 28 was very rich; when shaken it produced a fine dust that rose and dispersed into the air like smoke.

Bulk samples generally had more small particles and higher "richness" when they were collected using a vacuum cleaner as opposed to collected with a brush and dustpan. The greater richness of the sample generally resulted in higher sample weights. Samples 24-28 were collected using the Dirt Devil™ hand-held vacuum.

Table 4.2 demonstrates the progression of longer filtration times to obtain more sample. Generally it was found that the longer the sample time, the more effective the filtration apparatus was at attaining a sample for laboratory testing. Eventually it was determined that a forty minute filtration time was sufficient. For a total sub-sample time of forty minutes, this was broken into twenty 2-minute sampling times. After 2 minutes the vacuum was stopped and the filter was brushed off with a clean paint brush. A 2 minute sampling period was completed 4 times before the filter was changed. This means that 5 filters would be used for twenty 2-minute runs, for a total filtration time of forty minutes.

The nozzle of the filtration apparatus was generally held 2-3 inches above the mouth of the jar. If the filtration apparatus nozzle was too close, the filter would pick up the heavier, larger particles and clog quickly. The space of 2-3 inches ensured a steady and even filtration process.

To summarize the collection process and method that functions to produce a filtered PM sample for laboratory analysis, Graphic 4.1 is a flow chart of the process.

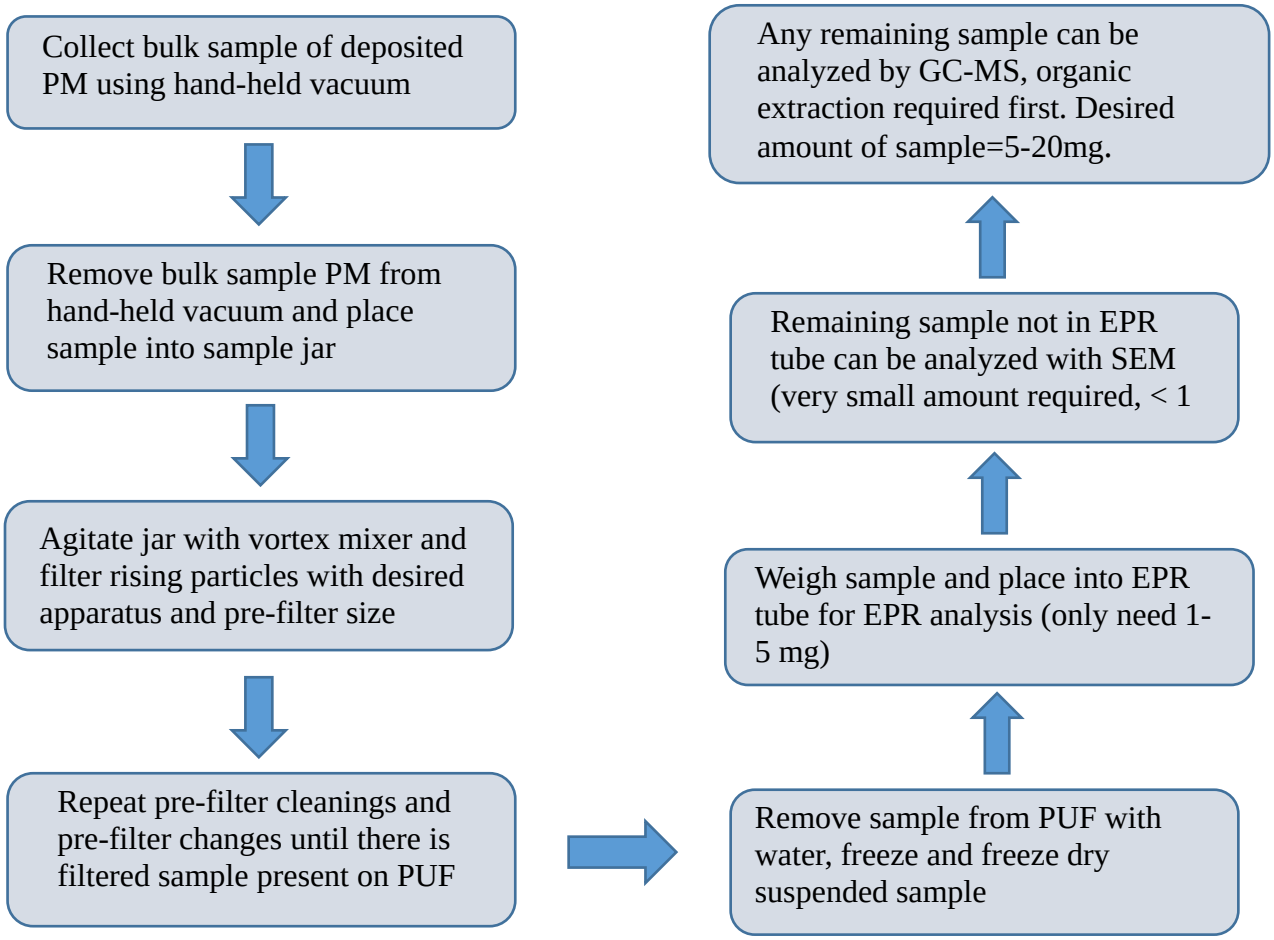

Graphic 4.1: Flow chart showing the recommendations for collection, filtering and analysis of PM from surfaces.

4.2: Scanning Electron Microscopy Imaging Results

Scanning electron microscopy was conducted on sample numbers 7, 11, 14, 15, 17, 22, 24, 27 and 28, with images were obtained only for samples 7, 11, 14, 15, 17, 22, and 24. This sample set was chosen to provide a diverse range of different pre-filters which would provide a good representative sample of particle sizes. Reference the map on page 35 and appendix 5 for sampling location numbers that reference the physical location.

Sample 7:

Sample 7 was collected with the B apparatus which utilizes a built in 40 micron pre-filter. The sample was taken from the replaceable foam filter of a home vacuum cleaner. The foam filter was a Eureka brand replaceable filter for a Eureka Envirovac 3041 BZ.

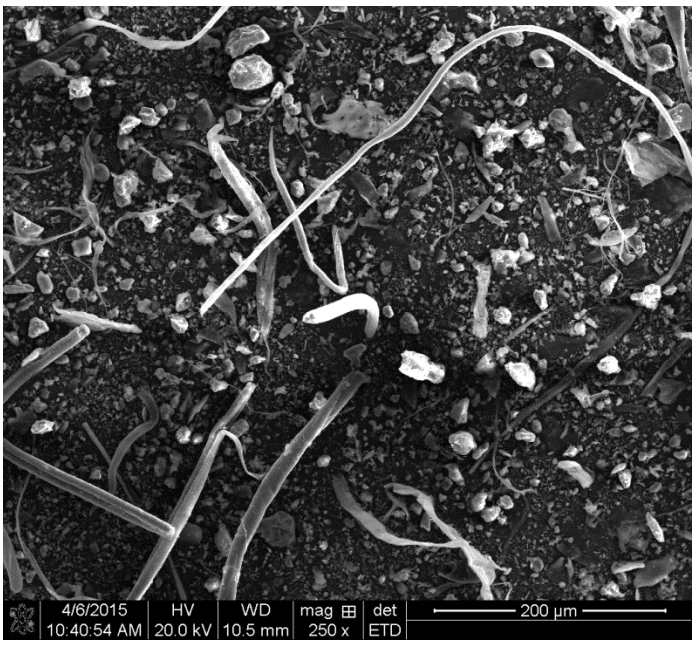

Figure 4.1: 250x magnification showing a sub 40 micron PM sample of PM which includes some fibrous material.

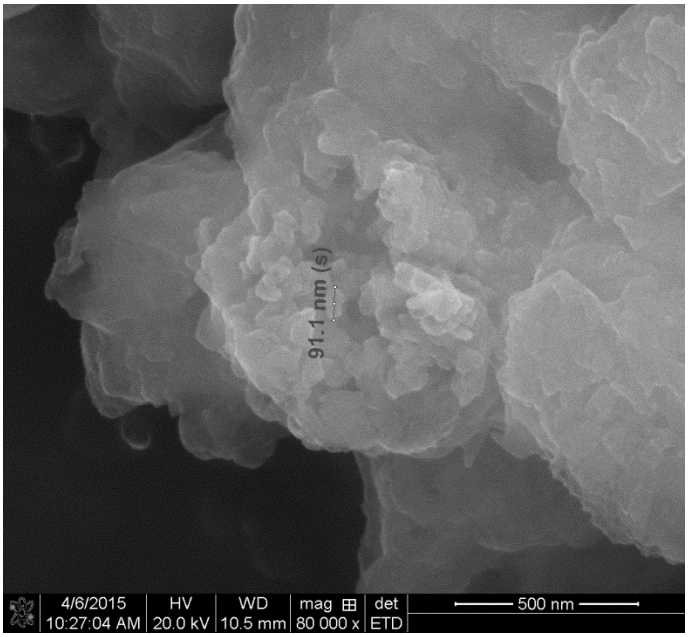

Figure 4.2: 80,000x magnification image of sub 40 micron PM sample showing nano-scale particles.

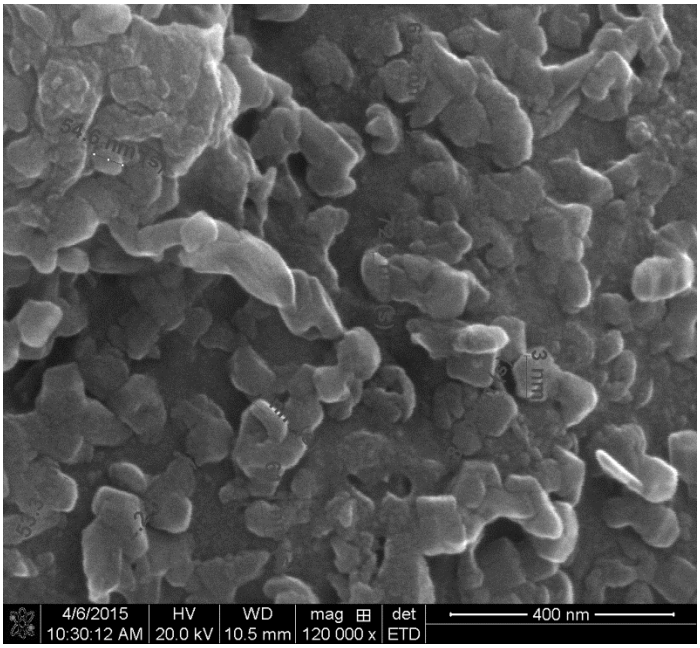

Figure 4.3: 120,000x magnification image of sub 40 micron PM sample showing nano-scale particles many of which are less than 100 nanometers and are therefore ultrafine.

Low magnification of sample 7 in Figure 4.1 shows a heterogeneous mix of fibrous particles. While higher magnification at 80,000x in figure 4.2 shows an agglomeration of particles in the sub-micron range with one of the particles in the agglomerate measuring 91

nanometers. At even higher magnification at 120,000x, Figure 4.3 also shows many ultrafine particles most of which are in the 50-70nm range. This shows that agglomerates of ultrafine particulates agglomerate in more coarse dust but can be seen with SEM.

Sample 11:

Sample 11 was also viewed with SEM. Sample 11 was sample taken from filtration where an 8 micron nitrocellulose pre-filter was used, therefore all particles that are not merely agglomerates should be 8 micron or smaller. Filtration apparatus C was used in this sample. Sample 11 was taken from the vacuum canister of the home vacuum of sampling location 1, from the same Eureka Envirovac 3041 BZ mentioned above.

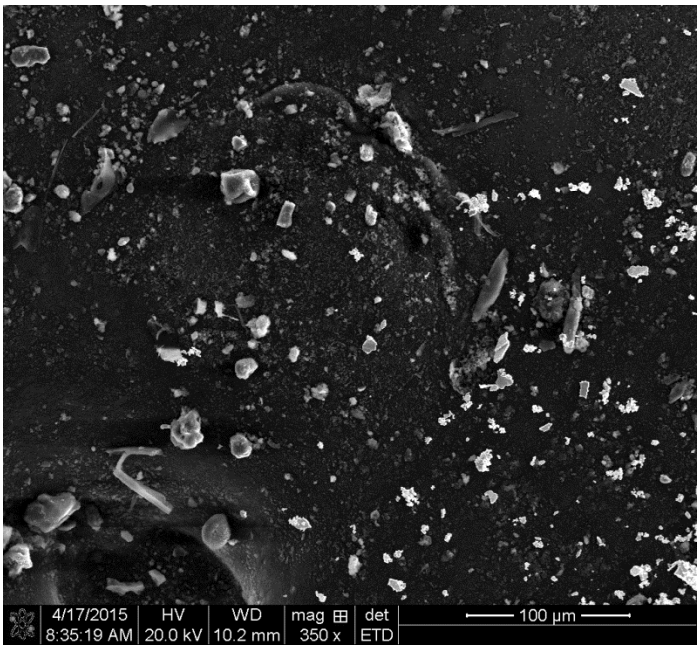

Figure 4.4: 350x magnification of sub 8 micron PM sample showing a diverse range of particle sizes.

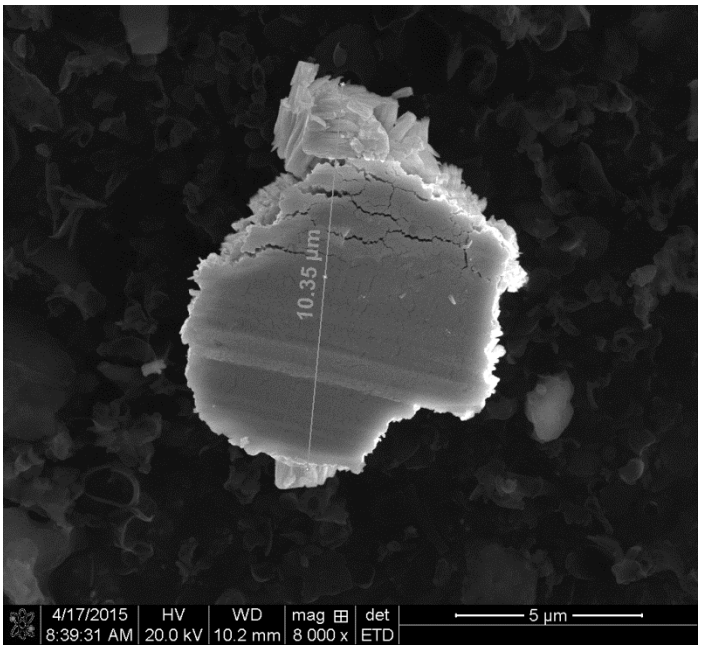

Figure 4.5: 8000x magnification image of sub 8 micron PM. This image shows a particle which by at least one dimension is larger than 8 micron.

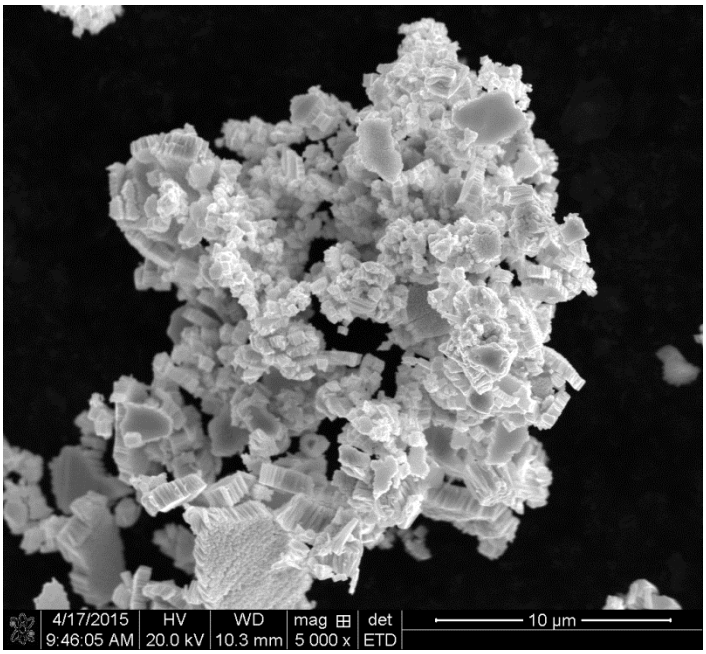

Figure 4.6: 5000x magnification image of sub 8 micron PM sample. This image shows an agglomeration of inhalable particles (less than 10 micron diameter).

Figure 4.4 at 350x magnification clearly shows many particles above 8 micron. Some of these may be agglomerates, however the image shows brightly contrasted larger particles against the background of darker, smaller particles. Some particles larger than 8 micron went through the

filtration system; Figure 4.5 shows a particle which is over ten microns. Figure 4.6 shows a collection of particles that have defined geometry, many of these particles are in the submicron range. However, it is impossible to determine when these particles actually agglomerated. However it may be possible that the 8 micron pre-filter used during this filtration failed in some way. Sample 11 was collected with filtration apparatus C. The 8 micron nitrocellulose filters became brittle when exposed to air.

Sample 14:

Sample 14 was filtered with a 20 micron pre-filter and filtration apparatus C, therefore all particles should be 20 micron or less. Samples 14 and 15 were both taken from a 3.0 HP Shopvac™ in Kenner, LA 70065.

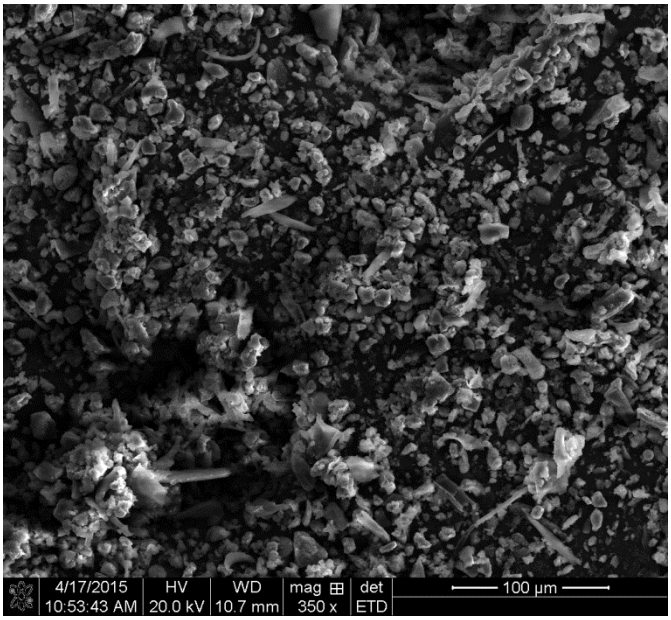

Figure 4.7: 350x magnification of a sub 20 micron PM sample. This image shows a more homogenous particle size distribution.

Figure 4.2.7 of sample 14 shows a more homogeneous distribution of particle size which would indicate that the pre-filter and the filtration apparatus combination used here was more effective. This was the use of filtration apparatus C paired with nylon net filters.

Sample 15:

Sample 15 was collected using an 11 micron nylon net pre-filter. All particles should be 11 micron or less in diameter.

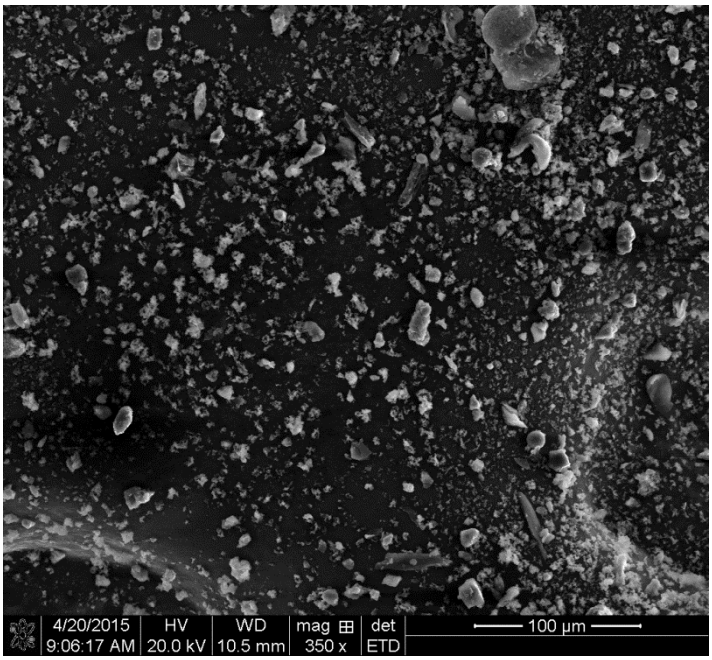

Figure 4.8: 350x magnification of a sub 11 micron sample of PM.

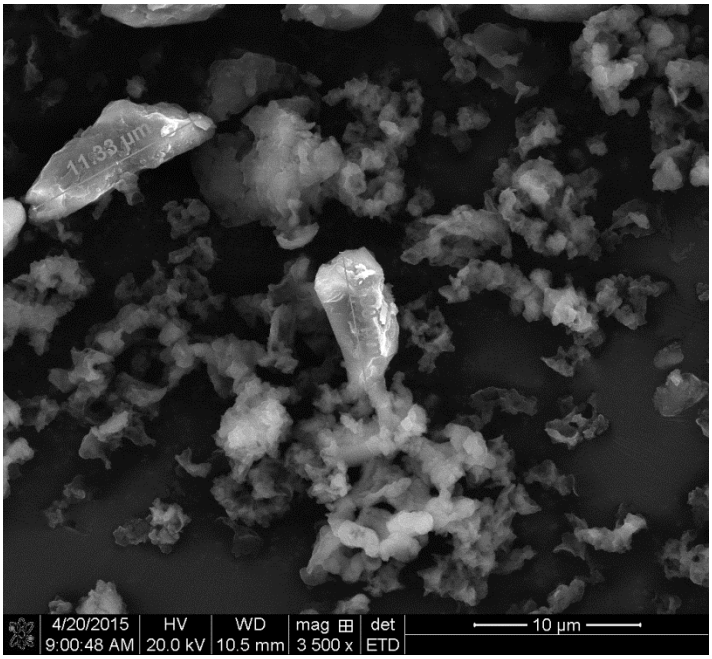

Figure 4.9: 3500x magnification of a sub 11 micron sample of PM. Particles show here appear to be 11 micron or less.

Figure 4.8 shows a fairly homogeneous size distribution of particles while figure 4.9 shows two large, light-colored particlesfrom the sample. These particles measure 11.3 micron and 8.3 micron, which can be seen measured in the image. The shape of the 11.3 micron particle is irregular so it is possible that the smaller end passed through the pore size of the pre-filter and does not indicate a malfunction of the filtration system. There are also smaller particles clearly visible in the background slightly out of focus that appear to be smaller particles, perhaps agglomerated together.

Sample 17:

Sample 17 is a sub 20 micron sample taken from a vacuum cleaner canister. The vacuum was used on various home surfaces at location number 1.

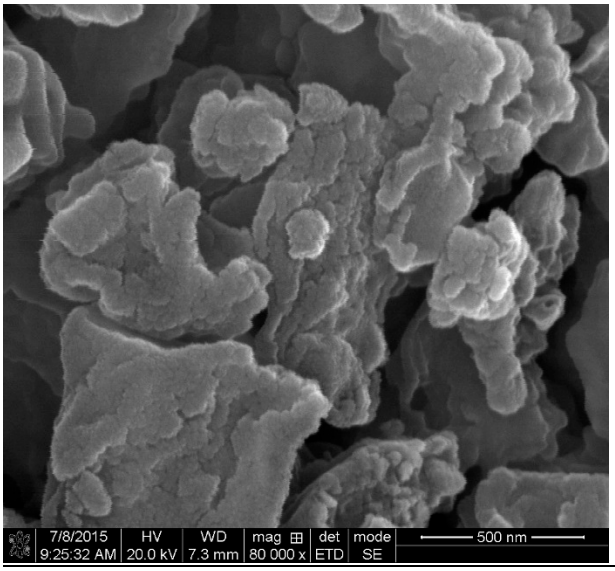

Figure 4.10

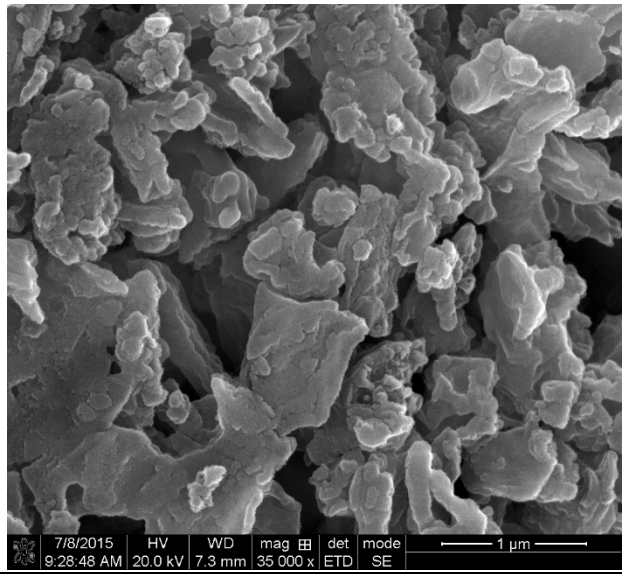

Figure 4.11

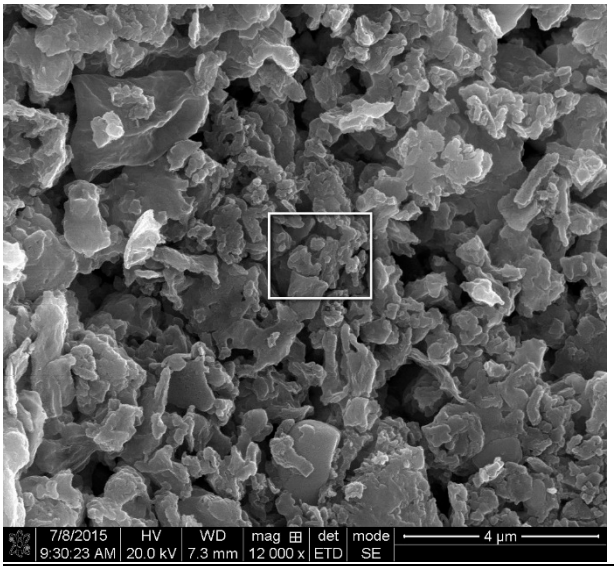

Figure 4.12

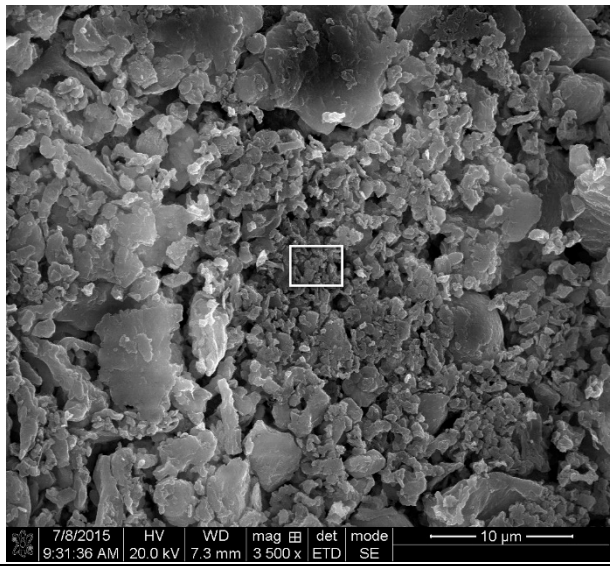

Figure 4.13

Figures 4.10 to 4.13: A range of magnification from 80,000x magnification to 3500x magnification. These figures show progression of a sub 20 micron PM sample with the area of detail highlighted by a box to show relative particle size.

Figures 4.10 to 4.13 are images taken of sample 17 that show a range of magnification. The white box around Figures 4.12 and 4.13 demonstrates the location of the nano-scale particles shown in figure 4.10. It is clear from the scale bars that many of the particles fall into the ultrafine and fine particle category, while others are coarse particles. However, it is also clear that nearly all of the particles shown from sample 17 are smaller than 10 microns and are therefore inhalable.

Sample 22:

Sample 22 is a sub 20 micron particulate sample taken from an outdoor porch at location number 2 in Baton Rouge. Sample 22 images seem to indicate a similar size fraction as sample 17, however, the images are blurry. The lack of clarity in the images may have been due to water adsorbed to particles in the sample.

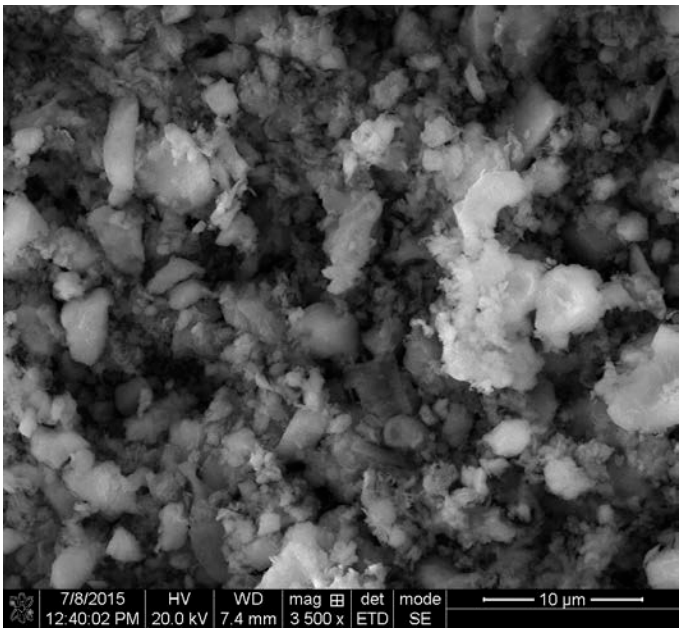

Figure 4.14: 3500x magnification image of a sub 20 micron PM sample of outdoor origin. It is possible that adsorbed water led to lack of clarity in this image.

Figure 4.14 shows many smaller particles forming aggregates, although all particles pictured appear to be less than 10 micron in diameter and are therefore inhalable.

Sample 24:

Sample 24 is a sub 20 micron sample taken from an attic at location number 4 in Baton Rouge.

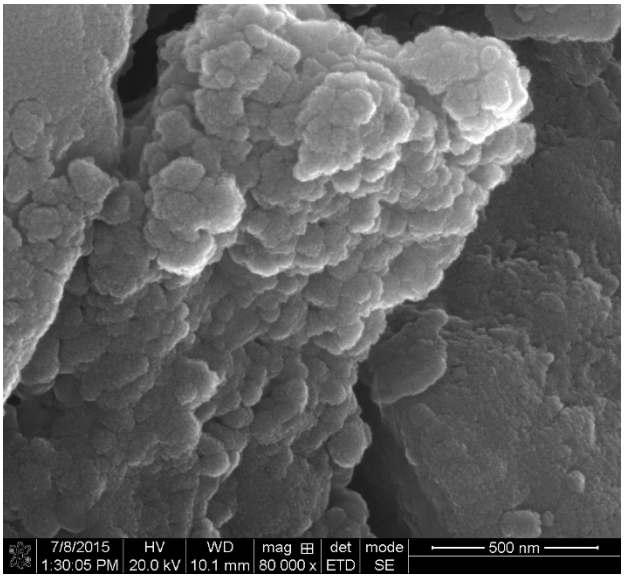

Figure 4.15

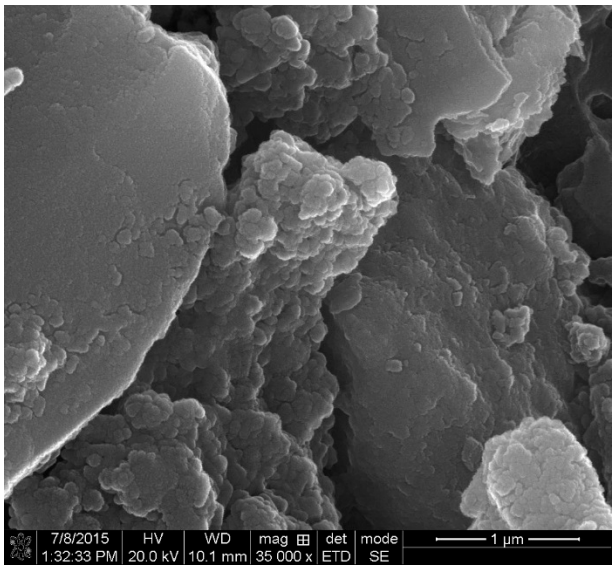

Figure 4.16

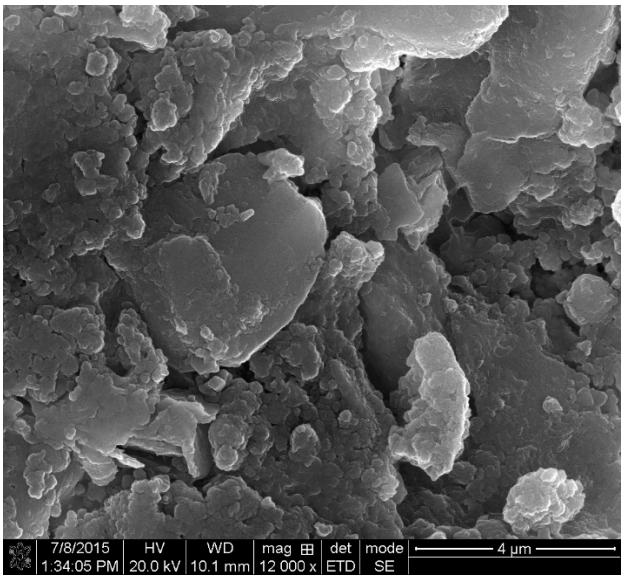

Figure 4.17

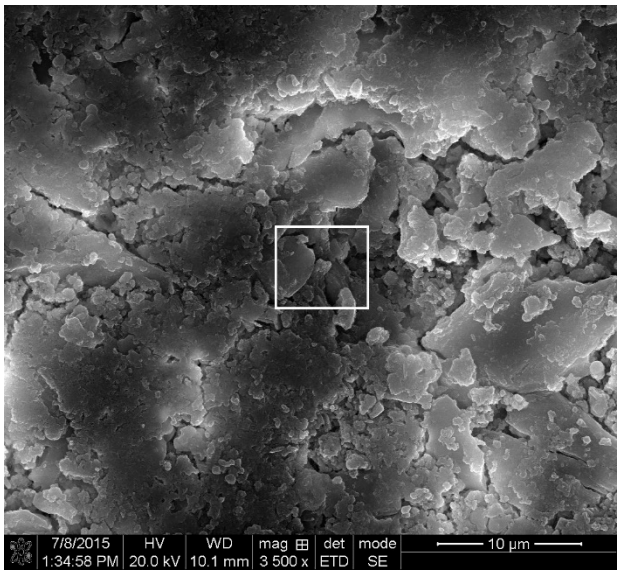

Figure 4.18

Figures 4.15 to 4.18: A progression from 80,000x magnification to 3500x magnification from a sub 20 micron PM sample. A boxed area highlights the original area of detail to show relative particle size.

Figures 4.15 to 4.18 show a progression of lower magnifications. Figure 4.15 would seem to indicate an agglomeration of ultrafine particles. Figure 4.18 shows many of these agglomerates caked together. Figure 4.18 also shows a box which indicates the particles referenced in 4.15. Almost all of the particles in the figures above appear to be inhalable. The particles were certainly inhalable when originally suspended in ambient air before precipitating out of suspension and agglomerating at some point. Even as agglomerates most appear to be smaller than 10 microns in diameter. The evidence of a high quantity of ultrafine particles in attics shows proof that combustion products enter into home spaces.

These results would indicate that all busk dust collected is potentially capable of providing a sample containing ultrafine and fine particles, the best stratification system tested was the use of apparatus C with a nylon net filter. Nylon net filters were also the most durable and provided the best flow rate. The use of the 11 micron nylon net filter is particularly useful because this is very close to the size cutoff for respirable particulate. All particulate matter ten

microns and smaller is inhalable, per the United States EPA (2015). The 11 micron and smaller samples filtered in laboratory are therefore relevant for study.

4.3: Scanning Electron Microscopy, Energy Dispersive X-Ray Spectroscopy Results

Samples described above: 7, 11, 14, 15, 17, 22, 24, 27, and 28 were also analyzed with energy dispersive x-ray spectroscopy (EDS) to ascertain elemental analysis on the samples. Samples 27 and 28 were also analyzed with SEM-EDS. SEM-EDS provides many several useful outputs used in this research: element overlay maps and elemental composition results.

Element overlay maps do not provide accurate quantification, therefore the “smart quant” elemental composition results from the EDS analysis is also provided to more accurately represent the elements in a portion of a given sample.

Sample 7 is a sub 40 micron sample from a vacuum canister taken from location number 1 in Baton Rouge. An EDS scan at 1000x magnification gives an element overlay map seen below.

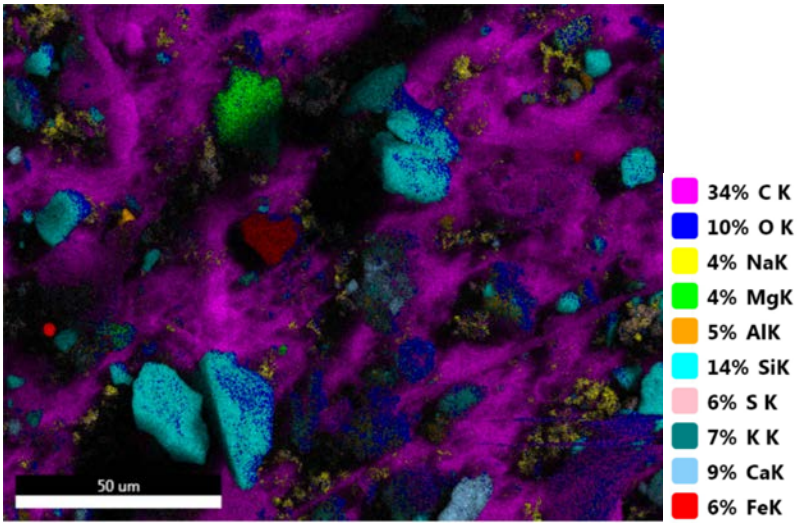

Figure 4.19: Element overlay map from a sub 40 micron PM sample at 1000x magnification.

Figure 4.19 shows an elemental makeup that is mostly carbon, but that also contains significant amounts of iron, calcium, silicon, oxygen and potassium. All of the listed elements are common crustal elements which are common in coarse particulate matter (Vallero 2014).

Table 4.3: Elemental composition results for sample 7

Element	Weight %	Atomic %	Net Int.	Error %
.C K	64.21	72.65	5,143.26	6.39
O K	28.03	23.80	1,655.25	9.78
NaK	0.76	0.45	170.73	9.00
MgK	0.10	0.06	40.28	12.63
AlK	0.64	0.32	319.04	5.03
SiK	4.07	1.97	2,293.08	2.80
P K	0.02	0.01	10.44	57.03
S K	0.32	0.13	159.00	3.82
ClK	0.06	0.02	28.19	16.49
K K	0.26	0.09	105.30	6.60
CaK	1.22	0.41	416.28	3.68
TiK	0.09	0.03	27.34	15.46
FeK	0.21	0.05	36.97	12.94

It is apparent from the weight percentage and the atomic percentage given by the elemental composition results in Table 4.3 that there is some difference between elemental constituency as indicated by the two methods. This is because the elemental overlay map is a representation of uncorrected net intensity from the analyzed elements.

Sample 11 is a sub 8 micron sample from a vacuum canister taken from sample location 1 in Baton Rouge. An EDS scan at 1000x magnification provides an overlay map:

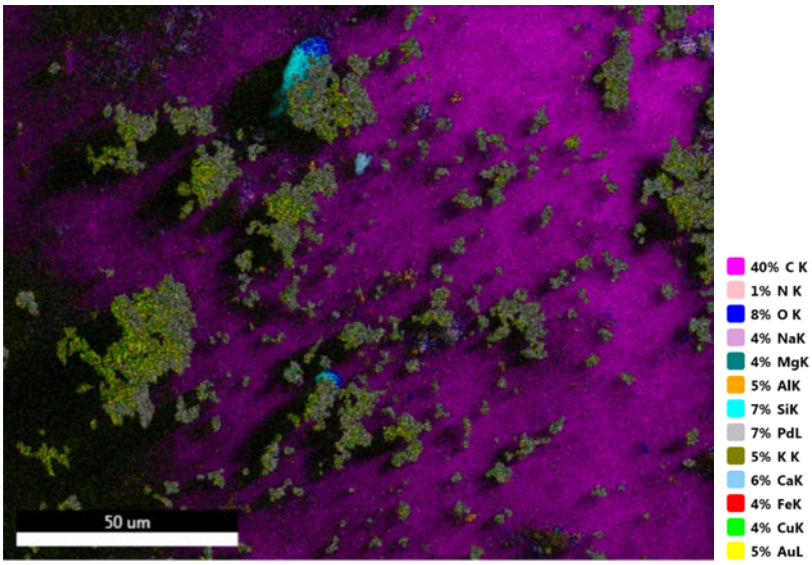

Figure 4.20: Element overlay map from sample 11, a sub 8 micron PM sample at 1000x magnification.

Figure 4.20 above shows a mostly carbon background that is highlighted by some gold particles. These are most likely gold from the gold and palladium plating that is required to view the particles with the scanning electron microscope, but it is possible that the gold came from the sample itself. There is also a blue and teal particle that appears to be made of silicon and oxygen. This could potentially be a clay particle.

Table 4.4: Elemental composition results from sample 11.

Element	Weight %	Atomic %	Net Int.	Error %
C K	69.17	75.52	5,645.07	4.69
O K	28.39	23.27	1,252.34	9.81
NaK	1.02	0.58	172.12	8.79
AlK	0.13	0.06	47.06	11.27
SiK	1.01	0.47	430.83	3.25
CaK	0.28	0.09	73.14	11.08

Sample 14 is a sub 20 micron sample from a vacuum canister in Kenner, Louisiana. An EDS scan at 1000x magnification provides an elemental overlay map:

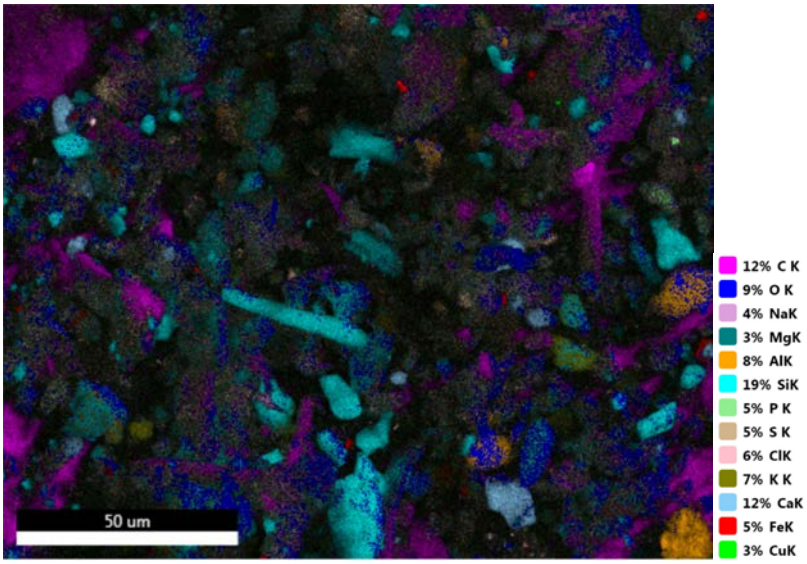

Figure 4.21: Element overlay map from sample 14, sub 20 micron PM sample viewed at 1000x magnification.

Figure 4.21 shows a more evenly balanced elemental composition than overlay maps from samples 7 and 11. There is a high amount of silicon compared to other similarly sized samples. There are also high proportions of calcium and carbon.

Table 4.5: Elemental composition results from sample 14

Element	Weight %	Atomic %	Net Int.	Error %
C K	42.50	54.87	1,338.23	8.41
O K	35.14	34.06	1,555.16	9.55
NaK	2.33	1.57	313.61	8.18
MgK	0.22	0.14	52.25	11.00
AlK	2.50	1.44	752.51	4.74
SiK	7.12	3.93	2,413.79	3.44
P K	0.75	0.37	208.87	4.44
S K	0.70	0.34	212.88	4.91
ClK	1.11	0.49	318.01	3.08
K K	1.37	0.54	344.93	3.07

Element	Weight %	Atomic %	Net Int.	Error %
CaK	4.61	1.78	980.96	1.93
TiK	0.36	0.12	64.73	10.33
FeK	1.00	0.28	106.41	6.76
CuK	0.29	0.07	20.02	27.31

Sample 14 shows the presence of metals like titanium and copper. However, the error percentage for copper and titanium is high, so the presence of copper cannot be determined with certainty.

Sample 15 is a sub 11 micron sample from a vacuum canister in Kenner, LA 70065. An EDS scan at 2000x magnification provides an elemental overlay map:

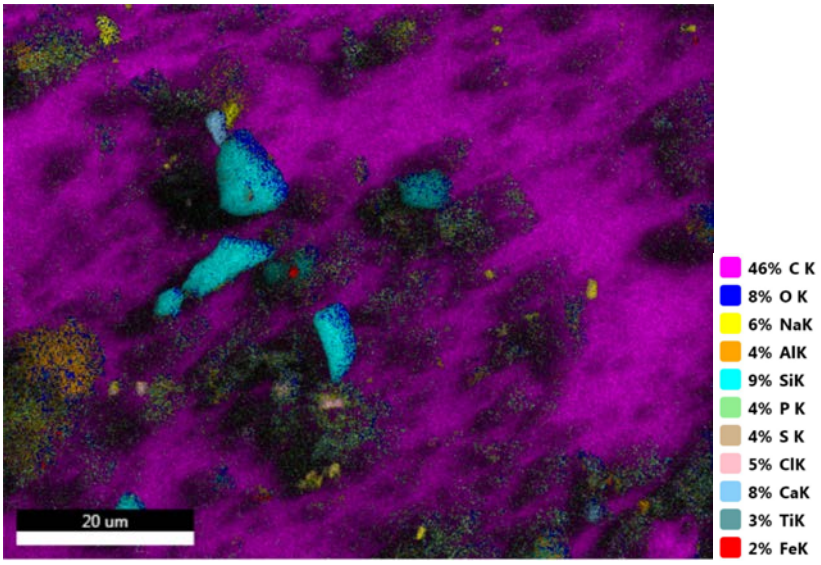

Figure 4.22: Element overlap map from sample 15, a sub 11 micron PM sample viewed at 2000x magnification.

Figure 4.22 is a heavily carbon based element composition. There are sizable chucks of silicon and oxygen near the center of the image. These could be clay soil particles as silicon and oxygen tetrahedrons are key components of clay minerals. It would also seem that aluminum and oxygen octahedrons may be present because of the presence of aluminum and the abundance of oxygen. There are also small quantities of sodium and phosphorous present.

Table 4.6: Element composition results from sample 15.

Element	Weight %	Atomic %	Net Int.	Error %
C K	71.59	79.75	7,758.57	5.86
O K	19.70	16.48	1,303.02	9.91
FeL	1.60	0.38	72.20	8.43
NaK	2.25	1.31	641.67	7.17
MgK	0.35	0.19	172.46	7.03
AlK	0.50	0.25	300.81	4.84
S K	0.27	0.11	172.73	3.02
ClK	0.45	0.17	259.16	2.40
CaK	1.34	0.45	565.36	2.53

It appears that the majority of sample 15 that is displayed by Figure 4.22 and Table 4.6 is background carbon. However, there are clearly silicon and oxygen particles as well as sodium, phosphorous, and iron.

Sample 17: a sub 20 micron sample from a vacuum canister at location 1 in Baton Rouge. An EDS scan at 2000x magnification provides an elemental overlay map:

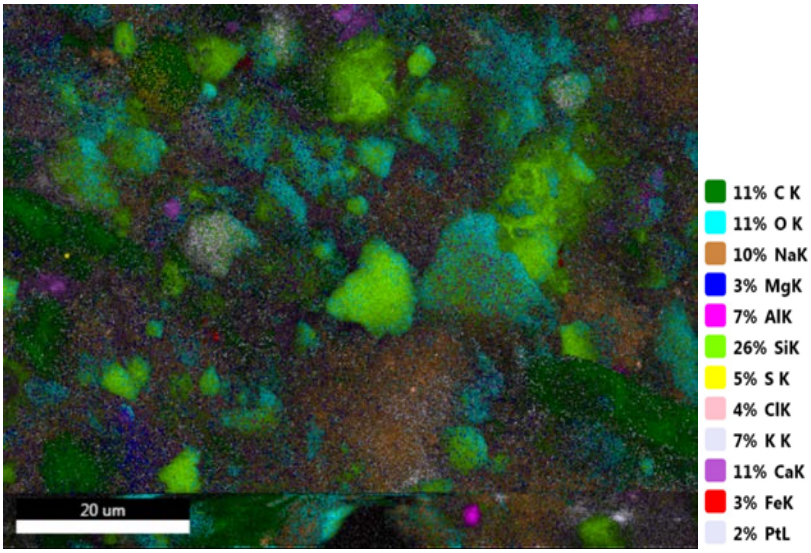

Figure 4.23: Element overlap map from sample 17, a sub 20 micron PM sample, viewed at 2000x magnification.

Sillicon and oxygen are both present in large chunks that appear to be correlated due to the color coding, and this may represent clay particles.

Table 4.7: Element composition results from sample 17.

Element	Weight %	Atomic %	Net Int.	Error %
C K	27.13	38.90	1,680.95	8.94
N K	5.72	7.04	197.47	11.40
O K	31.79	34.22	3,695.98	9.30
F K	2.19	1.99	288.96	21.51
NaK	6.96	5.22	2,279.69	7.38
MgK	0.74	0.52	394.97	7.34
AlK	3.05	1.95	2,048.58	5.00
SiK	10.04	6.16	7,666.24	3.82
PtM	4.00	0.35	1,150.73	5.67
S K	1.22	0.66	813.39	4.05
ClK	0.69	0.34	434.15	5.07
K K	1.66	0.73	934.16	2.96
CaK	3.65	1.57	1,776.47	2.21
FeK	1.15	0.35	275.25	4.31

The elemental composition results in table 4.7 indicate the presence of platinum, most likely from the sputter coating used to prepare the sample for SEM analysis. Platinum (or in other cases gold/palladium) coating reduces charging of the sample and improves secondary electron signal so that the sample can be better viewed by spectroscopy.

Sample 22: a sub 20 micron sample from an outdoor porch at location 2, Baton Rouge. An EDS scan at 2000x magnification provides an elemental overlay map:

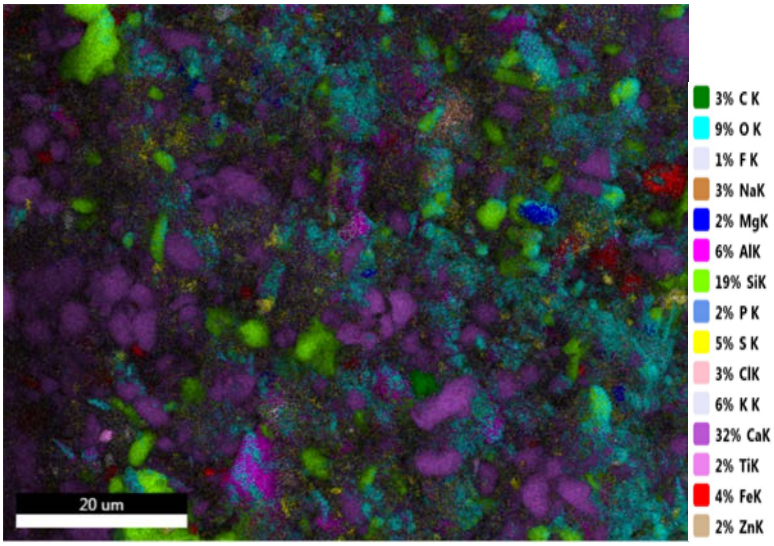

Figure 4.24: Element overlap map from sample 22, a sub 20 micron PM sample, viewed at 2000x magnification.

Many particles in sample 23 appear to be fine particulates, and many are coarse. Calcium, silicon, oxygen and carbon appear in high proportions.

Table 4.8: Element composition results from sample 22.

Element	Weight %	Atomic %	Net Int.	Error %
C K	12.58	20.54	422.36	9.22
O K	43.68	53.56	2,652.83	9.41
F K	1.91	1.97	111.92	14.78
NaK	1.43	1.22	214.72	9.42
MgK	0.67	0.54	188.46	8.10
AlK	3.02	2.20	1,085.43	5.36
SiK	9.93	6.93	4,109.57	4.06
P K	0.50	0.32	170.80	7.49
S K	1.53	0.94	584.15	4.00
ClK	0.69	0.38	249.69	4.68
CaK	19.40	9.50	5,317.91	1.72
TiK	0.28	0.12	62.54	12.54
FeK	2.18	0.76	290.76	4.01
ZnK	0.39	0.12	28.18	20.88

Sample 24: a sub 20 micron sample from an attic at location 4 in Baton Rouge. An EDS scan at 2000x magnification provides an elemental overlap map:

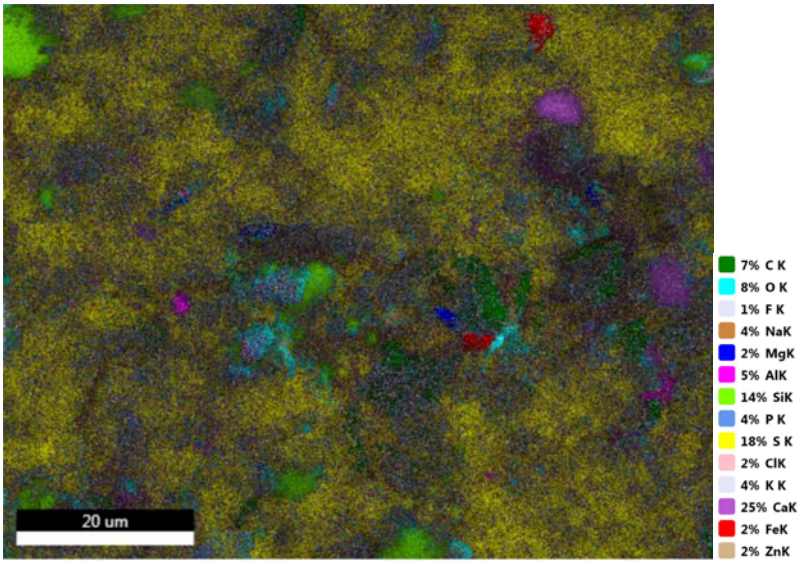

Figure 4.25: Elemental overlap map from sample 24, a sub 20 micron PM sample, viewed at 2000x magnification.

Figure 4.25 shows a heavy presence of sulfur throughout the sample. The high levels of sulfur, calcium and oxygen may indicate the presence of CaSO4, or gypsum. However, one might expect gypsum to exist in the coarse size fraction, while most of the sulfur particles in figure 4.25 appear to be smaller than coarse PM. Sulfates are the second most major constituent of ambient fine PM, and most of these sulfates come from power generation or industrial facilities (US EPA 2004). It is possible that the sulfur viewed here which makes up approximately 6.5% of the sample on a weight basis, comes from industrial processes. Iron is seen in this sample.

Table 4.9: Element composition results from sample 24.

Element	Weight %	Atomic %	Net Int.	Error %
C K	25.00	36.93	1,058.36	8.93
N K	6.24	7.90	122.40	11.56
O K	34.09	37.80	2,168.29	9.65

Element	Weight %	Atomic %	Net Int.	Error %
F K	2.06	1.92	155.24	17.37
NaK	0.93	0.72	181.97	9.13
MgK	0.50	0.37	180.02	8.19
AlK	1.44	0.95	652.65	5.29
SiK	5.23	3.31	2,750.04	3.68
S K	6.45	3.57	3,052.57	2.83
ClK	0.19	0.09	79.10	11.61
K K	1.17	0.53	454.54	3.67
CaK	11.96	5.29	3,899.33	1.89
FeK	0.30	0.09	49.34	12.43
ZnK	0.67	0.18	62.19	12.97
PtL	3.78	0.34	110.77	10.43

Sample 27:

Samples 17, 22 and 24 had better particulate coverage over the carbon tape. This led to higher percentage of other elements in the EDS scans and lower percentages of background carbon. Carbon value is therefore indeterminable.

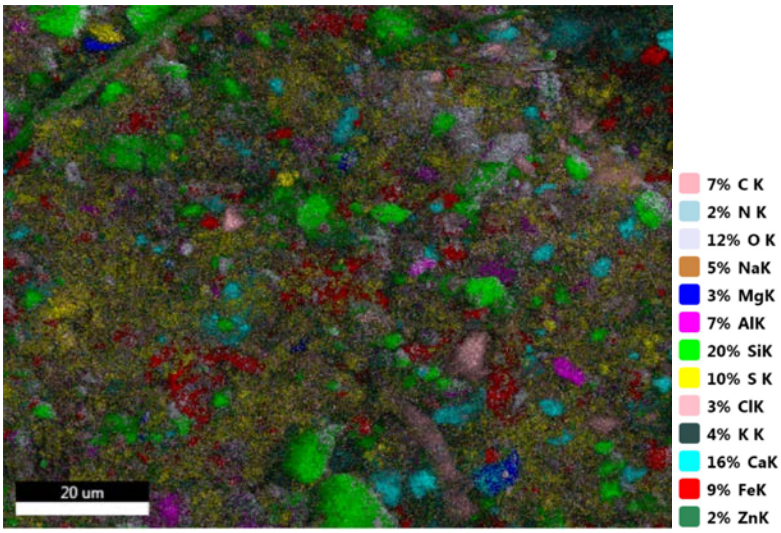

Figure 4.26: elemental overlap map of sample 27, a sub 11 micron sample of PM, viewed at 2000x magnification.

Samples 27 and 28 were taken from the same bulk sample at 405 St. Ferdinand Street in downtown Baton Rouge, sample location 3. The bulk sample source is an attic. This location is approximately one quarter mile away from the Mississippi River which is a major industrial corridor. Sample 27 is a sub 11 micron particulate matter sample, while sample 28 is a sub 40 micron particulate matter sample. Both samples contain fine and coarse particulates.

Table 4.10: Element composition results from sample 27.

Element	Weight %	Atomic %	Net Int.	Error %
C K	30.66	40.29	1315.26	8.26
N K	10.49	11.81	209.88	12.69
O K	38.27	37.75	2816.07	9.38
F K	1.94	1.61	162.22	35.94
NaK	0.64	0.44	147.67	9.39
MgK	0.49	0.32	213.84	7.29
AlK	1.58	0.92	886.47	5.06
SiK	4.95	2.78	3196.85	3.59
S K	2.32	1.14	1397.50	2.63
ClK	0.16	0.07	89.46	6.13
K K	0.55	0.22	280.55	3.96
CaK	3.78	1.49	1627.60	1.69
TiK	0.05	0.02	19.87	22.88
FeK	3.25	0.92	691.06	2.75
ZnK	0.86	0.21	99.28	5.49

The elemental composition results for sample 27 shows a diverse range of elements. Numerous small particles containing iron are present.

Sample 28:

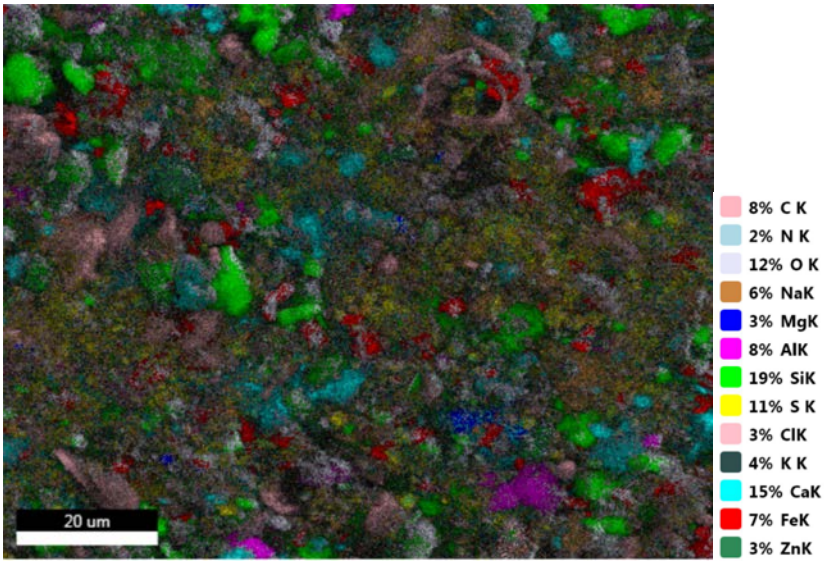

Figure 4.27: Elemental overlay map of sample 28, a sub 40 micron PM sample, viewed at 2000x magnification.

Table 4.11: Element composition results from sample 28.

Element	Weight %	Atomic %	Net Int.	Error %
C K	32.25	42.13	1345.55	8.30
N K	10.06	11.27	191.21	11.31
O K	38.66	37.92	2772.76	9.39
NaK	0.62	0.42	143.80	9.83
MgK	0.42	0.27	182.74	7.70
AlK	1.93	1.13	1085.64	4.87
SiK	4.87	2.72	3114.87	3.55
S K	2.62	1.28	1557.49	2.56
ClK	0.14	0.06	76.88	5.86
K K	0.61	0.25	304.82	3.78
CaK	3.65	1.43	1544.67	1.76
FeK	3.01	0.85	633.12	2.79
ZnK	1.15	0.28	130.33	4.71

Figures 4.26 and 4.27 for samples 27 and 28 from downtown Baton Rouge show higher levels of metals including iron and zinc, compared to suburban derived samples.

Samples 27 and 28 also show higher amounts of nitrogen than other samples, making up about 11% of atoms in the above samples. The nitrogen may be in the form of nitrates, other research indicated nitrogen and nitrate content to be 4-5% of coarse PM (Chan et al. 1997).. Stochiometrically, there is enough oxygen in the sample (38% atomically) to form nitrates, NO3.

Also worth noting in samples 27 and 28 is that chunks of carbon are present. Instead of carbon simply being present as background from the carbon tape used to affix PM for SEM viewing, in samples 27 and 28, carbon based particulates are visible in figures 4.26 and 4.27.

Across all samples elements found include: carbon, nitrogen, oxygen, sodium, magnesium, aluminum, silicon, sulfur, chlorine, potassium, calcium, iron, zinc, fluorine and copper. It was mentioned above that transition metals may play a key role in the formation of reactive oxygen species in biological systems (Vejerano et al. 2012).

4.4: Electron Paramagnetic Resonance Results

Filtered particulate matter from samples collected was tested with electron paramagnetic resonance (EPR) for paramagnetic species. Bulk samples were also collected and tested with EPR. Organic radical signal was the parameter most frequently tested for using electron paramagnetic resonance.

Most samples collected that were filtered and analyzed promptly demonstrate a significant organic radical signal. Sample 22 showed no radical signal. It was stored in a large jar, not under vacuum. However, it was collected in January 2015 and not filtered and scanned with the EPR until May 2015. Concentration values for most samples in spins per gram were

most frequently observed in the order of magnitude of 10^16 to 10^17, but overall varied from the order of magnitude of 10^15 to 10^17. These values are consistent with radical concentration taken from PM 2.5 from ambient air from monitors used by the Louisiana Department of Environmental quality in Baton Rouge in 2013 (Gehling and Dellinger 2013).

PMsamples taken from various sources showed significant organic radical signal, and also large signal from unidentified paramagnetic species. For example from sample 1, a sample of unfiltered dust from an attic demonstrated a strong organic radical in a June 26^{th,} 2014 100 gauss range scan with a large amount of paramagnetic species present in the 5000 gauss range scan:

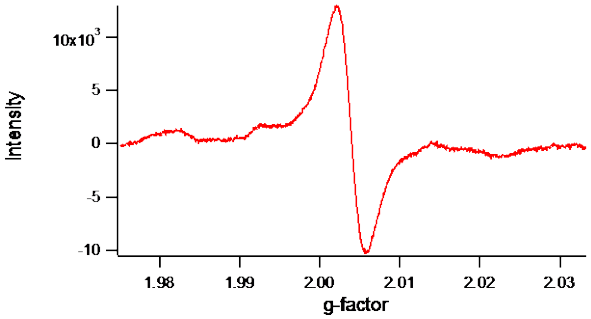

Figure 4.28

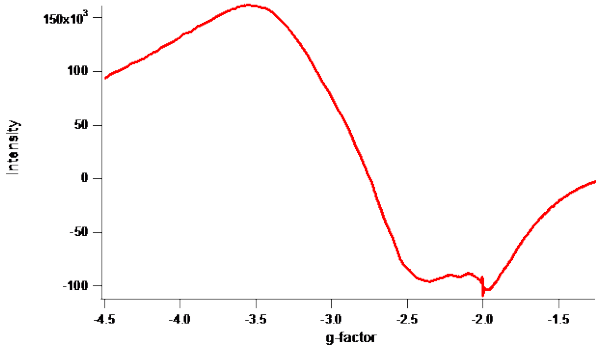

Figure 4.29

Figures 4.28 and 4.29: 100 gauss and 5000 gauss scans of the same sample, respectively. 4.28 shows a zoomed in area of detail on the organic radical, while 4.29 shows a more complete picture of paramagnetic species in the sample.

Figure 4.28: shows a 100 gauss scan of the organic radical that is viewed between 3000 and 4000 gauss on the long range, 5000 gauss scan. The organic radical concentration for the spectrum in Figure 4.28 is calculated to be 1.75 * 10^17 spins per gram with a g-factor of 2.00407, indicative of an oxygen centered radical. Figure 4.29 shows a long range scan depicting peaks from paramagnetic species. EPR can be used to detect free radicals, and also transition metal complexes (Massachusetts Institute of Technology 2003).

4.4.1: Particle Size and Radical Signal

Smaller particles have a larger surface area on a per weight basis than larger particles. Multiple samples consistently show PM filtered to a smaller particle size has a higher concentration of radicals in spins per gram. Environmentally persistent free radicals form as a surface complex by an organic reducing a metal cation (Vejerano et al. 2012), so a higher surface area would provide more room for surface reactions. The higher radical signal from smaller particles is also likely due to a higher concentration of smaller particles being the product of combustion, which equates to a higher radical concentration. The higher radical concentration for smaller particle sizes is seen in sample 21 where bulk sample had a radical concentration of 1.53 x10^16, while sample filtered with a 20 micron pre-filter had a radical concentration an entire order of magnitude higher, measured up to 1.79 x10^17 spins per gram.

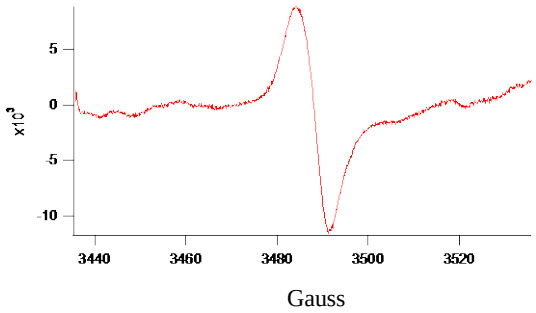

Figure 4.30

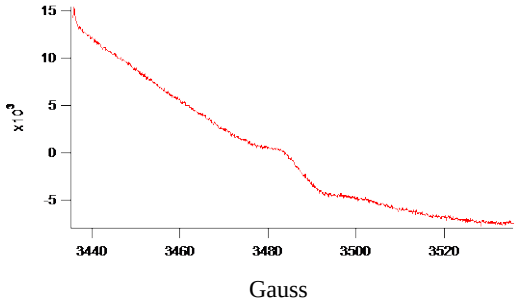

Figure 4.31

Figures 4.30 and 4.31: The organic radical signal portion for samples 21 and 21b. Figure 4.30 shows a baseline correction while figure 4.31 reflects an uncorrected baseline while the organic radical is on the shoulder of another peak.

Figures 4.30 and 4.31 show EPR spectra for sample 21 and 21b respectively. Figure 4.30 shows sub 20 micron filtered PM and a stronger radical signal than figure 4.31 which is the parent sample, bulk, un-filtered dust. Figure 4.30 shows a baseline correction to normalize the baseline and gain a more accurate peak area, while figure 4.31 is uncorrected in image, but for

quantification, the baseline was corrected. Figure 4.31 left uncorrected shows an organic radical on the steep peak of a shoulder of another paramagnetic species. The result of measuring the corrected peak gives a radical concentration of 1.53 x 10^16 spins per gram for sample 21b, which is an order of magnitude lower than the filtered sample number 21.

Samples 18, 19 and 20 were taken from the same location at the same time. Samples 18 and 19 (figures 4.4.5 and 4.4.6) were filtered with 11 and 20 micron pre-filters respectively, while sample 20 was bulk PM sampled from the same attic. Radical concentration on these scans for filtered sample was an order of magnitude higher, 10^17, than unfiltered particulate that had a radical concentration of 10^16 spins per gram. Seen below:

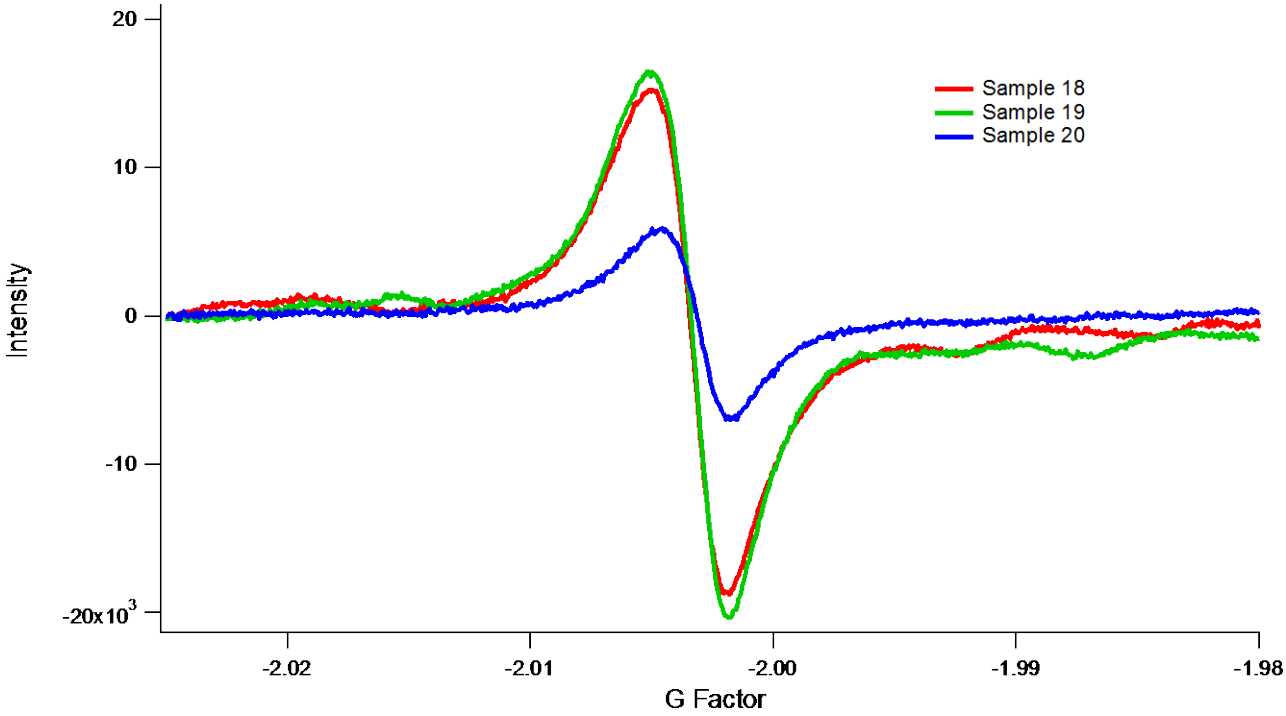

Figure 4.32: Sample 18: 11 micron pre-filter, radical concentration= 2.08*10^17: g-factor=2.0035. Sample 19: 20 micron pre-filter, radical concentration = 2.45*10^17: g-factor=2.0035. Sample 20: bulk dust, radical concentration = 4.49*10^16: g-factor = 2.0033. All measurements taken on April 24th.

Samples 18, 19 and 20 show filtered dust compared to bulk dust. In Figure 4.32 samples 18 and 19 also show the same g-factor for their organic radical, while bulk sample 20 shows a slightly lower g-factor at 2.0033. This indicates that deposited PM may contain many different species of organic radical and this difference may relate to particle size. It may be expected that sample 18 would show a higher radical concentration than sample 19 because of the smaller PM size, but this was not the case in this example.

The above two examples are reinforced by sample 6, where re-suspended and filtered dust excluded by the pre-filter was tested compared to dust that passed the filter and collected on the polyurethane foam. The dust collected from the pre-filter contained radicals in a concentration of 5.08 x 10^15 spins per gram. Filtered dust that was sub 40 micron consistently tested one order of magnitude higher (10^16 spins per gram) for six scans over a one month period after initial testing.

4.4.2: g-Factor

The g- factors of EPR spectra can generally be used to determine whether an organic radical signal is oxygen centered or carbon centered (Dellinger et al. 2008). The organic radical resides in the 3450-3550 gauss scan range on the EPR spectrum.Radicals tested for in this research had a g-factor between 2.0032-2.0044, indicative of a carbon centered radical with an adjacent oxygen atom. The closer the unpaired electron is to the oxygen atom, the greater the g-factor (Dellinger et al. 2008). Some radicals tested for in this research had a g-factor greater than 2.004, which is indicative of an oxygen-centered radical. Sub 20 micron filtered particulate from sample 21 had a g-factor of 2.0041-2.0042 (oxygen centered), while samples 18 and 19 consistently tested as a g-factor between 2.0033-2.0035, a carbon centered radical. In spite of g-factor differences radical concentration for samples 18, 19 and 21 had very similar values: 2.08,

2.45 and 1.50 * 10^17 spins per gram respectively that persisted in EPR tubes for months at a time. It is unknown from this research as to the genesis of these radicals and how long they persisted in the environment before collection.

In the literature review section it was mentioned that semiquinone radicals with a g-factor between 2.0031-2.0044 were noted for their ability to cause sustained radical generation in the body via redox cycling (Squadrito et al. 2001). This research consistently found similar g-factor values in PM from Baton Rouge homes ranging from 2.0032-2.0044. Oxygen centered radicals have values on the higher end of this spectrum, and are more reactive than carbon centered (Dellinger et al. 2007).

4.4.3 Radical Persistence

Some samples demonstrate almost indefinite persistence when kept in sealed EPR tubes. For example, sample 7 is sub 40 micron particulate matter filtered from dust from a vacuum cleaner using filtration apparatus B.

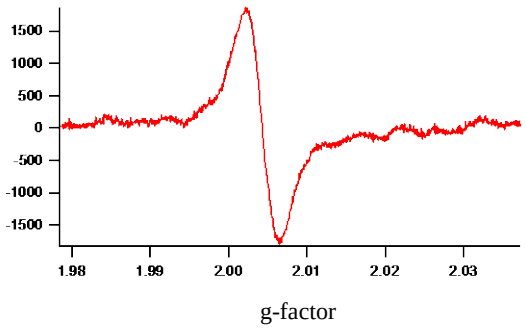

Figure 4.33

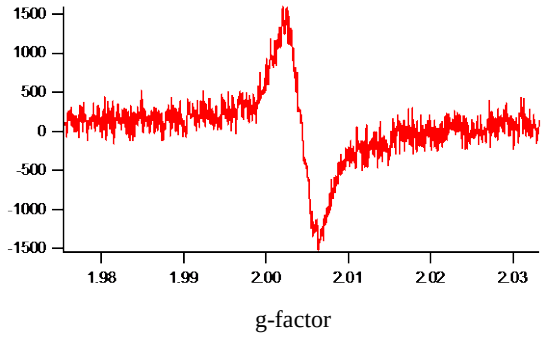

Figure 4.34

Figure 4.33: Sample 7, October 17th, 2014 scan of 8.1 mg of sub 40 micron particulate. Radical concentration is 2.45 x 10^16 spins per gram. g-factor=2.0044.

Figure 4.34: Sample 7 April 1st, 2015 scan of same 8.1 mg sample. Radical concentration is 1.70 x 10^16 spins per gram. g-factor=2.0044.

It is apparent from the two scans that they have a similar intensity and the same g-factor, however, Figure 4.34 is a much noisier signal than Figure 4.33. It is possible that the tube height position in the EPR differed, resulted in differing measurements. However, it can still be said that an organic radical signal was persistent in lasting at least six months in an EPR tube. Later sample scans on the EPR were marked at a specific height to ensure that the testing was consistent.

The persistence of EPFRs contained in tested particulate matter samples from homes in the Baton Rouge area can also be seen sample 8. Sample 8 is a particulate matter sample filtered from a vacuum canister. Sample 8 continues to show strong organic signal ten months after it was initially tested. An initial test on November 7, 2014 indicated a radical concentration of 1.80 x10^17 spins per gram while a later test nearly ten months later indicated a radical concentration of 1.49 x 10^17 spins per gram.

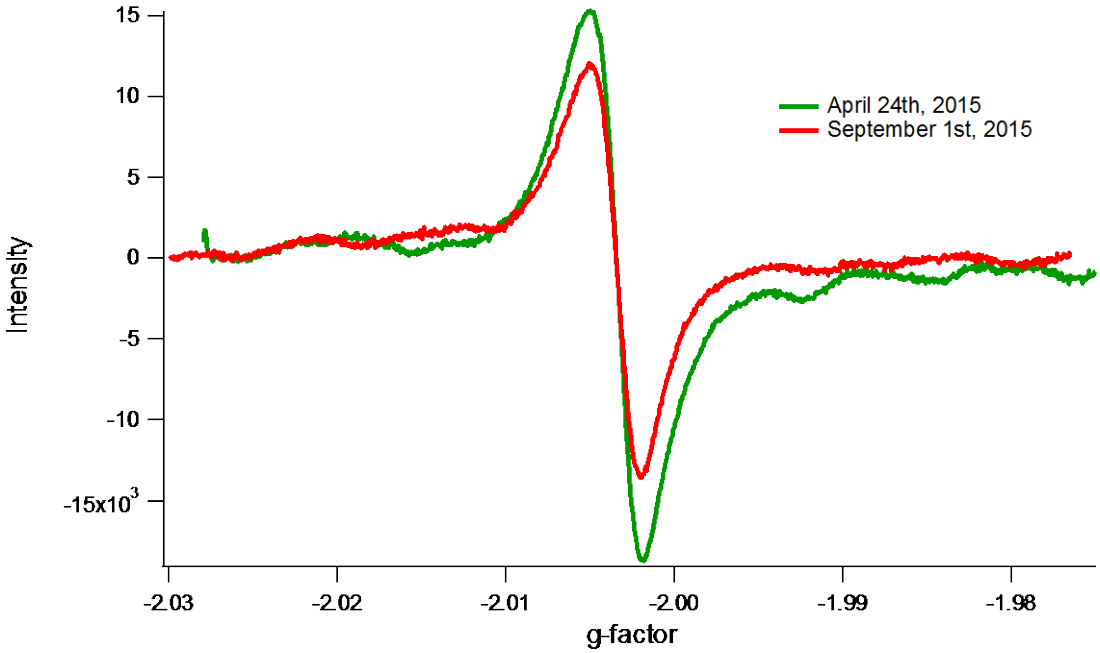

Figure 4.35: Sample 18, initial April scan, and final September scan show very little decay of the organic radical signal. The four month period results in a change in radical spins per gram from 1.86x10^17 to 1.27x10^17. The g-factor remained constant at 2.0035

Samples 18 and 19 showed radicals that were very persistent. Their decay from April 24th to September 1st was low level of degradation, seen in Figure 4.35 and Figure 4.36.

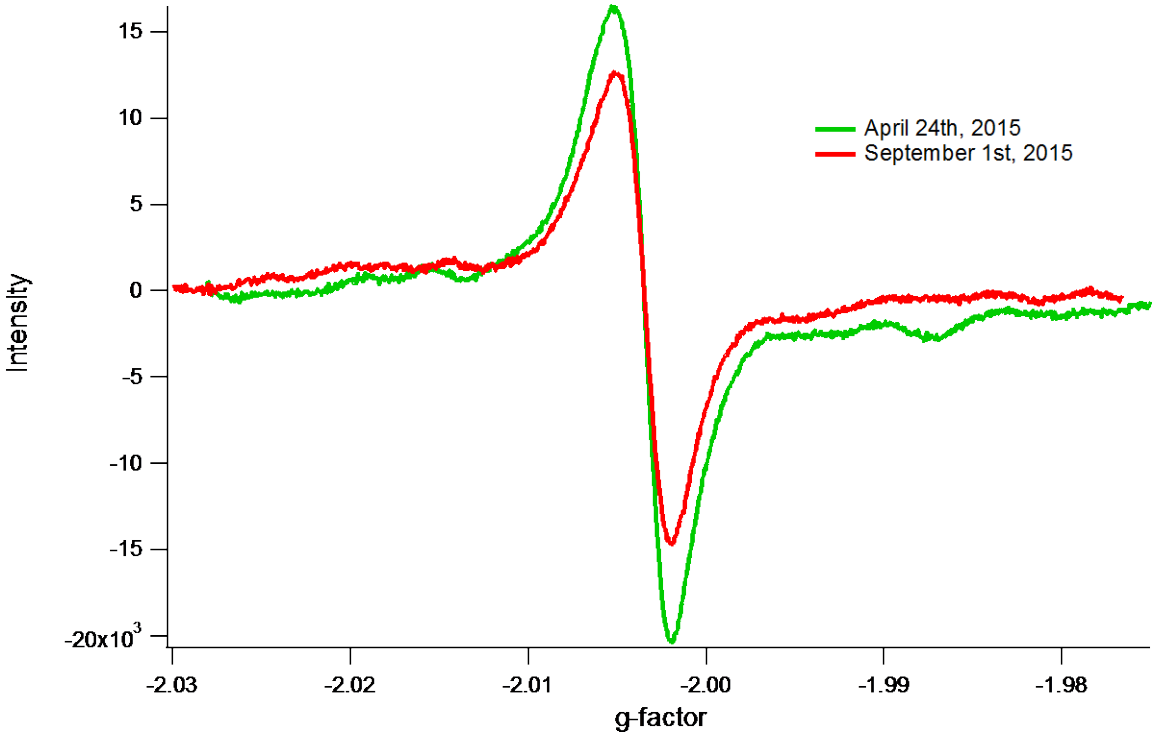

Figure 4.36: Sample 19, initial April scan, and final September scan show very little decay of the organic radical signal. The four month period results in a change in radical spins per gram from 2.33x10^17 to 1.42x10^17. The g-factor remained constant at 2.0035

Samples 27 and 28 were collected in downtown Baton Rouge near the Mississippi River and showed organic radical signal and the presence of other paramagnetic species. Sample 27 was a sub 11 micron sample, while sample 28 was a sub 40 micron sample. Sample 27 showed a slightly higher radical concentration of 1.24 x 10^17 spins per gram versus 8.75 x 10^16 spins per gram. These data are consistent with above described data where a smaller PM size resulted in a higher radical concentration. These samples caused the receiver level to drop and thus required the samples be run at 30 dB attenuation as opposed to 20 dB attenuation. 30 dB

attenuation is a lower power. This is possibly due to interference from a high level of metals in the sample. In spite of being tested at a lower power, the downtown Baton Rouge samples showed just as high of a quantitative radical concentration as other samples described in this research.

Samples 27 and 28 also showed a relatively high concentration of iron from SEM-EDS analysis: 3.25% by weight and 0.92% by atomic proportion for sample 27 and 3.01% and 0.85% for sample 28. Samples 27 and 28 were also tested with a long range (5000 gauss) EPR scan that resulted in broad, featureless peaks. Iron oxide species usually exhibit broad, featureless spectra at elevated concentrations (Herring et al 2015).

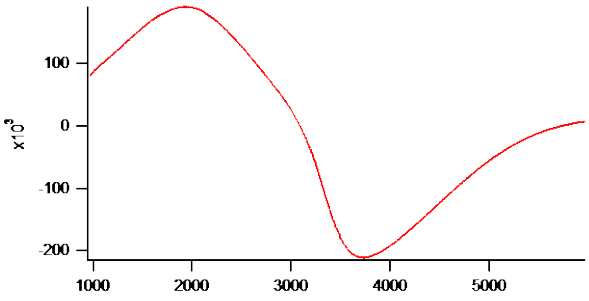

Figure 4.37

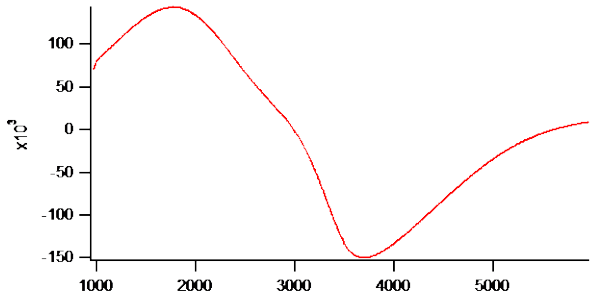

Figure 4.38

Figure 4.37: September 15th, 2015 5000 gauss scan of 2.6mg of sub 11 micron PM from sampling location 3. g-factor=2.27.

Figure 4.38: September 15th, 2015 5000gauss scan of 3.0 mg of sub 40 micron PM from sampling location 3. g-factor= 2.34

Figures 4.37 and 4.38 show the broad featureless spectra indicative of a high quantity of iron and may also indicate the presence of many different species or iron. Interestingly a g-factor of 2.28 is cited in literature as a g-factor characteristic of $FE(III)_2O_3$ (Herring et al. 2015). The g-factor of sample 27 was 2.27. This information regarding the broad featureless peaks mentioned in Herring (2013), paired with data from SEM-EDS, seems to indicate the presence of iron in

sample 27 and 28 as the spectra are typical of bulk paramagnetic iron species. However, it is not possible to determine definitively from these results.

4.5: Polycyclic Aromatic Hydrocarbon Analysis Results

Various samples of particulate matter were tested for organics that may be associated with PM. Specifically, polycyclic aromatic hydrocarbons were tested for using gas chromatography-mass spectrometry in scan mode as well as using selective ion monitoring (SIM mode). The full panel of PAHs tested for in SIM mode can be found in the appendix. Other organic compounds were detected, including many aromatics and alkanes. However, this research focuses on PAHs because of their health effects. SIM analysis here tests for 14 of the 16 PAHs on EPA's priority pollutant list.

Samples of particulate matter, both bulk samples and filtered samples, showed significantly higher levels of organic compounds than blank samples. The specific compounds were identified in SIM mode. Below are graphs showing the average blank sample and tested samples from organic extractions and GC-MS runs. The average blank was taken from four blanks run that were generally consistent in background concentrations or PAHs. The Figures 4.39 and 4.40 show the raw response numbers and not the concentration; a concentration for the blank samples is not possible to calculate, but these graphs illustrate the drastic difference in raw intensity response from background PAH levels to PAH levels actually found in samples. The other graphs shown below are calculated to actually show concentrations of PAHs from environmental samples. The SIM mode can identify many homologues of PAHs, for example it can detect many different types of pyrenes or chrysenes. Here the homologue PAHs are grouped together for simplicity.

Raw Responses Run 1**:**

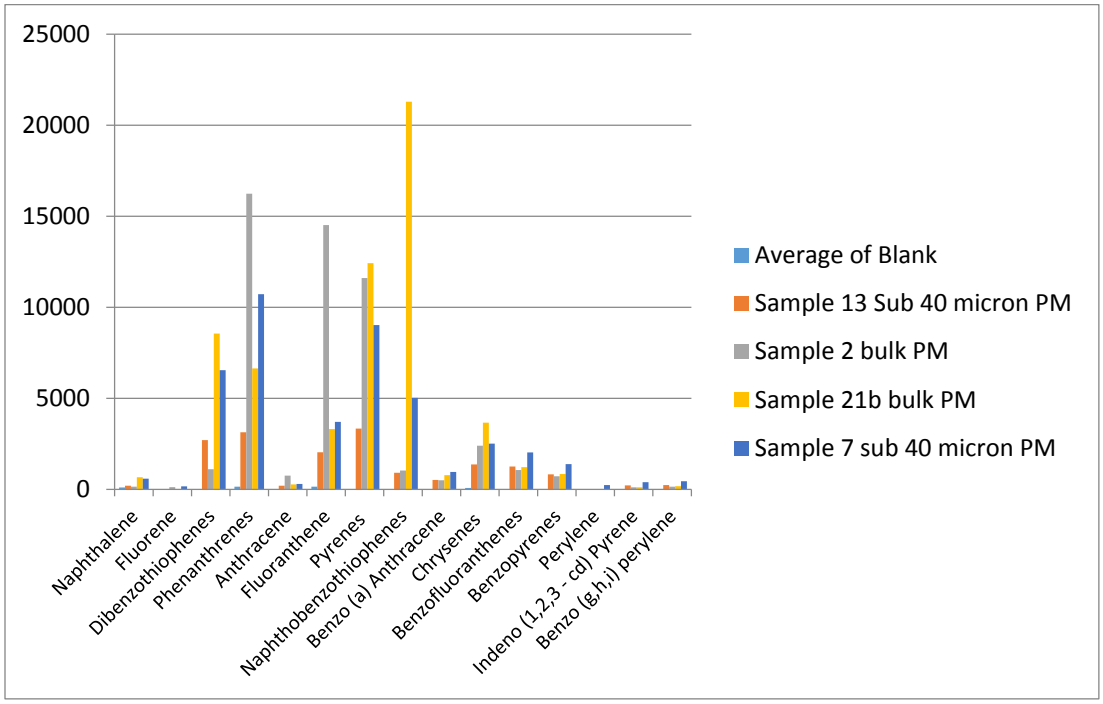

Figure 4.39: GC-MS raw responses for samples 2, 7, 13 and 21b. Differing weights of sample were extracted, therefore raw response numbers will vary regardless of concentration.

Raw Responses Run 2:

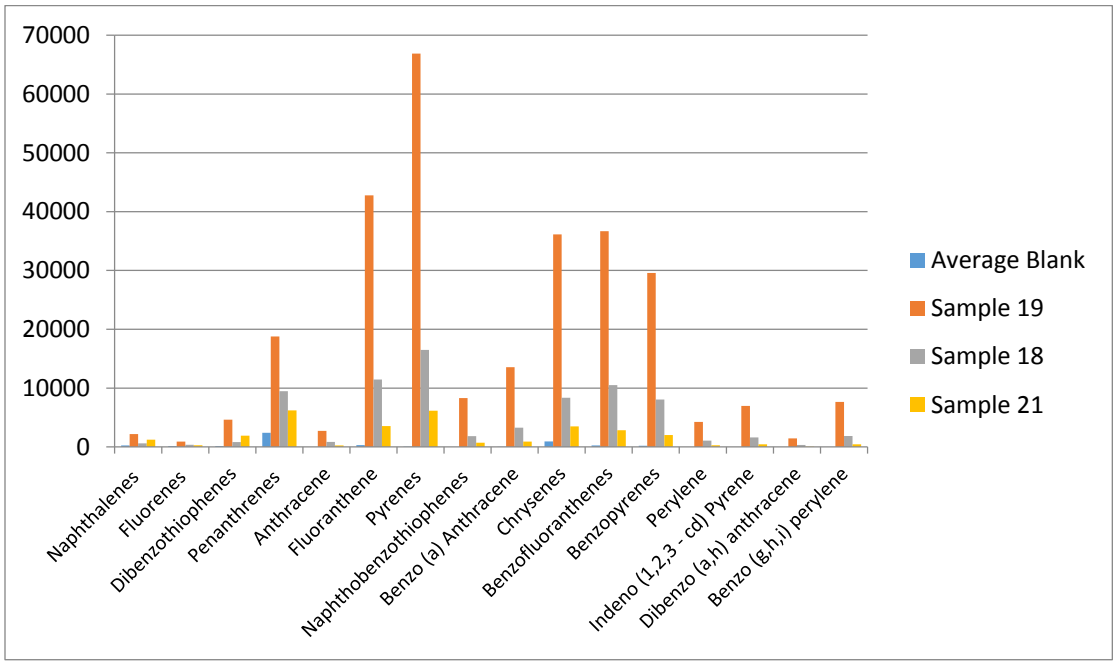

Figure 4.40: GC-MS raw responses for samples 18, 19 and 21. Differing weights of sample were extracted, therefore raw response numbers will vary regardless of concentration.

The raw responses show that samples tested had a significantly higher level of PAHs than blank samples which showed low background levels of PAHs. The raw response numbers can be viewed in the appendix.

4.5.1: PAH Concentrations

Below are bar graphs illustrating the concentration of samples in nanograms per gram which is equivalent to parts per billion. Sample concentrations were calculated using an internal standard average and a 5 point calibration curve.

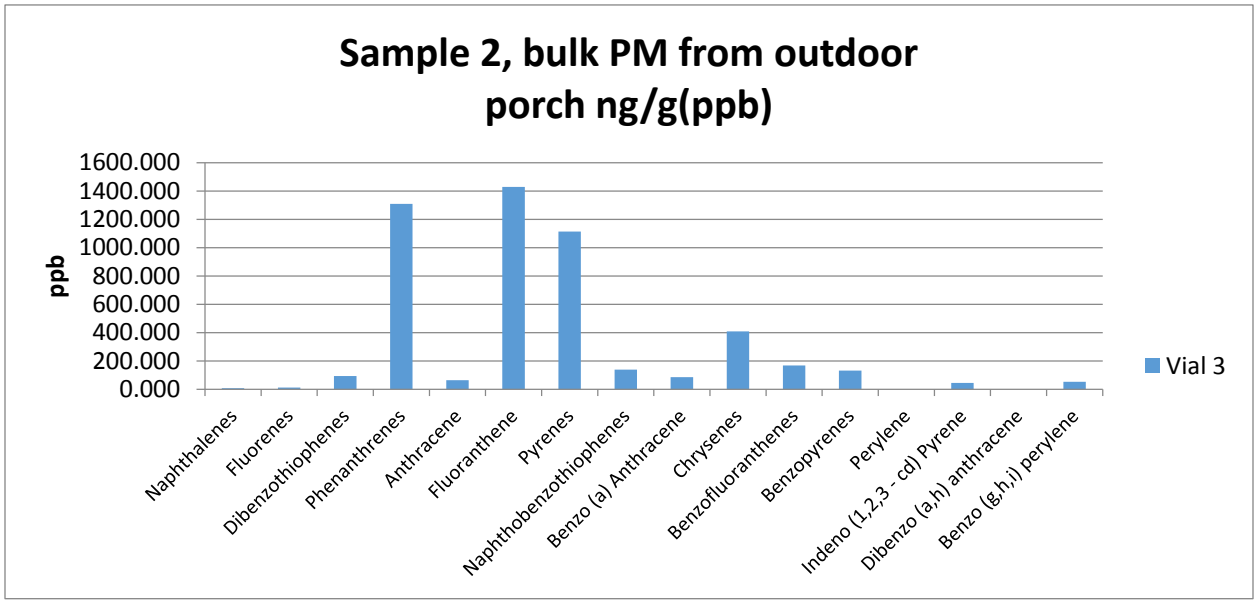

Figure 4.41: Concentration of PAHs (ppb) from sample 2.

Sample 2 was collected by hand and is an outdoor sample collected at location 2 in Baton Rouge. This is a bulk sample, meaning the PM was unfiltered and its particle size highly variable.

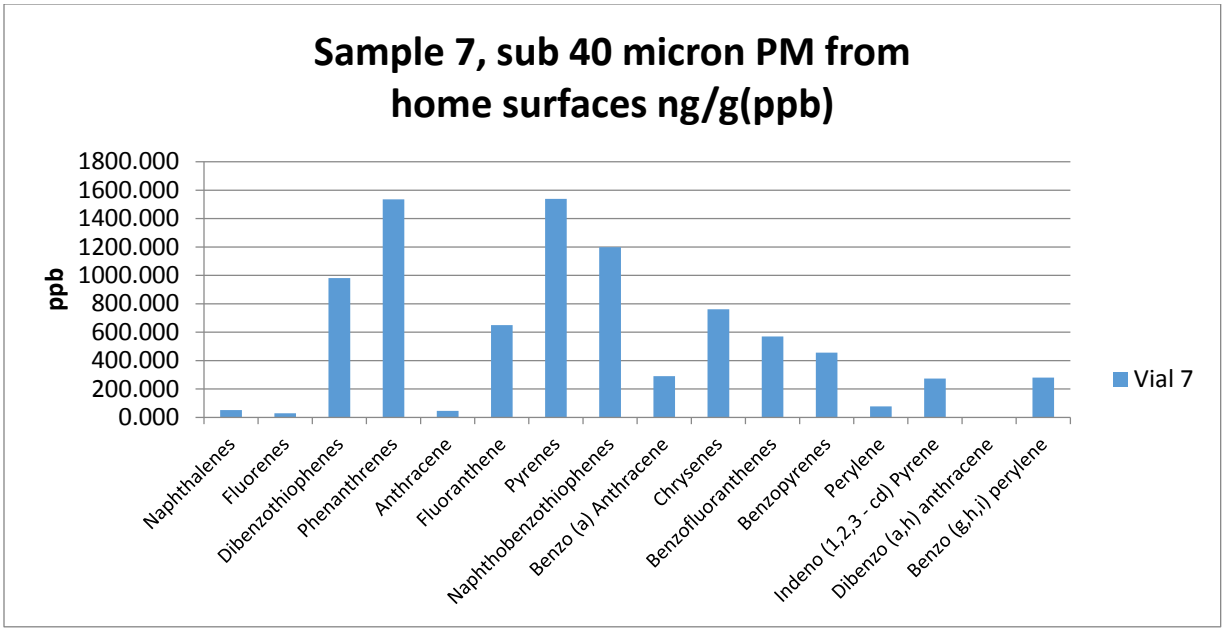

Figure 4.42: Concentration of PAHs (ppb) from sample 7.

Sample 7 was collected from a vacuum cleaner canister from location 1 in Baton Rouge. This sample was filtered using filtration apparatus B, meaning the PM is less than 40 micron in diameter.

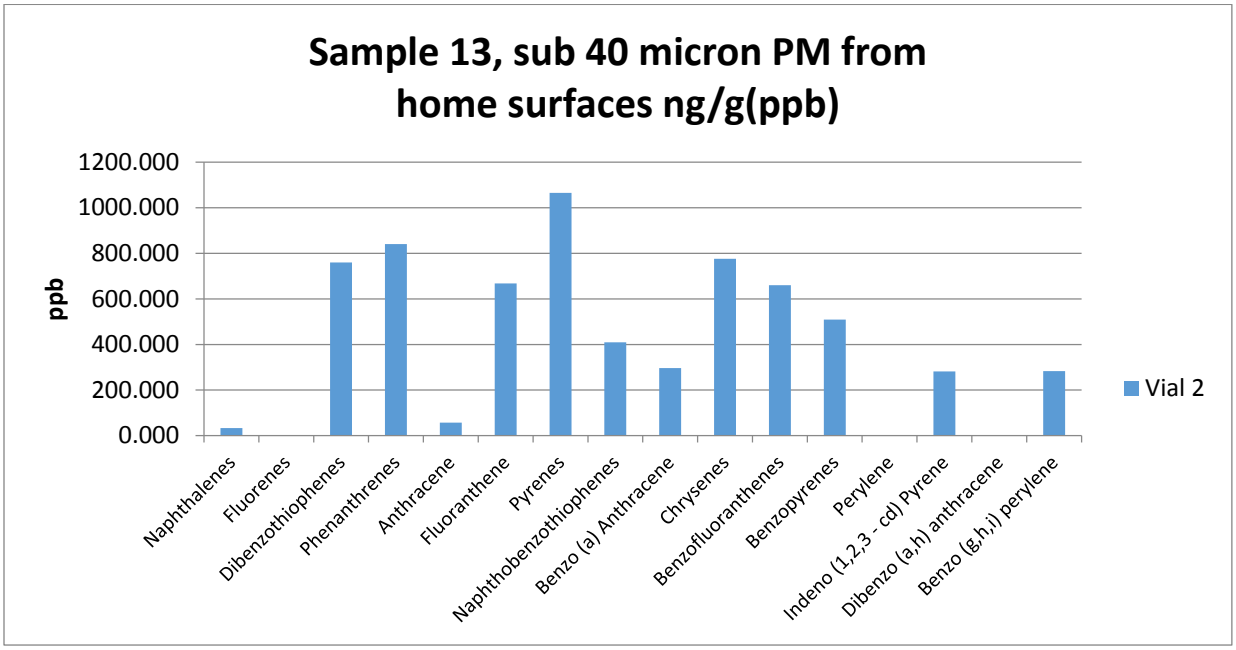

Figure 4.43: Concentration of PAHs (ppb) from sample 13.

Sample 13 was collected from a vacuum cleaner canister at location 5 in Baton Rouge. This sample was filtered using filtration apparatus B, meaning the PM is less than 40 micron in diameter.

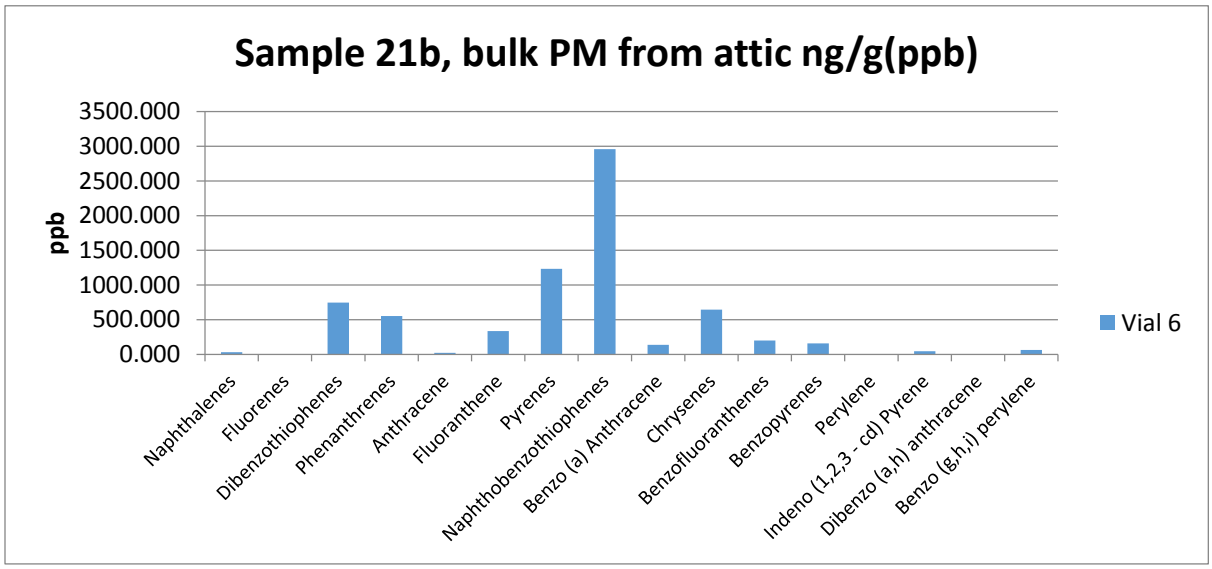

Figure 4.44: Concentration of PAHs (ppb) from sample 21b.

Sample 21b was collected by vacuum from an attic at location 4 in Baton Rouge. This is a bulk sample, meaning the PM was unfiltered and its particle size highly variable.

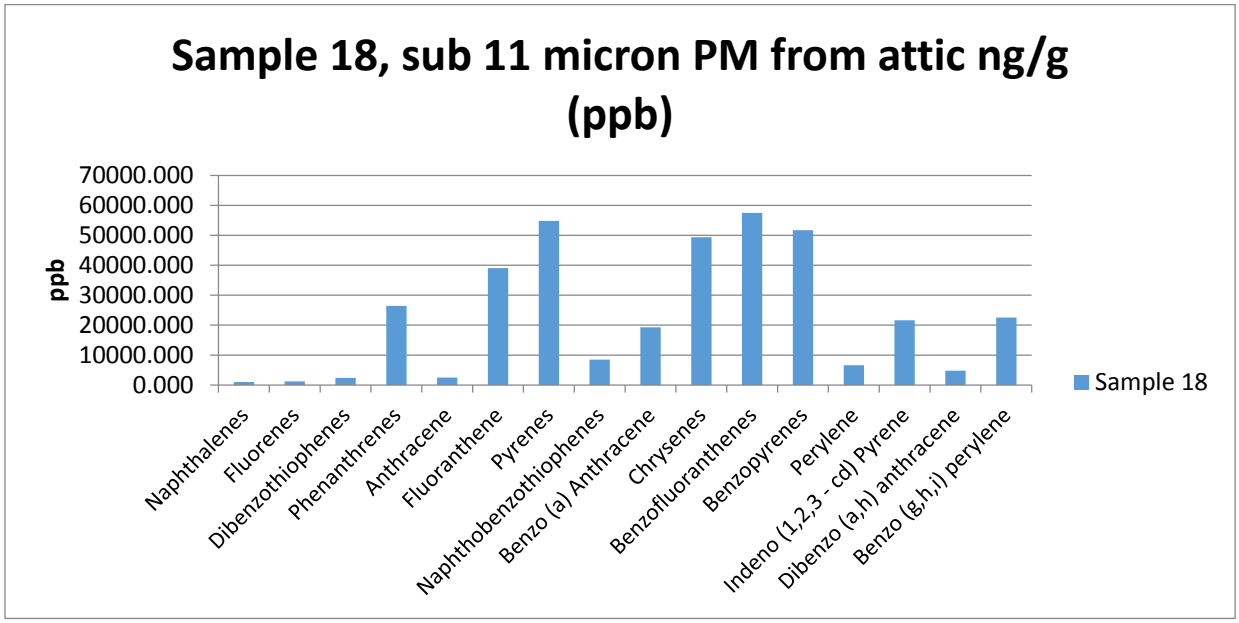

Figure 4.45: Concentration of PAHs (ppb) from sample 18.

Sample 18 was collected from an attic at location 1 in Baton Rouge. This sample was filtered using filtration apparatus C with an 11 micron nylon net filter, meaning the PM is less than 11 micron in diameter.

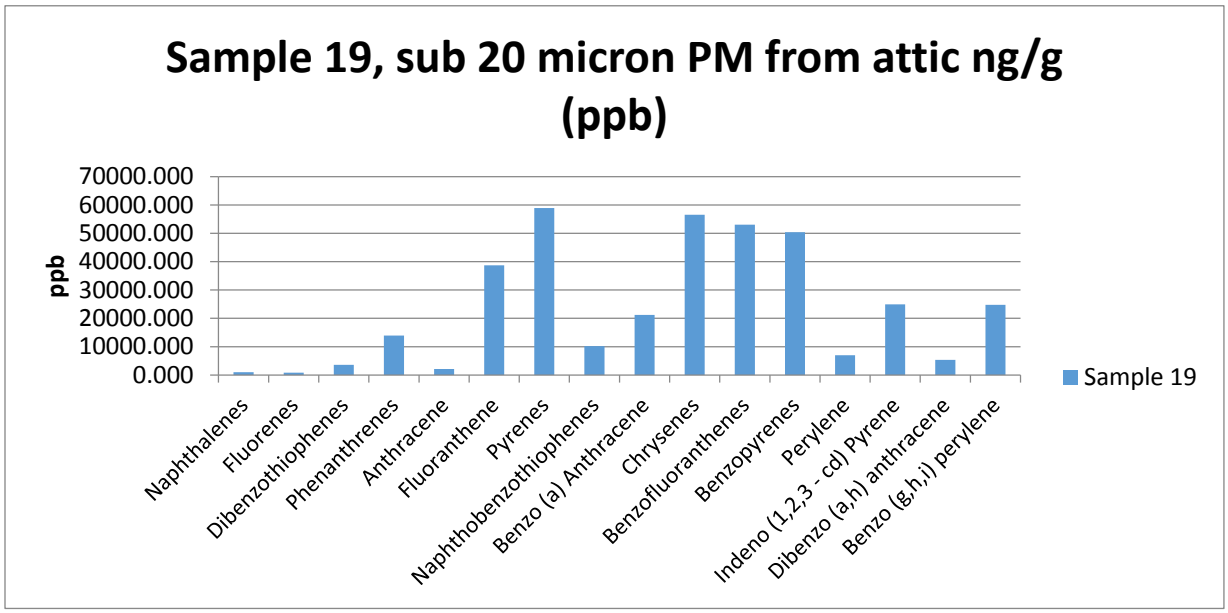

Figure 4.46: Concentration of PAHs (ppb) from sample 19.

Sample 19 was collected from an attic at location 1 in Baton Rouge. This sample was filtered using filtration apparatus C with a 20 micron nylon net filter, meaning the PM is less than 20 micron in diameter.

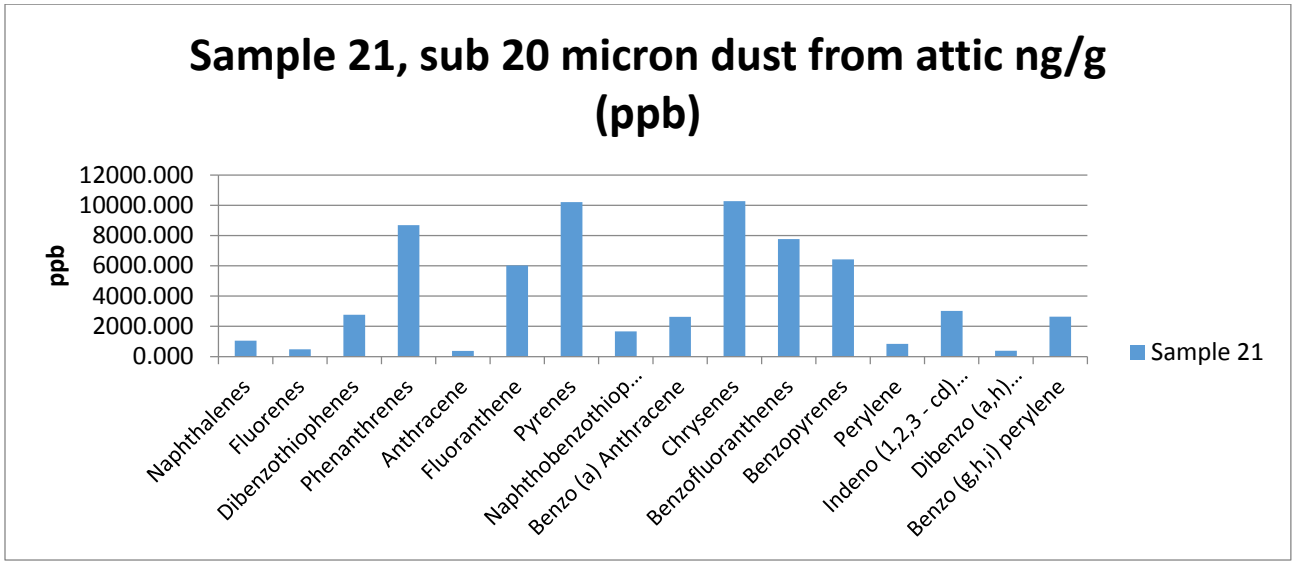

Figure 4.47: Concentration of PAHs (ppb) from sample 20.

Sample 21 was collected from an attic at location 4 in Baton Rouge. This sample was filtered using filtration apparatus C with a 20 micron nylon net filter, meaning the PM is less than 20 micron in diameter.

Surprisingly, samples 27 and 28 taken from a downtown attic at location 3 where there is less vegetation and more traffic in closer proximity to industrial facilities did not show a higher concentration of PAHs adsorbed to filtered particulate matter. Also, surprisingly, the sub 40 micron sample did not show a lower amount of PAHs than the sub 11 micron sample as expected.

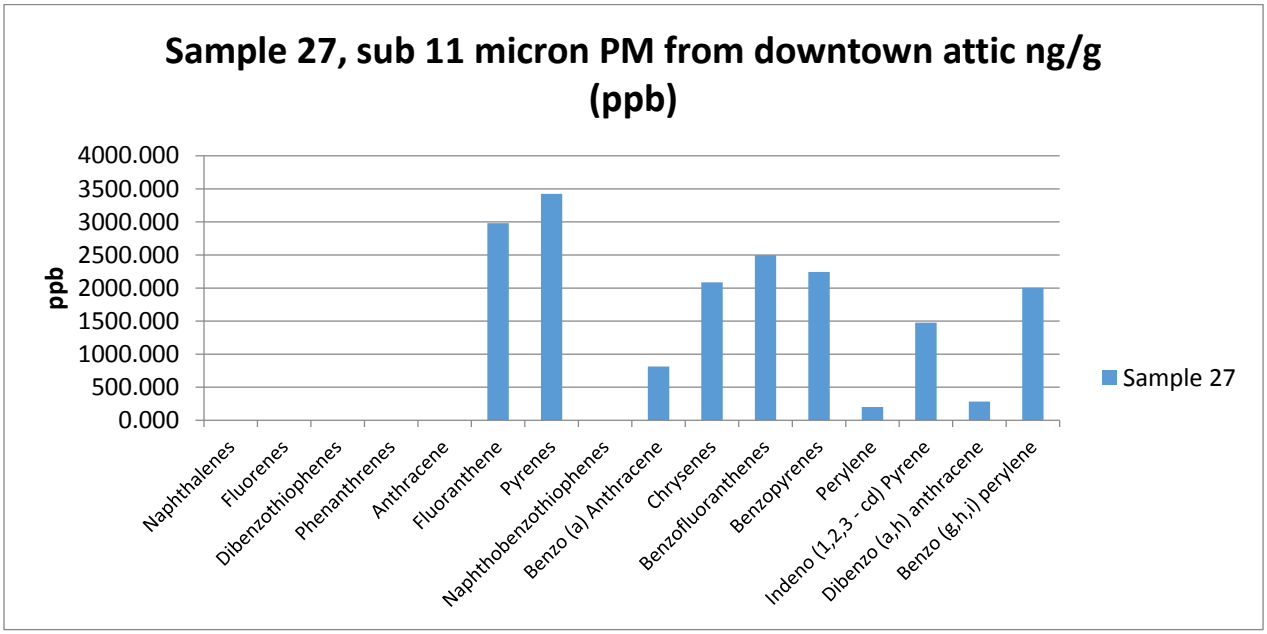

Figure 4.48: PAH concentration (ppb) from sample 27.

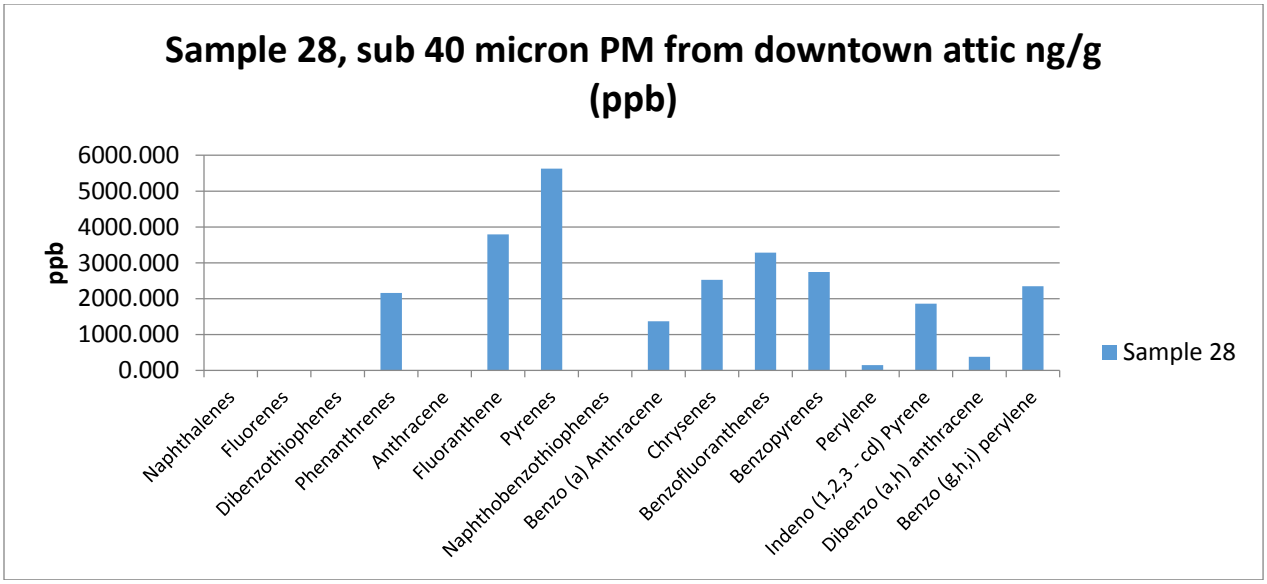

Figure 4.49: PAH concentration (ppb) from sample 28. Sample 27 and 28 were sub-sampled from the same bulk sample.

The sample concentration and raw response data given above show that samples tested definitively had more associated PAHs than blank samples, and that tested samples showed PAHs in the concentration range of the low parts per million, not more than ten ppm (10,000 ppb) with the samples tested. PM collected and tested from homes in the Baton Rouge area definitively showed levels of PAHs associated with the particles.

Some samples contained over 2000 ng/g for individual PAHs and much more than that for total concentration of PAHs. For total aromatics in ng/g, this research found samples 27 and 28 to have relatively high PAH concentrations for total aromatics. However, samples 18 and 19 had very high concentrations of PAHs, approximately double the amount found in soil samples near oil refineries.

Table 4.12: Samples and total PAH concentration compared to two example levels.

Sample	Total PAH Concentration in ng/g = ug/kg (ppb)
Average soil for cities with heavy traffic (ATSDR 2009)	2000
Example soil for area near refinery (ATSDR 2009)	200,000
Number 2 (extraction 1)-unfiltered	6,639
Number 7 (extraction 1)-sub 40 micron	5,062
Number 13 (extraction1)-sub 40 micron	7,145
Number 18 (extraction 2)-sub 11 micron	369, 180
Number 19 (extraction 2)-sub 20 micron	372,495
Number 21 (extraction 2)-sub 20 micron	65,245
Sample 21b (extraction1)-unfiltered	8,737
Sample 27 (extraction 3)-sub 11 micron	18,011
Sample 28 (extraction 3)-sub 40 micron	26,245

Table 4.12 shows the various total PAH concentration of given samples compared to environmental soil levels in areas contaminated by combustions byproducts and studied by the ATSDR.

Alkanes were also detected in SIM mode in each sample tested. Values for total alkanes in each sample were generally several hundred ppb, with the average total alkane ppb value being 237.5 per sample. Specific alkane concentrations from Baton Rouge samples can be viewed in Appendix 3.

Many organic compounds were present, detected in scan mode and identified through the program library. For samples run, compounds that were also found in any of the blanks were excluded from consideration of presence in samples from homes. A complete list of compounds

identified in scan mode with GC-MS can be found in Appendix 2. The compounds found here may originate from any number of processes external or internal to the home including combustion, aerosolization, or volatilization.

The presence of aromatics may be significant in these findings because hydroxyl and chlorine substituted aromatics chemisorbed onto metal oxide surfaces is a key part of the model for EPFR formation in industrial processes (Vejerano et al. 2012). Many of the organics found in this analysis are aromatic compounds which could play a role in EPFR formation.

Examples of aromatic compounds extracted from deposited PM samples include: benzenes, furans, phenols, biphenyls, acetophenone, pyridine, benzoic acid, isopropylbenzamide, benzofuranone, oxazole, pyrazine, indole and benzene dicarboxylic acid.

Some of the significant compounds present in sample number 2, a bulk outdoor sample, were: sulfurous acid and benzenemethanol, an aromatic. Sulfurous acid (H_2SO_3) is an intermediary in air pollution in the formation of sulfuric acid (H_2SO_4) which can lead to acid rain (Pauling 1970). Benzenemethanol is a suspected liver toxicant, suspected neurotoxicant and suspected immunotoxicant. Benzenemethanol is found in perfumes, dyes, ink and cosmetics (Thorp 2011).

Some of the significant compounds found in sample 7, a sub 40 micron sampled filtered from vacuum canister dust, include: acetophenone and choloropropionic acid. Acetophenone, an aromatic, is listed on the EPA's Clean Air Act list of Hazardous Air Pollutants (US EPA 2015). Chloropropionic acid may be used in agro-chemicals. Some forms of chloropropionic acids can act as neurotoxins (Simpson et al. 1996).

One of the significant compounds found in sample 13, a sub 40 micron sample of vacuum dust includes benzenedicarboxylic acid. Benzene dicarboxylic acid, or phthalic acid, is a carboxylic acid with a benzene ring attached, it is an aromatic.

Some of the significant compound in sample 21b, a bulk sample taken from an attic, include: vanillin, 1,1' biphenyl 4,4' diamine, 3,3', 5,5' tetramethyl, methylenedioxybenzophenone, indole, and 2,7 dichloromethoxy dibenzofuran. Vanillin is used in foods and fragrances. It is possible that vanillin's presence in the home is from an aerosolized spray. Biphenyl diamine is two phenyl rings with two amine groups, and in this case there are also four methyl groups attached. Biphenyls are aromatics and are on the CAA list of HAPs (US EPA 2015). Indole is an aromatic that has shown to be toxic in chronic exposure to humans lungs and mucous membranes. Although indole can be toxic to cells it is widespread in nature because various species of bacteria produce considerable quantities of indole (Kim et al. 2013).

One of the most interesting compounds found from sample 21b was dichloromethoxy dibenzofuran. As the name suggests it is two benzene rings fused by a furan, this structure is also chlorinated. It is known that chlorinated organics and in particular, polychlorinated dibenzofurans are persistent organic pollutants. Dibenzofurans are on Clean Air Act list of Hazardous Air Pollutants (US EPA 2015). Polychlorinated dibenzo dioxins and the related polychlorinated dibenzo furans (PCDDs and PCDFs) are highly toxic and exposure to them resulted in decreased body weights, hepatic lesions, thymic atrophy, and adverse reproductive effects, at a wide range of exposure concentrations (CDC 2014). The chemical structure of PCDF can be seen in Figure 4.50.

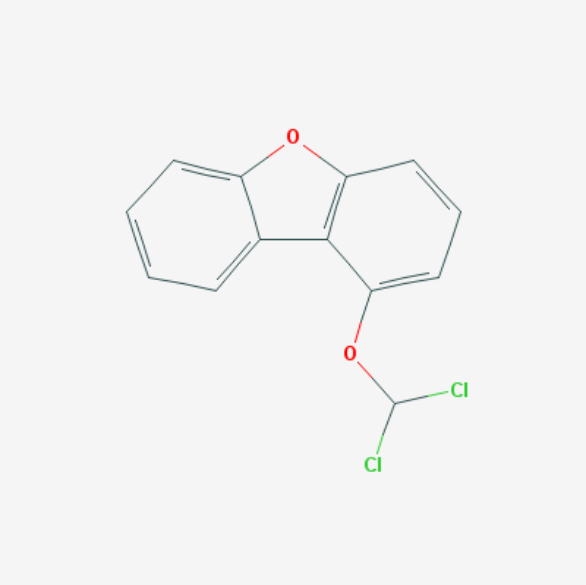

Figure 4.50: Chemical structure of dichloromethoxy dibenzofuran.

4.6: Summary of Results

Various locations were sampled in the Baton Rouge area: a downtown location, three garden district locations, and a location in mid-city. These locations are mapped in Figure 4.51

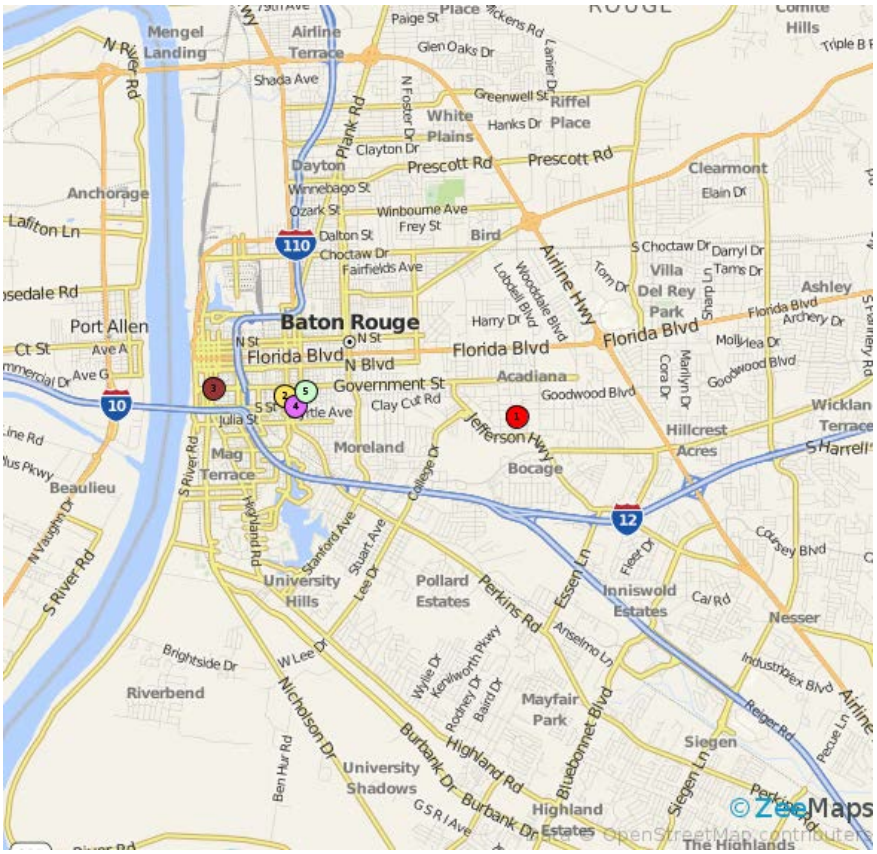

Figure 4.51: Approximate sampling locations in Baton Rouge.

Table 4.13 shows samples taken from some of the main sampling locations in the Baton Rouge area of this research. An effort was made was made to be as consistent with analysis as possible and use consistent particle sizes for comparison, yet this was difficult due to the experimental nature of the sampling and filtering and the variability of particulate available for analysis.

Table 4.13: Sub 11 micron samples: locations and chemical composition.

Location	Sample	Elements of Interest (atomic %)	PAHs	EPFR Radical Concentration	g-Factor
Kenner	15	Iron: 0.38 Aluminum: 0.25 Silicon: 0.78 Sulfur: 0.11 Calcium: 0.45	Not tested	3.57 x 10^16 spins/g	2.0041
Mid-City (location 1)	18	Not tested	benzofluoranthene, pyrenes, benzopyrenes, chrysenes, fluoranthene	2.08 x 10^17 spins/g	2.0034
Downtown (location 3)	27	Nitrogen: 11.8 Aluminum: 0.92 Silicon:2.78 Sulfur: 1.14 Calcium: 1.49 Titanium: 0.02 Iron: 0.92 Zinc: 0.21	pyrenes, fluoranthene, benzofluoranthene, benzopyrenes, chrysenes	2.31 x 10^17 spins/g	2.0035

Table 4.13 shows three sub 11 micron samples with chemical composition of organics and inorganics as well as radical concentrations and the g-factor characterization of the radical species. Elements of interest in sample 15 include metals shown to support EPFR formation such as iron and aluminum, as well as sulfur which is commonly an air pollutant in the form of SO_x emissions. Additional elements include calcium and silicon, which are commonly found in soils.

Sample 27 shows a higher composition of transition metals zinc and iron, as well as higher content of aluminum compared to sample 15. Titanium is also present, which can support EPFR formation. There is a relatively high percentage of nitrogen, which is common in combustion related NO_x emissions.

PAHs present in samples 18 and 27 are consistent in composition in that pyrenes, benzopyrenes, chrysenes, benzofluoranthene and fluoranthene appear to be most common.

Sub 11 micron samples in this group appear to have a variable organic radical concentration and g-factor.

Table 4.14: Sub 20 micron samples, locations and chemical composition.

Location	Sample	Elements of Interest (atomic %)	PAHs	EPFR Concentration	g-Factor
Kenner	14	Aluminum: 1.44 Silicon: 3.93 Sulfur: 0.34 Calcium: 1.78 Titanium: 0.12 Iron: 0.28 Copper: 0.07	Not tested	1.05 x 10^16 spins/g	2.0039
Mid-City (location 1)	17	Nitrogen: 7.04 Aluminum: 1.95 Silicon: 6.16 Sulfur: 0.66 Calcium: 1.57 Iron: 0.35	Not tested	4.01 x 10^16 spins/g	2.00395
Mid-City (location 1)	19	Not tested	pyrenes, chrysenes, benzofluoranthene, benzopyrenes, fluoranthene	2.33 x 10^17 spins/g	2.0035
Garden District (location 4)	21	Not tested	chrysenes, pyrenes, phenanthrenes, benzofluoranthene, benzopyrenes	3.36 x 10^17 spins/g	2.0042
Garden District (location 2)	22	Aluminum: 2.20 Silicon: 6.93 Sulfur: 0.94 Calcium: 9.50 Titanium: 0.12 Iron: 0.76 Zinc: 0.12	Not tested	No signal	No signal
Garden District (location 4)	24	Nitrogen: 7.90 Aluminum: 0.95 Silicon: 3.31 Sulfur: 3.57 Calcium: 5.29 Iron: 0.09 Zinc: 0.18	Not tested	4.16 x 10^16 spins/g	2.0033
Garden District (location 4)	25	Not tested	Not tested	4.11 x 10^17 spins/g	2.0037

Table 4.14 shows the most commonly filtered particulate size in this research, sub 20 micron. Elements of interest include sulfur and nitrogen which are common in fine PM. Metals present that can support EPFR formation include copper, iron, zinc, and aluminum and common

soil constituents calcium and silicon. Sub 20 micron samples in this group appear to have a variable organic radical concentration and g-factor. Of the sub 20 micron filtered group no samples were tested for both organic and inorganic composition.

Table 4.15: Sub 40 micron samples, locations and chemical composition.

Location	Sample	Elements of Interest (atomic %)	PAHs	EPFR Concentration	g-factor
Mid City (location 1)	7	Aluminum: 0.32 Silicon: 1.97 Calcium: 0.41 Titanium: 0.03 Iron: 0.05	phenanthrene, pyrene, naphthobenzothiophene, dibenzothiopene, benzopyrene	7.41 x 10^16 spins/g	2.0044
Garden District (location 5)	13	Not tested	pyrene, phenanthrene, dibenzothiophene, chrysene, benzofluoranthene	3.46 x 10^16 spins/g	2.0038
Garden District (location 4)	26	Not tested	fluoranthene, pyrene, benzofluoranthene, benzo (g,h,i) perylene, chrysene	4.44 x 10^17 spins/g	2.0038
Downtown (location 3)	28	Aluminum: 1.13 Sulfur: 1.28 Silicon: 2.72 Calcium: 1.43 Iron: 0.85 Zinc: 0.28	pyrene, phenanthrene, benzofluoranthene, benzopyrene, chrysene	2.31 x 10^17 spins/g	2.0035

Among samples in the sub 40, seen in Table 4.15, micron range downtown sample 28 has a higher transition metal composition than sample 7. Across all 40 micron samples, pyrenes and chrysenes are the most common PAHs. Samples in the sub 40 micron range appear to have a variable organic radical concentration and g-factor.

Most samples showed a similar elemental composition with elements such as carbon, oxygen, calcium, silicon, magnesium, aluminum, iron, and sulfur being the most common. The most significant difference among samples was a higher presence of the metals iron, zinc or copper present. For example, downtown locations 27 (sub 11 micron) and 28 (sub 40 micron) had higher levels of transition metals iron and zinc than similarly sized samples from more

suburban locations. However, no conclusions can be made regarding each individual filtered size: 11, 20, and 40 micron. PAH types, elements, and organic radical concentration and species are fairly consistent among and across particle size types.

5. DISCUSSION

5.1 Sampling methodology

It became evident through the course of testing of the citizen sampler that a one-step process utilizing using a small diameter membrane filter (47 mm) was not effective at collecting and filtering particulate from surfaces coated in deposited PM, the pre-filter became quickly occluded and prohibited effective filtration. This finding required the adaptation of a two-step method: collection of a bulk sample of deposited PM; and subsequent sub-sampling of the bulk sample in the laboratory. The sub-sampling was determined to be most effective using a custom designed filtration apparatus then re-suspending the collected particles for collection. Successful collection of a bulk sample rich in small PM that rises easily when agitated was also found to be important to the collection of a filtered sample substantial enough for laboratory testing.

This research found the most effective way to collect a bulk sample and filter it using membrane technology, thereby producing a sub 11 micron sample of an adequate amount for laboratory testing. Yet not all parameters to determine the success of filtration are quantifiable. Another factor in producing a testable amount of filtered particulate was the “richness” of the bulk sample. A “rich” sample contains a high quantity of small particulates that when shaken will rise and dissipate in the air in a manner similar to smoke. Specifically the bulk sample that produced filtered samples 27 and 28 was very rich.

It was determined from review of literature that smaller particles have higher diffusion coefficients and greater mobilities (Hinds 1999). This information is very applicable to the research at hand. When particles are re-suspended, the fine and ultrafine particles will be transported much more quickly out of the sample jar than larger particles. As the smaller particles have less inertia than larger particles it is also logical to assume they will be more

influenced by the suction near the filtration apparatus entrance point. It remains to be seen from this research whether fine and ultrafine particles can exist by themselves in re-suspension as they were originally formed, or if they are irrevocably agglomerated to other particles. It is important to minimize the surfaces that PM comes into contact with to minimize particle loss from adhesion to these surfaces because particles adhere to any surface they contact. As noted in the literature review, the smaller fraction of particles are especially difficult to remove from surfaces once they adhere, but vibration may free them (Hinds 1999).

The optimum pre-filters in this research were 8, 11, 20 and 40 micron pore size. Smaller pore sizes such as 2.7 micron glass microfiber filter were used, yet these fibrous filters and their pore size rating is for liquid filtration. The specifications for liquid filtration compared to air filtration are quite different. The technical specifications for the 2.7 micron glass microfiber filter specify that 99.9% of particles 0.3 micron and larger would be retained on the pre-filter (Millipore).

It is possible that flow rate through the filtration apparatus was inhibited and prevented more successful particle filtration and the production of a larger filtered sample. As mentioned in the results, the most effective setup for flow rate was filtration apparatus C which when paired with 20 and 11 micron pre-filters resulted in a flow rate of approximately 12 and 10 CFM, or approximately 23% and 19% of maximum flow rate respectively. A stronger vacuum may aid in producing higher flow rate for increased particle penetration through pre-filters.

5.2: Analytical findings

5.2.1: Particle Size and Elemental Composition

Scanning electron microscopy showed that samples of filtered particulates contained a wide range of particle sizes, including coarse, fine, and ultrafine particles. As described in the literature review, ultrafine particles make up the dominant fraction of particles in urban aerosols and a higher proportion of these particles are from combustion compared to other size fractions (Yinon et al. 2010). Around the world, the primary source for urban outdoor ultrafine PM is traffic from motor vehicles (Kumar et al. 2014), so many of the ultrafine particles found in attics potentially come from motor traffic or other combustion. Ultrafine particles may also result from indoor sources like cooking, which is another major source (Kearney et al. 2011). Further, a report from the Combustion Byproducts International Congress found that 70% of airborne fine particles were a result of combustion emissions (Dellinger et al. 2008). Therefore, many of the fine particles in homes are also a result of combustion, both indoor and outdoor sources. No homes sampled were inhabited by cigarette smokers, but we have no information on previous residents.

PM is extremely heterogeneous, therefore it is difficult to say how strong a correlation is from one small scan of a sample to the actual chemical makeup of the entire sample. However, the SEM-EDS scans clearly indicate the presence of carbon, which could be elemental or organic carbon. Ultrafine particles have a higher percentage of carbon than other particles (US EPA 2005). The presence of sulfur and nitrogen may indicate the presence of sulfates and nitrates, which are common particle constituents and associated with air pollution in the form of SO_x and NO_x. Also common in the SEM-EDS scans were crustal elements and metals which are most common in coarse particles that may represent wind-blown soil or sand (US EPA 2005).

SEM-EDS also indicated the presence of metals including iron, copper, zinc, and titanium in deposited PM from homes. The Beauchemin et al. (2014) study indicates that metals become more bio-accessible when stored in humid or oxygenated conditions. This is very applicable to Baton Rouge because of the humid climate where bio-accessable zinc would be potentially dangerous if inhaled in adequate quantities (Beauchemin et al. 2014).

In sample 23 there is a wide range of particle sizes. Calcium, silicon, oxygen and carbon appear in high proportions. It is possible that a mineral like CaCO3, calcium carbonate, may be present from crushed rock, stone or concrete and form coarse particles that show up in this sample. This mineral may originate from roadways.

Many of the samples have a high percentage of carbon. This may be in part from the carbon background tape that the particles are adhered to in the SEM instrument. However, some samples clearly demonstrate carbon based particles, so it is not possible to completely disregard all carbon from the sample composition. Perhaps future work could utilize a different backing when using SEM-EDS analysis.

Samples 27 and 28 from downtown Baton Rouge show higher levels of metals including iron and zinc compared to suburban derived samples of equal particle size. These higher concentrations may be due to the closer proximity to industrial facilities, heavier traffic from cars and busses, and less vegetation to capture pollutants. Motor oil has been found to contain traces of iron, copper and zinc in the parts per million range. Also, it has been shown that metals in diesel fuel lead to a high correlation of those metals incorporated into particulates produced from combustion (Herring et al. 2013). Additional house PM samples would need to be collected and more SEM-EDS scans of those samples taken to draw reliable conclusions regarding spatial correlations to chemical makeup of deposited PM.

It is difficult to draw conclusions regarding the elemental makeup of coarse particulate matter because of the highly variable nature of PM. Also, ambient PM 10 collected would be best compared to local soil samples to compare elemental enrichment. This was not accomplished in this research but in other research an enrichment factor can be calculated for PM to demonstrate the magnitude an element is elevated (Sattar et al. 2014).

Samples 27 and 28, collected from downtown Baton Rouge, show a similar concentration of iron compared to PM 10 samples at other locations (Sattar et al. 2014). The Sattar study sampled in Indonesia and found PM10 to contain a concentration of 1.3% iron compared to 0.92% and 0.85% compared to samples 27 and 28. However, the Sattar study only found a concentration of 0.12% of zinc while samples 27 and 28 displayed 0.21% and 0.28% zinc respectively. Further elements comparisons can be made from Table 5.1.

Table 5.1: Elemental composition of PM10 from two studies.

Element	Percent Composition Sattar et al. 2014	Percent Composition Chan et al. 1997
Aluminum	1.53	2.00
Calcium	1.93	2.50
Iron	1.30	1.80
Magnesium	0.73	0.55
NO_3	---	4.30
Silicon	1.84	5.40
Sodium	1.65	3.30
Sulfur	---	2.40
Titanium	0.11	0.18
Zinc	0.12	0.09

A study by Chan in Australia found that PM10 contained a higher percentage of iron (1.8%) than what was seen in samples 27 and 28. But a wide range in zinc concentrations was reported by Chan (.048%-.31%). Sulfur (2-3%) in Chan was comparable to what was found in this research. Chan sulfur levels were lower than what was found in other samples in this research, specifically sample 24. Samples 27 and 28 had 11% of their chemical makeup as nitrogen, while

the Chan samples demonstrated less (Chan et al. 1997). This high presence of nitrogen may be due to nitrates in air pollution. Samples 27 and 28 show higher amounts of nitrogen than other samples of the same particle size, making up about 11% of atoms in these samples. This could be hypothesized to be due to the presence of nitrates, which often result from motor traffic like cars and trucks, or from power generation (US EPA 2005). This nitrogen could also result from the engines of boats and barges on the Mississippi River. Stochiometrically, there is enough oxygen in the sample (38% atomically) to form nitrates, NO3.

Across all samples for SEM-EDS analysis elements found include: carbon, nitrogen, oxygen, sodium, magnesium, aluminum, silicon, sulfur, chlorine, potassium, calcium, iron, zinc, fluorine and copper. It was mentioned above that transition metals may play a key role in the formation of reactive oxygen species in biological systems (Vejerano et al. 2012). Therefore it is significant to positively identify transition metals like iron and zinc in the above described PM samples which also contain an organic radical. Also, titanium and copper were potentially identified, however, with a high error percentage on the quantification results. Metals and metal oxide presence is crucial in the formation of EPFRs in combustion processes. Free radicals are thought to chemisorb to metal oxides like iron and copper by reducing the metal (Vejerano et al. 2012). In research conducted by the LSU Superfund Research Center the formation of radical species was promoted by the addition of iron oxide nanoparticles. It was also found that iron oxide nanoparticles may contribute molecular growth of PAHs (Herring et al. 2013). Therefore, all three pollutants (metals, PAHs,and EPFRs) studied in this research may have a correlation as pollutants from combustion that are known to associate with particulate matter. Yet no correlation can definitively be identified here.

5.2.2: Environmentally Persistent Free Radicals

Tested particles in this research had an organic radical concentration typically from 10^15 to 10^17. Research by Gehling and Dellinger (2013) found radical concentrations in the order of magnitude range of 10^16 to 10^18 for ambient PM. The values from this research are also consistent with PM 2.5 radical concentration values from a study by Squadrito et al. (2001) who found PM 2.5 containing radical concentration in the range of 10^16 to 10^17. This research found that sampled radicals were stable for months after initial scans, a point that echoes the earlier work of Squadrito et al. (2001). Other research has indicated that tested soot had a high spin density of 10^18-10^20 spins per gram (Herring et al. 2013). While, this research did not find deposited PM in the house with as high of a radical concentration as soot, it is still apparent that house PM contains significant and persistent organic radicals that are generally more abundant in sub 11 and sub 20 micron samples compared to sub 40 micron and unfiltered samples. This is to be expected given that EPFRs studied are a surface complex, and smaller particles have a higher surface area to weight ratio. It is important to note that in addition to the greater surface area to weight ratio influencing the concentration of radicals, that a higher proportion of ultrafine and fine particles are the result of combustion compared to larger particles. Therefore fractions of smaller particles will contain comparatively more particles resulting from combustion, which bear a higher radical concentration.

A sample that contains free radicals in concentrations of 10^16 to 10^17 spins per gram is comparable to the level found in cigarette smoke (Dellinger et al. 2008). Another study by Gehling et al. (2014) used samples from an air monitoring station north of LSU campus near a major highway in Baton Rouge. Gehling et al. (2014) again found radical concentration in the range of 10^16 to 10^17 spins per gram.

One sample that did not show radical signal was sample 22. Similar samples taken from the exact same location showed radical signal on more than one occasion. However, sample 22 was not filtered and tested with EPR for over four months after it was collected. During those four months the sample was kept in a large jar not under vacuum and its radical signal may have decayed.

It was not clear from this research if there was any correlation between urban locations and higher radical concentration. However, it would be interesting in future research to study the differences in EPR spectra from downtown locations compared to those of more suburban setting with more vegetation and less traffic to determine if organic radical scans and long range scans would indicate any difference in peaks between urban, rural, and more suburban locations. An increased number of sampling locations would be required to test this.

Further research could dedicate more analysis to the g-factor of radicals found in homes to determine whether oxygen centered or carbon centered radicals are more prevalent.

5.2.3: Polycyclic Aromatic Hydrocarbons

Most of the samples tested contained PAHs that which have been identified as known animal carcinogens by the U.S. Department of Health and Human Services or as probable human carcinogens by the U.S. Environmental Protection Agency. The PAHs which are listed as known or probable carcinogens by the two agencies are: benzo (a) anthracene, chrysene, benzo (b) fluoranthene, benzo (a) pyrene, dibenz (a,h) anthracene, indeno (1,2,3-c,d) pyrene, and benzo (k) fluoranthene (Agency for Toxic Substances and Disease Registry 2014). Other PAHs could potentially have health effects, but have not been officially declared as such. The most serious chronic outcome of PAHs is cancer, while PAHs generally have a low acute toxicity (Agency for Toxic Substances and Disease Registry 2014). The SIM GC-MS tests and bar graphs given in the

results section demonstrate levels for 14 of the 16 PAHs originally listed on the EPA's priority pollutant list (Yan et al. 2004). This research found that levels of the above seven PAHs that are known or probable carcinogens varied widely and was often in the range of hundreds to thousands ppb.

As the literature review mentioned, PAHs are found in ambient PM but also in soil, primarily from atmospheric fallout. PAH concentration in soil near refineries has been shown to be as high as 200,000 ug/kg, while levels in soil samples near cities and areas with heavy traffic has been shown to be usually lower than 2000 ug/kg (Agency for Toxic Substances and Disease Registry 2013). This research showed that deposited particulate matter in homes can contain PAHs adsorbed to PM within this range of 2000-200,000 ug/kg (ppb) or even well above it in some instances

All samples indicate that PAHs found adsorbed to PM in attics or other home surfaces from deposited ambient air have higher concentrations of PAHs than average soil samples taken near cities or areas with heavy traffic. Samples 18 and 19 showed total PAH concentrations to be in the range of 369,000 and 372,000 ppb, approximately. The PAH concentrations for samples 18 and 19 are the highest tested in this research and higher than soils tested by ATSDR. This is consistent with studies that found that PAH concentrations from house dust were higher than found in outdoor soil (Chuang 1995). This research undertaken in Baton Rouge, plus evidence from the literature in Chuang, would indicate that it is common for PAHs to exist in relatively high concentrations in deposited PM and house dust.

Research noted in the literature review by Langer (2010) found that three PAHs: pyrene, benzo (a) anthracene, and benzo (a) pyrene were found in all homes sampled and found a median concentrations of 98, 15 and 11 ppb respectively in Danish homes (Langer 2010). These numbers

are significantly less than the levels of individual PAHs found in Baton Rouge homes in this study. Pyrene and its homologues were found in the above samples in the range of 1000-10,000 ppb, a level 10 to 100 times higher than the levels found in the Danish study. Levels in the Baton Rouge area also had higher levels than the Langer study for benzo (a) anthracene and benzo (a) pyrene, which frequently measured in the hundreds to thousands in level of ppb, compared to 15 and 11 ppb from the Langer study of Danish homes. Pyrene and its homologues, benzo (a) anthracene and, benzo (a) pyrene consistently tested in high quantities for this research of Baton Rouge PM samples, much higher than the Langer study (2010). Benzo (a) pyrene and benzo (a) anthracene are probable human carcinogens.

A study in North Carolina found house dust from vacuum cleaners in the 4-25 micron range to contain all 10 PAHs they tested for, and in concentrations of 40-650 ppb per PAH, at an average of 464 ppb (Lewis et al. 1999). The level in the Lewis study is generally lower, as in the Langer study, than what was measured in this research of deposited PM in the Baton Rouge area compared to the graphs from this research in the PAH results section. It would require additional testing to be certain, but it appears that house dust from the Baton Rouge area contains comparatively higher levels of PAHs in house dust, or deposited PM, than other tested areas. Also, further PAH testing with this research could potentially draw spatial relations throughout Baton Rouge to potential sources and PAH concentrations. This would also require more testing locations and a broader effort overall for future research.

This information would be significant because of the health effects associated with some PAHs. PAH data would also be significant because the LSU Superfund Resarch Center has determined that substituted aromatic hydrocarbons chemisorb to the surface of transition metal containing PM, which can create EPFRs (Patterson et al. 2012).

This research shows that deposited PM has detectable levels of organic compounds, notably PAHs, other aromatics and alkanes. This research also shows PM to contain metals and free radicals which associate with PM as part of complex particle-pollutant systems. More research would be required to analyze the specific role of organics, metals and their potential influence on EPFR formation.

5.2.4: Citizen Science

Future work associated with this research could have tie-ins with citizen science. The goal of this research for the future is not only to collect and identify hazardous pollutants in the household but also to encourage public understanding of science and the importance of research conducted at the Louisiana State University Superfund Research Center and other institutions. This is done through research translation and community engagement with the Superfund Research Center. This research may eventually use citizen scientists to collect samples of deposited PM and provide the sample to LSU researchers for laboratory filtration and analysis. This will encourage public understanding of science and will make individuals more informed about the scientific process in general. It will also make individuals more specifically aware of issues like local air pollution and pollutants in the home.

The research, or an offshoot of it, could seek to establish a training program where disseminated literature, data collected , journal publications, and dispersal of results would provide a community building experience and advance important and useful science. Scientists in the LSU Superfund Research Center have shown important health correlations to specific pollutant systems and this research could contribute to an understanding of these pollutants in a real world scenario.

6. CONCLUSIONS

6.1: Sampling

The collections and filtration method described in this research serves as a much simpler and less expensive alternative technique for collecting size specific PM and analysis than other methods of PM collection/filtration such as cyclones, electrostatic precipitators, and impactors

A filtering time of 40 minutes usually produced a sample amount sufficient for laboratory testing. Between 1 and 5 milligrams is required for EPR testing; GC-MS analysis 5-20 milligrams of sample was sufficient to detect PAHs, alkanes and other organic compounds, and less than 1 milligram is sufficient for SEM analysis.

The Dustream™ design, and the constructed apparatus C were found to offer the best filtered PM samples of the tested filtration apparatuses. Porous nylon net filters were the most successful for use in filtration apparatus C, most likely in part because they allowed a higher flow rate than other filter types. The success of using smaller pore sizes could be determined by their further testing, however this is not possible unless smaller pore sizes for nylon net become commercially available.

6.2: Analysis

Particulate matter from homes was found to demonstrate a persistent radical signal that decayed slowly over time. The spectra for radicals found in PM from homes in Baton Rouge are consistent with semiquinone radicals that can be carbon centered or oxygen centered. Samples tested demonstrated a wide variety of organic compounds, including PAHs and alkanes. Many of the PAHs found are probable human carcinogens. Overall, no pattern of differences among EPFRs, organic compounds, or metals was found among size fractions.

Avenues for future research include further sampling to test for a correlation between organic and metal composition of PM and radical concentration, intensity, and persistence. Future research may also test for spatial correlations between potential sources of particle pollution and particle abundance and chemical composition on surfaces in homes in Baton Rouge and other urban areas.

BIBLIOGRAPHY

Agency for Toxic Substances and Disease Registry, (2014, May 7). *Priority List of Hazardous Substances*. Retrieved October 7, 2015, from http://www.atsdr.cdc.gov/spl/

Agency for Toxic Substances and Disease Registry: Case Studies in Environmental Medicine. (2009, July 1). *Toxicity of Polycyclic Aromatic Hydrocarbons (PAHs)*. Retrieved October 7, 2015, from http://www.atsdr.cdc.gov/csem/pah/docs/pah.pdf

Balakrishna, S., Saravia, J., Thevenot, P., Ahlert, T., Lominiki, S., Dellinger, B., & Cormier Stephania, A. (2011). "Environmentally persistent free radicals induce airway hyperresponsiveness in neonatal rat lungs." Particle and Fibre Toxicology(1): 11.
Beauchemin, S., Rasmussen, P. E., MacKinnon, T., Chénier, M., & Boros, K. (2014). "Zinc in House Dust: Speciation, Bioaccessibility and Impact of Humidity." Environmental Science & Technology. 2014, 48, 9022−9029.

Bekö, G., Weschler, C. J., Wierzbicka, A., Karottki, D. G., Toftum, J., Loft, S., & Clausen, G. (2013). "Ultrafine Particles: Exposure and Source Apportionment in 56 Danish Homes." Environmental Science & Technology 47(18): 10240-10248.

Bhangar, S., Mullen, N. A., Hering, S. V., Kreisberg, N. M., & Nazaroff, W. W. (2011). "Ultrafine particle concentrations and exposures in seven residences in northern California." Indoor Air 21(2): 132-144.

Boasen, J., Chisholm, D., Lebet, L., Akira, S., & Horner, A. A. (2005). "House dust extracts elicit Toll-like receptor-dependent dendritic cell responses." Journal of Allergy and Clinical Immunology 116(1): 185-191.

Brauer, M., Amann, M., Burnett, R. T., Cohen, A., Dentener, F., Ezzati, M., Henderson, S. B., Krzyzanowski, M., Martin, R. V., Van Dingenen, R., van Donkelaar, A., & Thurston, G. D. (2012). "Exposure Assessment for Estimation of the Global Burden of Disease Attributable to Outdoor Air Pollution." Environmental Science & Technology 46(2): 652-660.

Brossard, D., Lewenstein, B., & Bonney, R. (2005). "Scientific Knowledge and Attitude Change: The Impact of a Citizen Science Project. Research Report." International Journal of Science Education 27(9): 1099-1121.

Burn, B. R., & Varner, K. J. (2015). Environmentally persistent free radicals compromise left ventricular function during ischemia/reperfusion injury. *American Journal Of Physiology. Heart And Circulatory Physiology, 308*(9), H998-H1006Centers for Disease Control and Prevention. (2013, July 23). *Factsheet: Polycyclic Aromatic Hydrocarbons (PAHs)*. Retrieved October 7, 2015, from http://www.cdc.gov/biomonitoring/PAHs_FactSheet.html

Chan, W., Simpson, W., McTainsh, G., & Vowles, P. (1997). “Characterisation of Chemical Species in PM 2.5 and PM 10 aerosols in Brisbane, Australia.” Atmospheric Environment 31 (22): 3773-3785.

Chalvatzaki, E., Aleksandropoulou, V., & Lazaridis, M. (2014). "A Case Study of Landfill Workers Exposure and Dose to Particulate Matter-Bound Metals." Water, Air & Soil Pollution 225(1): 1-19.

Cheng, S., Lang, J., Zhou, Y., Han, L., Wang, G., & Chen, D. (2013). "A new monitoring-simulation-source apportionment approach for investigating the vehicular emission contribution to the PM2.5 pollution in Beijing, China." Atmospheric Environment 79: 308-316.

Choi, H. S., Ashitate, Y., Lee, J. H., Kim, S. H., Matsui, A., Insin, N., Bawendi, M. G., Semmler-Behnke, M., Frangioni, J. V., & Tsuda, A. (2010). Rapid translocation of nanoparticles from the lung airspaces to the body. *Nat Biotech*, *28*(12), 1300-1303.

Chuang, J. C., Callahan, P. J., Menton, R. G., Gordon, S. M., Lewis, R. G., & Wilson, N. K. (1995). “Monitoring methods for polycyclic aromatic hydrocarbons and their distribution in house dust and track-in soil.” Environmental Science & Technology, 29: 494-500.

Cormier, S. A., Lomnicki, S., Backes, W., & Dellinger, B. (2006). Origin and Health Impacts of Emissions of Toxic By-Products and Fine Particles from Combustion and Thermal Treatment of Hazardous Wastes and Materials, National Institute of Environmental Health Sciences. National Institutes of Health. Department of Health, Education and Welfare: 810.

Costa, M. A. M., Carvalho Jr, J. A., Soares Neto, T. G., Anselmo, E., Lima, B. A., Kura, L. T. U., & Santos, J. C. (2012). "Real-time sampling of particulate matter smaller than 2.5 μm from Amazon forest biomass combustion." Atmospheric Environment 54(0): 480-489.

Cronin, D. P., & Messemer, J. E. (2013). "Elevating Adult Civic Science Literacy Through a Renewed Citizen Science Paradigm." Adult Learning 24(4): 143-150.

Davis, J. J., & Gulson, B. L. (2005). Ceiling (attic) dust: “A ‘museum’ of contamination and potential hazard.” Environmental Research, 99(2), 177-194.

Dellinger, B., D'Alessio, A., D'Anna, A., Ciajolo, A., Gullett, B., Henry, H., Keener, M., Lighty, J., Lomnicki, S., Lucas, D., Oberdörster, G., Pitea, D., Suk, W., Sarofim, A., Smith, K. R., Stoeger, T., Tolbert, P., Wyzga, R., & Zimmermann, R. (2008). "Combustion Byproducts and Their Health Effects: Summary of the 10th International Congress." Environmental Engineering Science 25(8): 1107-1114.

Dellinger, B., Lomnicki, S., Khachatyran, L., Maskos, Z., Hall, R., Adounkpe, J., McFerrin, C., & Truong, H. (2007). “Formation and Stabilization of Persistent Free Radicals.” Proceedings of the Combusion Institute 31 (1): 521-528.

Dellinger, B., Pryor, W. A., Cueto, R., Squadrito, G. L., Hegde, V., & Deutsch, W. A. (2001). "Role of Free Radicals in the Toxicity of Airborne Fine Particulate Matter." Chemical Research in Toxicology 14(10): 1371-1377.

Dorevitch, S., Karandikar, A., Washington, G. F., Walton, G. P., Anderson, R., & Nickels, L. (2008). "Efficacy of an Outdoor Air Pollution Education Program in a Community at Risk for Asthma Morbidity." Journal of Asthma. 45(9): 839-844.

Eaton, G., Eaton, S., Barr, D., & Weber, R. *Quantitative EPR*. Vienna: Springer-Verlag/Wien, 2010. Print.

Ebelt, S. T., Wilson, W. E., & Brauer, M. (2005) "Exposure to ambient and nonambient components of particulate matter - A comparison of health effects." Epidemiology. 16(3):396-405.

Elder, A., Gelein, R., Silva, V., Feikert, T., Opanashuk, L., Carter, J., Potter, R., Maynard, A., Ito, Y., Finkelstein, J., & Oberdörster, G. (2006). Translocation of Inhaled Ultrafine Manganese Oxide Particles to the Central Nervous System, 1172.

Fahmy, B., Ding, L., You, D., Lomnicki, S., Dellinger, B., & Cormier, S. A. (2010). "In vitro and in vivo assessment of pulmonary risk associated with exposure to combustion generated fine particles." Environmental Toxicology and Pharmacology 29(2): 173-182.
Gehling, W., & Dellinger, B. (2013). "Environmentally Persistent Free Radicals and Their Lifetimes in PM2.5". Environmental Science & Technology. 47(15): 8172-8178.

Freitag, A., & Pfeffer, M. (2013). "Process, not product: investigating recommendations for improving citizen science success". PLoS One, 15;8(5).

Gilgenast, E., Boczkaj, G., Przyjazny, A., & Kamiński, M. (2011). "Sample preparation procedure for the determination of polycyclic aromatic hydrocarbons in petroleum vacuum residue and bitumen." Analytical & Bioanalytical Chemistry 401(3): 1059-1069.

Guo, S., Hu, M., Zamora, M. L., Peng, J., Shang, D., Zheng, J., Du, Z., Wu, Z., Shao, M., Zeng, L., Molina, M. J., & Zhang, R. (2014). "Elucidating severe urban haze formation in China." Proceedings of the National Academy of Sciences 111(49): 17373-17378.

Hasheminassab, S., Daher, N., Shafer, M. M., Schauer, J. J., Delfino, R. J., & Sioutas, C. (2014). "Chemical characterization and source apportionment of indoor and outdoor fine particulate matter (PM2.5) in retirement communities of the Los Angeles Basin." Science of The Total Environment 490(0): 528-537.

Herring, M., Potter, P. M., Wu, H., Lomnicki, S., & Dellinger, B. (2012). "Fe2O3 nanoparticle mediated molecular growth and soot inception from the oxidative pyrolysis of 1-methylnaphthalene." Proceedings of the Combustion Institute. 34: 1749-1757.

Herring, P., Khachatryan, L., Lomnicki, S., & Dellinger, B. (2013). “Paramagnetic centers in particulate formed from the oxidative pyrolysis of 1-methylnaphthalene in the presence of Fe(III)2O3 nanoparticles.” Combustion and Flame. 160: 2996-3003.

Herring, M. P., Khachatryan, L., & Dellinger, B. (2015). “Speciation of Iron (III) Oxide Nanoparticles and Other Paramagnetic Intermediates during High-Temperature Oxidative Pyrolysis of 1-Methylnaphthalene. Intenational Journal of Chemical, Molecular, Nuclear, Materials and Metallurgical Engineering. 9,7: 818-826.

Herzog, N., & Egbers, C. (2013). "Numerical prediction of pressure drop and particle separation efficiency of some vane-type dust filters." Powder Technology 245(0): 265-272.

Hinds, W. (1999*). Aerosol Technology: Properties, Behavior, and Measurement of Airborne Particles, 2nd Edition.* New York: John Wiley & Sons, Inc.

Jamriska, M., & Morawska, L. (2003). "Quantitative Assessment of the Effect of Surface Deposition and Coagulation on the Dynamics of Submicrometer Particles Indoors." Aerosol Science & Technology 37(5): 425-436.

Japuntich, Daniel. (1995). “DOP Testing: History and Persepective.” 3M Job Health Highlights, Technical Information for Occupational Health and Safety Professionals, 13, 1: 1-5.

Jing, W., Shejun, C., Mi, T., Xiaobo, Z., Gonzales, L., Ohura, T., Bixian, M., & Massey Simomch, S. L. (2012). "Inhalation Cancer Risk Associated with Exposure to Complex Polycyclic Aromatic Hydrocarbon Mixtures in an Electronic Waste and Urban Area in South China." Environmental Science & Technology 46(17): 9745-9752.

Kearney, J., Wallace, L., MacNeill, M., Xu, X., VanRyswyk, K., You, H., Kulka, R., & Wheeler, A. J. (2011). "Residential indoor and outdoor ultrafine particles in Windsor, Ontario." Atmospheric Environment 45(40, Sp. Iss. SI): 7583-7593.

Kelley, M. A., Hebert, V. Y., Thibeaux, T. M., Orchard, M. A., Hasan, F., Cormier, S. A., Thevenot, P. T., Lomnicki, S. M., Varner, K. J., Dellinger, B., Latimer, B. M., & Dugas, T. R. (2013). "Model Combustion-Generated Particulate Matter Containing Persistent Free Radicals Redox Cycle to Produce Reactive Oxygen Species." Chemical Research in Toxicology 26(12): 1862-1871.

Kelly, F. J., & Fussell, J. C. Fussell (2012). "Size, source and chemical composition as determinants of toxicity attributable to ambient particulate matter." Atmospheric Environment 60: 504-526.

Kheirbek, I., Haney, J., Douglas, S., Ito, K., Caputo, S., & Matte, T. (2014). "The Public Health Benefits of Reducing Fine Particulate Matter through Conversion to Cleaner Heating Fuels in New York City." Environmental Science & Technology 48(23): 13573-13582.

Kim, J., Hong, H., Heo, A., & Park, W. (2013). “Indole toxicity involves the inhibition of adenosine triphosphate production and protein folding in Pseudomonas putida.” FEMS Microbiology Letters 343 (1): 89-99.

Kim, K.-H., Jahan, S. A., Kabir, E., & Brown, R. J. C. (2013). A review of airborne polycyclic aromatic hydrocarbons (PAHs) and their human health effects. Environment International, 60, 71-80.

Kim, S., Jaques, P. A., Chang, M., Froines, J. R., & Sioutas, C. (2001). "Versatile aerosol concentration enrichment system (VACES) for simultaneous in vivo and in vitro evaluation of toxic effects of ultrafine, fine and coarse ambient particles Part I: Development and laboratory characterization." Journal of Aerosol Science 32(11): 1281-1297.

King, L. E., & Weber, R. J. (2013). "Development and testing of an online method to measure ambient fine particulate reactive oxygen species (ROS) based on the 2',7'-dichlorofluorescin (DCFH) assay." Atmospheric Measurement Techniques 6(7): 1647-1658.

Kiruri, L. W., Dellinger, B., & Lomnicki, S. (2013). "Tar Balls from Deep Water Horizon Oil Spill: Environmentally Persistent Free Radicals (EPFR) Formation During Crude Weathering." Environmental Science & Technology 47(9): 4220-4226.

Klaassen, C., & Watkins, B. (2010). *Casarett & Doull’s Essentials of Toxicology*. New York: McGraw Hill Medical.

Kumar, P., Morawska, L., Birmili, W., Paasonen, P., Hu, M., Kulmala, M., Harrison, R. M., Norford, L., & Britter, R. (2014). “Ultrafine particles in cities.” Environment International 66: 1-10.

Langer, S., Weschler, C. J., Fischer, A., Bekö, G., Toftum, J., & Clausen, G. (2010). “Phthalate and PAH concentrations in dust collected from Danish homes and daycare centers.” Atmospheric Environment 44: 2294-2301.

Lee, S. W. (2010). "Fine particulate matter measurement and international standardization for air quality and emissions from stationary sources." Fuel 89(4): 874-882.

Lee, S. W., He, I., & Young, B. (2004). "Important aspects in source PM2.5 emissions measurement and characterization from stationary combustion systems." Fuel Processing Technology 85(6–7): 687-699.

Lee, S. W., Herage, T., He, I., & Young, B. (2008). "Particulate characteristics data for the management of PM2.5 emissions from stationary combustion sources." Powder Technology 180(1–2): 145-150.

Lee, S. W., Pomalis, R., & Kan, B. (2000). "A new methodology for source characterization of oil combustion particulate matter." Fuel Processing Technology 65–66(0): 189-202.

Lee, W.-C., Wolfson, J. M., Catalano, P. J., Rudnick, S. N., & Koutrakis, P. (2014). "Size-Resolved Deposition Rates for Ultrafine and Submicrometer Particles in a Residential Housing Unit." Environmental Science & Technology 48(17): 10282-10290.

Lepeule, J., Laden, F., Dockery, D., & Schwartz, J. (2012). "Chronic Exposure to Fine Particles and Mortality: An Extended Follow-up of the Harvard Six Cities Study from 1974 to 2009." Environmental Health Perspectives 120(7): 965-970.

Lewis, R. G., Fortune, C. R., Willis, R. D., Camann, D. E., & Antley, J. T. (1999). “Distribution of Pesticides and Polycyclic Aromatic Hydrocarbons in House Dust as a Function of Particle Size.” Environmental Health Perspectives 107 (9): 721-726.

Liao, S., Pan, B., Li, H., Zhang, D., & Xing, B. (2014). "Detecting Free Radicals in Biochars and Determining Their Ability to Inhibit the Germination and Growth of Corn, Wheat and Rice Seedlings." Environmental Science & Technology 48(15): 8581-8587.

Lieberman, A. and Scott, R. (1973). “Atmospheric particle penetration though high efficiency filters.” Powder Technology 8: 183-189.

Liu, C., Hsu, P., Lee, P., Ye, M., Zheng, M., Liu, N., & Cui, Y. (2015). “Transparent air filter for high-efficiency PM2.5 capture.” Nature Communications 6:6205.

Lomnicki, S., Hieu, T., Vejerano, E., & Dellinger, B. (2008). "Copper Oxide-Based Model of Persistent Free Radical Formation on Combustion-Derived Particulate Matter." Environmental Science & Technology 42(13): 4982-4988.

Lu, S., Yi, F., Hao, X., Yu, S., Ren, J., Wu, M., Jialiang, F., Yonemochi, S., & Wang, Q. (2014) "Physicochemical properties and ability to generate free radicals of ambient coarse, fine, and ultrafine particles in the atmosphere of Xuanwei, China, an area of high lung cancer incidence." Atmospheric Environment. 97: 519-528.

Mahne, S., Chuang, G. C., Pankey, E., Kiruri, L., Kadowitz, P. J., Dellinger, B., & Varner, K. J. (2012). "Environmentally persistent free radicals decrease cardiac function and increase pulmonary artery pressure." American Journal Of Physiology. Heart And Circulatory Physiology 303(9): 1135-1142.

Massachusetts Institute of Technology. (2003, November 20). *Introductory Training for the Bruker EMX EPR Spectrometer*. Retrieved October 7, 2015, from http://web.mit.edu/speclab/www/PDF/DCIF-EPR-training-n03.pdf

Meier, R., Eeftens, M., Aguilera, I., Phuleria, H. C., Ineichen, A., Davey, M., Ragettli, M. S., Fierz, M., Schindler, C., Probst-Hensch, N., Tsai, M.-Y., & Künzli, N. (2015). "Ambient Ultrafine Particle Levels at Residential and Reference Sites in Urban and Rural Switzerland." Environmental Science & Technology 49(5): 2709-2715.

Mouret, G., Thomas, D., Chazelet, S., Appert-Collin, J.-C., & Bemer, D. (2009). "Penetration of nanoparticles through fibrous filters perforated with defined pinholes." Journal of Aerosol Science 40(9): 762-775.

Mueller, A., Wichmann, G., Massolo, L., Rehwagen, M., Graebsch, C., Loffhagen, N., Herbarth, O., & Ronco, A. (2006). "Cytotoxicity and oxidative stress caused by chemicals adsorbed on particulate matter." Environmental Toxicology 21(5): 457-463.

Murillo-Tovar, M. A., Marriott, P. J., Villalobos-Pietrini, R., & Amador-Mułoz, O. (2010). "Selective Separation of Oxy-PAH from n-Alkanes and PAH in Complex Organic Mixtures Extracted from Airborne $PM_{2.5}$. Chromatographia 72(9-10): 913-921.

The National Institute for Occupational Safety and Health. (2014, December 24). *Polychlorinated Biphenyls (PCB's): Current Intelligence Bulletin 45*. Retrieved October 7, 2015, from http://www.cdc.gov/niosh/docs/86-111/

Nemzer, B., Pietrzkowski, Z., Chang, T., & Ou, B. (2013). "A Novel Approach for Measurement of Total Reactive Oxidant Species (ROS) In Vivo by A Fluorometric Method." American Journal of Biomedical Sciences 5(2): 154-160.

Okuda, T. (2013). "Measurement of the specific surface area and particle size distribution of atmospheric aerosol reference materials." Atmospheric Environment 75: 1-5.

Patterson, M. C., Keilbart, N. D., Kiruri, L. W., Thibodeaux, C. A., Lomnicki, S., Kurtz, R. L., Poliakoff, E. D., Dellinger, B., & Sprunger, P. T. (2013). "EPFR Formation from Phenol adsorption on $Al2O_3$ and TiO_2: EPR and EELS studies." Chemical Physics, 422, 277–282.

Patterson, S. L., Rusiecki, J. A., Barnes, S. L., Heller, J. M., Sutphin, J. B., & Kluchinsky, T. A., Jr. (2010). "Effectiveness, suitability, and performance testing of the SKC® Deployable Particulate Sampler (DPS) as compared to the currently eployed airmetrics MiniVol[TM] portable air sampler." Journal of Environmental Health 73(3): 16-22.

Pauling, Linus. (1970). *General Chemistry, third edition.* San Francisco: W.H. Freeman and Company.

Pavagadhi, S., Betha, R., Venkatesan, S., Balasubramanian, R., & Hande, M. P. (2013). "Physicochemical and toxicological characteristics of urban aerosols during a recent Indonesian biomass burning episode." Environmental Science and Pollution Research International 20(4): 2569-2578.

Pope, C. A., 3rd, Ezzati, M., & Dockery, D. W. (2013). "Fine particulate air pollution and life expectancies in the United States: the role of influential observations." Journal Of the Air & Waste Management Association (1995) 63(2): 129-132.

Qiao, L., Cai, J., Wang, H., Wang, W., Zhou, M., Lou, S., Chen, R., Dai, H., Chen, C., & Kan, H.. (2014). "PM2.5 Constituents and Hospital Emergency-Room Visits in Shanghai, China." Environmental Science & Technology 48(17): 10406-10414

Reist, P. C., & Taylor, L. (2000). "Development and operation of an improved turntable dust feeder." Powder Technology 107: 36-42.

Rim, D., Persily, A., Emmerich, S., Dols, W. S., & Wallace, L. (2013) Multi-zone modeling of size-resolved outdoor ultrafine particle entry into a test house. Atmospheric Environment 69: 219-230.

Saravia, J., Lee, G. I., Lomnicki, S., Dellinger, B., & Cormier, S. A. (2013). "Particulate Matter Containing Environmentally Persistent Free Radicals and Adverse Infant Respiratory Health Effects: A Review." Journal of Biochemical and Molecular Toxicology 27(1): 56-68.

Sattar, Y., Rashid, M., Ramli, M., & Sabariah, B. (2014). “Black carbon and elemental concentration of ambient particulate matter in Makassar, Indonesia.” IOP Conference Series: Earth and Environmental Sciences (18): 012099.

Simpson M.G., Wyatt I., Jones H.B., Gyte A.J., Widdowson P.S., Lock E.A. (1996). "Neuropathological changes in rat brain following oral administration of 2-chloropropionic acid". Neurotoxicology **17** (2): 471–80.

Souza, K. F., Carvalho, L. R. F., Allen, A. G., & Cardoso, A. A. (2014). "Diurnal and nocturnal measurements of PAH, nitro-PAH, and oxy-PAH compounds in atmospheric particulate matter of a sugar cane burning region." Atmospheric Environment 83: 193-201.

Squadrito, G., Cueto, R., Dellinger, B., Pryor, W.A. (2001). “Quinoid redox cycling as a mechanism for sustained free radical generation by inhaled airborne particulate matter.” Free Radical Biology & Medicine 1;31(9):1132-8.

Stephens, B., & Siegel, J. A. (2012). "Penetration of ambient submicron particles into single-family residences and associations with building characteristics." Indoor Air 22(6): 501-513.

Tantra, R., Tompkins, J., & Quincey, P. (2010). Characterisation of the de-agglomeration effects of bovine serum albumin on nanoparticles in aqueous suspension. Colloids and Surfaces B: Biointerfaces, 75(1), 275-281.

Thevenot, P. T., Saravia, J., Jin, N., Giaimo, J. D., Chustz, R. E., Mahne, S., Kelley, M. A., Hebert, V. Y., Dellinger, B., Dugas, T. R., DeMayo, F. J., & Cormier, S. A. (2013). "Radical-Containing Ultrafine Particulate Matter Initiates Epithelial-to-Mesenchymal Transitions in Airway Epithelial Cells." American Journal of Respiratory Cell and Molecular Biology 48(2): 188-197.

Thorp, Nick. (2011, June 22). *Benzenemethanol*. Retrieved October 7, 2015, from

http://www.toxipedia.org/display/toxipedia/Benzenemethanol

Umbuzeiro, G. A., Franco, A., Martins, M. H., Kummrow, F., Carvalho, L., Schmeiser, H. H., Leykauf, J., Stiborova, M., & Claxton, L. D. (2008). "Mutagenicity and DNA adduct formation of PAH, nitro-PAH, and oxy-PAH fractions of atmospheric particulate matter from São Paulo, Brazil." Mutation Research 652(1): 72-80.

United States Environmental Protection Agency. (2015, September 10). *Particulate Matter (PM)*. Retrieved October 7, 2015, from http://www3.epa.gov/pm/

United States Environmental Protection Agency. (February 2007). *Method 3500C: Organic Extraction and Sample Preparation*. Retrieved October 20, 2015, from http://www3.epa.gov/epawaste/hazard/testmethods/sw846/pdfs/3500c.pdf

United States Environmental Protection Agency (2015, September 15). *The Clean Air Act Amendments of 1990 List of Hazardous Air Pollutants*. Retrieved October 7, 2015, from http://www3.epa.gov/airtoxics/orig189.html

United States Environmental Protection Agency (2004, December). *The Particle Pollution Report: Current Understanding of Air Quality and Emissions through 2003*. Retrieved October 7, 2015, from www3.epa.gov/airtrends/aqtrnd04/pmreport03/report_2405.pdf#page=1

United States National Library of Medicine, TOXNET: Toxicology Data Network. (2000, May). *Oxalic acid*. Retrieved October 7, 2015, from http://toxnet.nlm.nih.gov/cgi-bin/sis/search2/f?./temp/~UtYItS:1

University of Buffalo. (n.d.). *SEM/EDS: Scanning Electron Microscopy with X-ray Microanalysis*. Retrieved October 7, 2015, from http://wings.buffalo.edu/faculty/research/scic/sem-eds.html

Urso, P., Cattaneo, A., Garramone, G., Peruzzo, C., Cavallo, D. M., & Carrer, P. (2015). "Identification of particulate matter determinants in residential homes." Building and Environment 86(0): 61-69.

Vallero, Daniel. (2014). *Fundamentals of Air Pollution*. New York: Elsevier, Academic Press.

Vejerano, E., Lomnicki, S. M., & Dellinger, B. (2012). "Formation and Stabilization of Combustion-Generated, Environmentally Persistent Radicals on Ni(II)O Supported on a Silica Surface." Environmental Science & Technology 46(17): 9406-9411.

Vu, V.-T., Lee, B.-K., Kim, J.-T., Lee, C.-H., & Kim, I.-H. (2011). "Assessment of carcinogenic risk due to inhalation of polycyclic aromatic hydrocarbons in PM10 from an industrial city: A Korean case-study." Journal of Hazardous Materials 189(1–2): 349-356.

Walgraeve, C., Demeestere, K., Wispelaere, P., Dewulf, J., Lintelmann, J., Fischer, K., & Langenhove, H. (2012). "Selective accurate-mass-based analysis of 11 oxy-PAHs on atmospheric particulate matter by pressurized liquid extraction followed by high-performance liquid chromatography and magnetic sector mass spectrometry." Analytical & Bioanalytical Chemistry 402(4): 1697-1711.

Wallace, L., Kindzierski, W., Kearney, J., MacNeill, M., Heroux, M.-E., & Wheeler, A. J. (2013). "Fine and Ultrafine Particle Decay Rates in Multiple Homes." Environmental Science & Technology 47(22): 12929-12937.

Wang, D. B., Pakbin, P., Saffari, A., Shafer, M. M., Schauer, J. J., & Sioutas, C. (2013). "Development and Evaluation of a High-Volume Aerosol-into-Liquid Collector for Fine and Ultrafine Particulate Matter." Aerosol Science and Technology 47(11): 1226-1238.

Wang, P., You, D., Saravia, J., Shen, H., & Cormier, S. A. (2013). Maternal exposure to combustion generated PM inhibits pulmonary Th1 maturation and concomitantly enhances postnatal asthma development in offspring. Particle and Fibre Toxicology, 10, 29-29.

Wertz, J.E. & Bolton, J.R. (1986). *Electron Spin Resonance: Elementary Theory and Practical Applications*. New York: Chapman and Hall.

Win Lee, S., Herage, T., Dureau, R., & Young, B. (2013). "Measurement of PM2.5 and ultra-fine particulate emissions from coal-fired utility boilers." Fuel 108(0): 60-66.

World Health Organization. (2014, March). Ambient (Outdoor) Air Quality and Health. Retrieved October 20, 2015 from: http://www.who.int/mediacentre/factsheets/fs313/en/

Yan, J., Wang, L., Fu, P. P., & Yu, H. (2004). “Photomutagenicity of 16 Polycyclic Aromatic Hydrocarbons From the US EPA Priority Pollutant List.” Mutation Research 557(10): 98-108.

Yinon, L., Themelis, N., & McNeil, F. (2010). Proceedings of the 18th Annual North American Waste-to-Energy Conference: “Ultrafine Particle from WTE and Other Combustions Sources”. Orlando, FL: N.J.Themelis.

APPENDICES

Appendix 1: Substances Tested for in GC-MS Selected Ion Monitoring Mode

PAHs tested for: Naphthalene, C1-Naphthalenes, C2-Naphthalenes, C3-Naphthalenes, C4-Naphthalenes, Fluorene, C1-Fluorenes, C2-Fluorenes, C1-Fluorenes, C2-Fluorenes, C3- Fluorenes, Dibenzothiophene, C1-Dibenzothiophenes, C1-Dibenzothiophenes, C2-Dibenzothiophenes, C3- Dibenzothiophenes, Phenanthrene, C1-Phenanthrenes, C2-Phenanthrenes, C3-Phenanthrenes, C4-Phenanthrenes, Anthracene, Fluoranthene, Pyrene, C1- Pyrenes, C2- Pyrenes, C3- Pyrenes, C4- Pyrenes, Naphthobenzothiophene, C-1 Naphthobenzothiophenes, C-2 Naphthobenzothiophenes, C-3 Naphthobenzothiophenes, Benzo (a) Anthracene, Chrysene, C1- Chrysenes, C2- Chrysenes, C3- Chrysenes, C4- Chrysenes, Benzo (b) Fluoranthene, Benzo (k) Fluoranthene, Benzo (e) Pyrene, Benzo (a) Pyrene, Perylene, Indeno (1,2,3 - cd) Pyrene, Dibenzo (a,h) anthracene, Benzo (g,h,i) perylene

Alkanes tested for: nC-10 Decane, nC-11 Undecane, nC-12 Dodecane, nC-13 Tridecane, nC-14 Tetradecane, nC-15 Pentadecane, nC-16 Hexadecane, nC-17 Heptadecane, Pristane, nC-18 Octadecane, Phytane, nC-19 Nonadecane, nC-20 Eicosane, nC-21 Heneicosane, nC-22 Docosane, nC-23 Tricosane, nC-24 Tetracosane, nC-25 Pentacosane, nC-26 Hexacosane, nC-27 Heptacosane, nC-28 Octacosane, nC-29 Nonacosane, nC-30 Triacontane, nC-31 Hentriacontane, nC-32 Dotriacontane, nC-33 Tritriacontane, nC-34 Tetratriacontane, nC-35 Pentatriacontane

Appendix 2: Substances Found in Scan Mode

Extraction 1:

Sample 21b (71.6 mg): Bicycloheptanone, exo-hydroxycineole, ethyl-nonanol, vanillin, biycyloundecanone, n-hexylamine, tetradecanoic acid, cyclopentadecane, n-acetyl propanamide, n-hexadecanoic acid, carbamic acid, nonadecanol, dodecenyl succinc ahydrid, propanol, methoxy acetic acid, biphenyl diamine, heptadecane, methylenedioxybenzophenone, dimethylhexenynol, estratetrone, eicosane, octadecanoic acid, indole, benzenebutanoic acid, octadecane, dichloromethoxy dibenzofuran, 9-octadecanamide, heptadecane, octadecane, hexadecane.

Sample #7 (41.7 mg): Benzene 1-methoxyethyl, dodecanoic acid, trimethylsilylborate, farnesene epoxide, heptadecane, acetyl methyl ideoxy glucofuranoside, hexanoic acid, ethanedioic acid, hexadecanol, alpha epoxymurulan, nitroundecene, n-hexadecanoic acid, ethanedioic acid ester, pentadecane, mercaptoacetic acid, oleic acid, ethanol, eicosane, methyl octatrienone, methoxyacetic acid, heptadecene, m-tolyl isothiocyanate, methoxyacetic acid, hexadecane, actadecane, choloropropionic acid, metanephrine, octadecenamide.

Sample #13 (22.3 mg): alpha methyl styrene, cyclotetra siloxane, acetophenone, ethyl methyl benzyl alcohol, benzoic acid, ethanedioic acid, hexadecane, adamantan trifluoropentane, nonadecane, hexenedioic acid, dodecanol, benzenedicarboxylic acid, cyclopentadecane,

spirodecene, acetyl, oxiranyl, hexadecanoic acid, dioxa disiladecene, hexanoic acid, methyl pentadecanol, chlorooctadecane, kaurene, mercaptoacetic acid, bisbolene epoxide, eicosane, heneicosane, octenem octadecenamide, acetoxymethyl cyclo hexanol, otctadecane.

Sample #2 (74.1 mg): hydroxyl methylenezene aldehyde, acetamido deoxy gluconic acid, butyl methylphosphonofluoridate, heptadienol, benzene dicarboxylic acid, cyclopentadecane, piperidinone, neoisolongifolene, pyrene, cyclohexadecane, isoaromadendrene epoxide, benzoisothiazole, chloro octadecane, eicosanol, phthalic acid, dodecanamide, heneicosane, sulfurous acid, benzenemethanol, spirio dioxabicyclo undecadiene oxirane.

Extraction 2:

Sample #18 (3.3 mg): Malonic acid, benzyl butyl phthalate

Sample #19 (8.0 mg): Ethanedioic acid, silane, benzyl butyl phthalate,

Sample #21 (7.0 mg): Spiroheptene trimethylsilyl, heptacosane, malonic acid, ethanedioic acid, butanoic acid, mercaptoacetic acid, benzyl butyl phthalate

Appendix 3: Concentrations of Alkanes and PAHs

Extraction 1:

Compound	Sample 13	Sample 2	Sample 21b	Sample 7
	ng/g	ng/g	ng/g	ng/g
nC-10 Decane	0.000	0.000	0.000	0.000
nC-11 Undecane	0.000	0.000	0.000	0.000
nC-12 Dodecane	0.000	0.000	0.000	0.000
nC-13 Tridecane	0.000	0.000	0.000	0.000
nC-14 Tetradecane	0.000	0.000	0.000	0.000
nC-15 Pentadecane	0.000	0.050	0.000	0.000
nC-16 Hexadecane	1.012	0.248	0.591	1.100
nC-17 Heptadecane	5.672	1.352	2.559	5.498
Pristane	1.984	0.472	1.044	2.308
nC-18 Octadecane	4.423	1.298	2.192	4.480
Phytane	1.798	0.491	1.000	2.203
nC-19 Nonadecane	2.253	0.435	0.956	2.442
nC-20 Eicosane	2.319	0.324	1.248	3.488
nC-21 Heneicosane	3.764	0.433	2.764	8.455
nC-22 Docosane	7.709	0.486	5.551	13.820
nC-23 Tricosane	12.972	0.760	10.554	13.269
nC-24 Tetracosane	24.357	3.321	17.675	11.028

nC-25 Pentacosane	38.057	2.075	22.551	18.428
nC-26 Hexacosane	34.513	0.669	20.261	15.649
nC-27 Heptacosane	28.544	1.940	19.179	20.510
nC-28 Octacosane	17.667	0.761	14.003	20.472
nC-29 Nonacosane	21.371	8.069	18.294	34.338
nC-30 Triacontane	8.479	0.340	6.318	16.893
nC-31 Hentriacontane	12.622	3.005	12.962	29.263
nC-32 Dotriacontane	5.856	0.262	5.381	16.538
nC-33 Tritriacontane	6.666	0.688	12.940	21.536
nC-34 Tetratriacontane	3.969	0.190	3.994	13.043
nC-35 Pentatriacontane	5.186	0.341	5.385	15.164
Total Alkanes	**251.192**	**28.011**	**187.403**	**289.925**
Naphthalene	32.881	7.631	33.932	51.526
C1-Naphthalenes	0.000	0.000	0.000	0.000
C2-Naphthalenes	0.000	0.000	0.000	0.000
C3-Naphthalenes	0.000	0.000	0.000	0.000
C4-Naphthalenes	0.000	0.000	0.000	0.000
Fluorene	0.000	12.395	0.000	29.019
C1-Fluorenes	0.000	0.000	0.000	0.000
C2-Fluorenes	0.000	0.000	0.000	0.000
C3- Fluorenes	0.000	0.000	0.000	0.000
Dibenzothiophene	40.875	55.861	22.322	52.252
C1-Dibenzothiophenes	138.864	37.662	97.922	153.611
C2-Dibenzothiophenes	262.329	0.000	262.287	349.743
C3- Dibenzothiophenes	317.483	0.000	364.045	425.201
Phenanthrene	489.877	1108.394	215.471	547.006
C1-Phenanthrenes	170.613	130.499	145.233	340.751
C2-Phenanthrenes	179.988	70.207	193.449	313.250
C3-Phenanthrenes	0.000	0.000	0.000	334.448
C4-Phenanthrenes	0.000	0.000	0.000	0.000
Anthracene	56.781	64.122	23.900	45.247
Fluoranthene	668.111	1429.310	337.399	649.486
Pyrene	486.715	800.573	245.202	525.336
C1- Pyrenes	244.154	120.287	146.029	199.089
C2- Pyrenes	334.358	192.709	264.958	295.906
C3- Pyrenes	0.000	0.000	240.239	287.725
C4- Pyrenes	0.000	0.000	337.029	230.793
Naphthobenzothiophene	101.206	63.062	102.756	125.650
C-1 Naphthobenzothiophenes	308.523	75.808	679.020	0.000
C-2 Naphthobenzothiophenes	0.000	0.000	1054.633	575.318
C-3 Naphthobenzothiophenes	0.000	0.000	1120.729	497.115
Benzo (a) Anthracene	296.138	85.543	138.790	289.783

Chrysene	463.741	312.350	276.875	411.812
C1- Chrysenes	311.992	96.108	283.047	349.435
C2- Chrysenes	0.000	0.000	31.567	0.000
C3- Chrysenes	0.000	0.000	54.493	0.000
C4- Chrysenes	0.000	0.000	0.000	0.000
Benzo (b) Fluoranthene	415.580	96.722	131.588	365.374
Benzo (k) Fluoranthene	244.633	71.923	69.004	204.600
Benzo (e) Pyrene	315.796	90.503	114.122	270.722
Benzo (a) Pyrene	193.393	42.034	46.454	184.874
Perylene	0.000	0.000	0.000	77.313
Indeno (1,2,3 - cd) Pyrene	281.910	45.533	47.123	273.854
Dibenzo (a,h) anthracene	0.000	0.000	0.000	0.000
Benzo (g,h,i) perylene	282.924	52.995	65.448	280.627
Total Aromatics	**6,639**	**5,062**	**7,145**	**8,737**

Extraction 2:

Compound	Sample 19	Sample 18	Sample 21
	ng/g	ng/g	ng/g
nC-10 Decane	0.000	0.000	0.000
nC-11 Undecane	0.000	0.000	0.000
nC-12 Dodecane	0.000	0.000	0.000
nC-13 Tridecane	0.000	0.000	0.000
nC-14 Tetradecane	0.000	0.000	0.000
nC-15 Pentadecane	0.000	0.000	0.000
nC-16 Hexadecane	8.548	25.267	17.139
nC-17 Heptadecane	31.787	119.417	68.184
Pristane	10.406	26.963	17.306
nC-18 Octadecane	25.403	88.836	51.096
Phytane	6.099	18.355	10.863
nC-19 Nonadecane	7.669	21.859	11.546
nC-20 Eicosane	4.604	11.465	6.321
nC-21 Heneicosane	4.516	9.609	5.819
nC-22 Docosane	5.428	11.042	5.726
nC-23 Tricosane	8.299	16.523	8.582
nC-24 Tetracosane	10.891	22.844	12.893
nC-25 Pentacosane	13.475	21.134	16.953
nC-26 Hexacosane	13.111	14.277	16.449
nC-27 Heptacosane	17.095	21.669	24.732
nC-28 Octacosane	11.797	14.479	19.463

nC-29 Nonacosane	18.268	22.497	27.436
nC-30 Triacontane	9.486	8.918	9.663
nC-31 Hentriacontane	12.892	13.452	16.390
nC-32 Dotriacontane	4.869	6.389	8.293
nC-33 Tritriacontane	7.185	9.121	9.387
nC-34 Tetratriacontane	3.464	4.194	6.222
nC-35 Pentatriacontane	5.900	8.708	9.567
Total Alkanes	**241.191**	**517.017**	**380.031**
Naphthalene	506.042	653.223	834.010
C1-Naphthalenes	193.101	373.514	214.898
C2-Naphthalenes	284.903	0.000	0.000
C3-Naphthalenes	0.000	0.000	0.000
C4-Naphthalenes	0.000	0.000	0.000
Fluorene	608.179	1220.127	483.961
C1-Fluorenes	201.521	0.000	0.000
C2-Fluorenes	0.000	0.000	0.000
C3- Fluorenes	0.000	0.000	0.000
Dibenzothiophene	996.858	849.408	364.866
C1-Dibenzothiophenes	1139.267	1561.627	972.003
C2-Dibenzothiophenes	862.190	0.000	880.057
C3- Dibenzothiophenes	592.852	0.000	550.218
Phenanthrene	12968.632	19142.444	6868.102
C1-Phenanthrenes	619.740	3672.110	1077.897
C2-Phenanthrenes	258.410	2314.965	737.214
C3-Phenanthrenes	62.937	1295.710	0.000
C4-Phenanthrenes	0.000	0.000	0.000
Anthracene	2114.423	2485.221	375.128
Fluoranthene	38688.636	39051.620	6024.210
Pyrene	35429.015	34364.896	5524.769
C1- Pyrenes	8902.192	8756.552	2086.950
C2- Pyrenes	8780.594	9009.112	1689.832
C3- Pyrenes	3189.739	2648.566	927.164
C4- Pyrenes	2625.807	0.000	0.000
Naphthobenzothiophene	4041.418	3686.136	699.576
C-1 Naphthobenzothiophenes	3659.338	3379.346	962.207
C-2 Naphthobenzothiophenes	1668.826	1417.745	0.000
C-3 Naphthobenzothiophenes	855.366	0.000	0.000
Benzo (a) Anthracene	21222.580	19251.264	2627.051
Chrysene	34023.750	31636.774	5555.179
C1- Chrysenes	12663.422	11027.709	2860.238
C2- Chrysenes	7596.488	6700.455	1859.598
C3- Chrysenes	2271.276	0.000	0.000

C4- Chrysenes	0.000	0.000	0.000
Benzo (b) Fluoranthene	29415.719	34163.330	4549.193
Benzo (k) Fluoranthene	23635.765	23286.385	3218.922
Benzo (e) Pyrene	26116.857	27960.927	3851.696
Benzo (a) Pyrene	24290.591	23754.216	2569.804
Perylene	6988.330	6587.446	840.489
Indeno (1,2,3 - cd) Pyrene	24909.995	21625.978	3020.087
Dibenzo (a,h) anthracene	5324.916	4770.298	382.458
Benzo (g,h,i) perylene	24784.859	22533.224	2637.648
Total Aromatics	**372,495**	**369,180**	**65,245**

Extraction 3:

Compound	Sample 26	Sample 27	Sample 28	Sample 29
	ng/g	ng/g	ng/g	ng/g
nC-10 Decane	0.000	0.000	0.000	0.000
nC-11 Undecane	0.000	0.000	0.000	0.000
nC-12 Dodecane	0.000	0.000	0.000	0.000
nC-13 Tridecane	0.000	0.000	0.000	0.000
nC-14 Tetradecane	0.000	0.000	0.000	0.000
nC-15 Pentadecane	0.000	0.000	0.000	0.000
nC-16 Hexadecane	0.552	0.535	0.635	0.000
nC-17 Heptadecane	3.520	4.013	2.840	3.594
Pristane	2.176	3.673	1.621	2.404
nC-18 Octadecane	3.129	4.754	4.265	2.426
Phytane	2.090	2.793	2.456	2.011
nC-19 Nonadecane	2.241	2.964	1.667	1.486
nC-20 Eicosane	1.579	3.459	2.102	1.164
nC-21 Heneicosane	2.326	6.453	2.755	1.575
nC-22 Docosane	3.068	10.741	3.888	3.939
nC-23 Tricosane	4.361	14.950	5.303	5.439
nC-24 Tetracosane	7.423	11.389	5.613	7.302
nC-25 Pentacosane	12.814	14.591	11.178	25.087
nC-26 Hexacosane	16.844	9.977	8.003	33.541
nC-27 Heptacosane	25.090	8.398	11.569	30.705
nC-28 Octacosane	18.012	7.086	6.804	20.193
nC-29 Nonacosane	27.209	11.325	14.729	18.353
nC-30 Triacontane	6.464	3.004	4.058	7.343
nC-31 Hentriacontane	6.262	5.481	7.512	6.052
nC-32 Dotriacontane	4.726	2.257	2.952	3.655

nC-33 Tritriacontane	5.554	3.837	4.851	4.066
nC-34 Tetratriacontane	4.255	2.012	2.309	2.545
nC-35 Pentatriacontane	5.073	2.573	3.388	4.861
Total Alkanes	**164.766**	**136.268**	**110.500**	**187.743**

Naphthalene	0.000	0.000	0.000	0.000
C1-Naphthalenes	0.000	0.000	0.000	0.000
C2-Naphthalenes	0.000	0.000	0.000	0.000
C3-Naphthalenes	0.000	0.000	0.000	0.000
C4-Naphthalenes	0.000	0.000	0.000	0.000
Fluorene	0.000	0.000	0.000	0.000
C1-Fluorenes	0.000	0.000	0.000	0.000
C2-Fluorenes	0.000	0.000	0.000	0.000
C3- Fluorenes	0.000	0.000	0.000	0.000
Dibenzothiophene	0.000	0.000	0.000	0.000
C1-Dibenzothiophenes	0.000	0.000	0.000	0.000
C2-Dibenzothiophenes	0.000	0.000	0.000	0.000
C3- Dibenzothiophenes	0.000	0.000	0.000	0.000
Phenanthrene	0.000	0.000	849.453	0.000
C1-Phenanthrenes	0.000	0.000	665.977	0.000
C2-Phenanthrenes	0.000	0.000	643.568	0.000
C3-Phenanthrenes	0.000	0.000	0.000	0.000
C4-Phenanthrenes	0.000	0.000	0.000	0.000
Anthracene	0.000	0.000	0.000	0.000
Fluoranthene	503.092	2980.940	3794.348	2487.049
Pyrene	442.369	2363.082	3124.197	2043.639
C1- Pyrenes	0.000	1062.017	1317.271	2137.253
C2- Pyrenes	0.000	0.000	1184.283	2492.668
C3- Pyrenes	0.000	0.000	0.000	4041.264
C4- Pyrenes	0.000	0.000	0.000	5667.607
Naphthobenzothiophene	0.000	0.000	0.000	0.000
C-1 Naphthobenzothiophenes	0.000	0.000	0.000	0.000
C-2 Naphthobenzothiophenes	0.000	0.000	0.000	0.000
C-3 Naphthobenzothiophenes	0.000	0.000	0.000	0.000
Benzo (a) Anthracene	109.303	812.623	1372.694	1025.996
Chrysene	315.660	1501.667	2358.143	3331.668
C1- Chrysenes	0.000	1156.396	1548.254	6773.264
C2- Chrysenes	0.000	930.209	979.670	8498.290
C3- Chrysenes	0.000	0.000	0.000	4585.976
C4- Chrysenes	0.000	0.000	0.000	0.000
Benzo (b) Fluoranthene	194.688	1278.228	1500.773	1462.486
Benzo (k) Fluoranthene	204.472	1220.604	1782.600	1414.599
Benzo (e) Pyrene	150.297	1485.428	1771.020	5173.263

Benzo (a) Pyrene	0.000	758.266	963.601	521.108
Perylene	0.000	200.175	148.189	376.674
Indeno (1,2,3 - cd) Pyrene	222.779	1475.630	1862.670	1643.820
Dibenzo (a,h) anthracene	0.000	283.555	380.922	811.814
Benzo (g,h,i) perylene	333.219	2004.044	2346.672	4822.567
Total Aromatics	**2,476**	**19,513**	**28,594**	**59,311**

APPENDIX 4: EPR Scan Data

Sample number	Date of Collection	Date of scan	pre filter	filter tested	Q value	g-value	ΔH (p-p)	Relative Intensity	Spins from sample	Amount of Sample	Spins/g
1	6/25/2014	6/26/2014	8 micron nitro cellulose	pre-filter		2.0041	6.18	23314	8.77E+14	0.005	1.75E+17
2	7/24/2014	7/28/2014	8 micron nitro cellulose	pre-filter		2.0038	6.11	9195	3.39E+14	0.01	3.39E+16
3	8/15/2014	NA	8 micron nitro cellulose	NA	NA	NA	NA	NA	NA	NA	NA
4	8/31/2014	NA	8 micron nitro cellulose	NA	NA	NA	NA	NA	NA	NA	NA
5	9/9/2014	9/10/2014	40 micron mesh	pre-filter		2.0037	5.11	25312	6.53E+14	0.021	3.11E+16
6	9/19/2014	10/1/2014	40 micron mesh	pre-filter		2.0037	5.33	3080	8.63E+13	0.017	5.08E+15
		10/1/2014	40 micron mesh	PUF		2.0039	6.33	1048	4.14E+13	0.0027	1.53E+16
		10/3/2014	40 micron mesh	PUF		2.0040	7	1827	8.83E+13	0.0027	3.27E+16
		10/13/2014	40 micron mesh	PUF		2.0041	7.778	997	5.95E+13	0.0027	2.20E+16
		10/20/2014	40 micron mesh	PUF		2.0045	6.222	1288	4.92E+13	0.0027	1.82E+16
		10/27/2014	40 micron mesh	PUF	2600	2.0042	7	1345	6.50E+13	0.0027	2.41E+16
		11/5/2014	40 micron mesh	PUF	2500	2.0041	6.556	1308	5.55E+13	0.0027	2.05E+16
7	10/5/2014	10/17/2014	40 micron mesh	PUF		2.0044	7.413	3652	1.98E+14	0.0081	2.45E+16
		10/20/2014	40 micron mesh	PUF		2.0044	7.312	3777	1.99E+14	0.0081	2.46E+16
		10/27/2014	40 micron mesh	PUF		2.0043	7.609	3782	2.16E+14	0.0081	2.67E+16
		11/5/2014	40 micron mesh	PUF		2.0042	7.393	3759	2.03E+14	0.0081	2.50E+16
		11/17/2014	40 micron mesh	PUF		NA	NA	NA	NA	NA	NA
		3/23/2015	40 micron mesh	PUF		2.0044	7.4	6954	3.76E+14	0.0081	4.64E+16
		3/23/2015	40 micron mesh	PUF		2.0045	7.321	11346	6.00E+14	0.0081	7.41E+16
		4/1/2015	40 micron mesh	PUF		2.0044	6.711	3095	1.38E+14	0.0081	1.70E+16
8	10/5/2014	11/7/2014	8 micron nitro cellulose	PUF		2.0037	6.667	69726	3.06E+15	0.017	1.80E+17
		11/17/2014	8 micron nitro cellulose	PUF		2.0035	7.111	58596	2.92E+15	1.70E-02	1.72E+17
		3/10/2015	8 micron nitro cellulose	PUF		2.0042	7.168	91594	4.64E+15	1.40E-02	3.32E+17
		3/10/2015	8 micron nitro cellulose	PUF		2.0042	7.11	14347	7.15733E+14	0.01	7.16E+16
		3/23/2015	8 micron nitro cellulose	PUF	2500	2.0044	7.337	11597	6.16075E+14	0.01	6.16E+16
		4/1/2015	8 micron nitro cellulose	PUF	3200	2.0041	6.681	4337	1.91039E+14	0.01	1.91E+16
		5/7/2015	8 micron nitro cellulose	PUF	2900	2.0039	6.55	11527	4.88033E+14	0.01	4.88E+16
		6/2/2015	8 micron nitro cellulose	PUF	3200	2.0039	6.18	9317	3.51159E+14	0.01	3.51E+16
		6/26/2015	8 micron nitro cellulose	PUF	2600	2.00387	6.672	12605	5.5374E+14	0.01	5.54E+16
		8/21/2015	8 micron nitro cellulose	PUF	3400	2.00396	6.682	33839	1.49101E+15	0.01	1.49E+17
9	11/18/2014	3/6/2015	2.7 micron glass fiber	PUF		2.0042	7.06	11579	5.69549E+14	0.008	7.12E+16
10	1/13/2015	NA	2.7 micron glass fiber	PUF		NA	NA	NA	NA	NA	NA
11	10/5/2014	2/6/2015	8 Micron Nitrocellulose	PUF		2.0043	6.993	3583	1.73E+14	0.0013	1.33E+17
		2/22/2015	8 Micron Nitrocellulose	PUF		2.0041	1.049	2690	2.92E+12	0.0013	2.25E+15
no signal		3/25/2015	8 Micron Nitrocellulose	PUF	3200	NA	NA	NA	NA	0.0013	NA
		4/1/2015	8 Micron Nitrocellulose	PUF	3400	2.0043	7.348	1365	7.27E+13	0.0013	5.59E+16
13	3/4/2015	3/10/2015	40 micron mesh	PUF	3000	2.0039	7.255	6200	3.22E+14	0.0235	1.37E+16
		3/23/2015	40 micron mesh	PUF	2900	2.0039	6.826	6826	3.14E+14	0.0235	1.34E+16
		3/25/2015	40 micron mesh	PUF	3000	2.0037	6.421	13254	5.39E+14	0.0235	2.29E+16
		5/7/2015	40 micron mesh	PUF	3000	2.00376	6.749	18113	8.14E+14	0.0235	3.46E+16
14	3/18/2015	3/25/2015	20 micron nylon net	PUF	3000	2.0039	6.206	1663	6.32E+13	0.006	1.05E+16

15	3/18/2015	3/25/2015	11 micron nylon net	PUF	2900	NA	NA	NA	NA	0.0014	NA
		4/1/2015	11 micron nylon net	PUF	3400	2.0041	6.993	1036	5.00E+13	0.0014	3.57E+16
16		3/25/2015	NA-raw dust	NA-raw dust	2900	2.00415	6.28	8875	3.45E+14	0.015	2.30E+16
17	9/19/2014	4/2/2015	20 micron- nylon net	PUF	3200	none	none	none	NA	0.0039	NA
		5/7/2015	20 micron- nylon net	PUF	3000	2.00395	5.507	5230	1.57E+14	0.0039	4.01E+16
		5/18/2015	20 micron- nylon net	PUF	2600	none	none	none	NA	0.0039	NA
17b	9/19/2014	4/2/2015	None-Raw dust	NA-raw dust	3200	2.0042	6.772	2283	1.03E+14	0.0263	3.93E+15
		5/7/2015	None-Raw dust	NA-raw dust	3000	2.0039	6.712	50028	2.22E+15	0.0263	8.46E+16
		5/18/2015	None-Raw dust	NA-raw dust	3200	2.00398	6.642	19195	8.36E+14	0.0263	3.18E+16
18	4/15/2015	4/24/2015	11 micron nylon net	PUF	2900	2.0333	5.702	35079	1.13E+15	0.0054	2.08E+17
		5/7/2015	11 micron nylon net	PUF	3000	2.00349	5.485	26902	7.99E+14	0.0054	1.48E+17
		5/19/2015	11 micron nylon net	PUF	3000	2.0035	5.162	15879	4.18E+14	0.0054	7.73E+16
		6/1/2015	11 micron nylon net	PUF	3600	2.00342	5.192	16439	4.37E+14	0.0054	8.10E+16
		6/26/2015	11 micron nylon net	PUF	3400	2.00344	5.19	24835	6.60E+14	0.0054	1.22E+17
		7/6/2015	11 micron nylon net	PUF	2900	2.00344	5.097	31984	8.20E+14	0.0054	1.52E+17
		7/24/2015	11 micron nylon net	PUF	3000	2.00338	5.178	24027	6.36E+14	0.0054	1.18E+17
		7/27/2015	11 micron nylon net	PUF	2900	2.00347	5.119	34680	8.97E+14	0.0054	1.66E+17
		8/7/2015	11 micron nylon net	PUF	3200	2.00349	5.273	32231	8.84E+14	0.0054	1.64E+17
		8/21/2015	11 micron nylon net	PUF	3400	2.00349	5.225	32233	8.68E+14	0.0054	1.61E+17
		9/1/2015	11 micron nylon net	PUF	2200	2.0035	5.218	25468	6.84E+14	0.0054	1.27E+17
19	4/15/2015	4/24/2015	20 micron nylon net	PUF	2900	2.0035	5.884	36815	1.26E+15	0.0054	2.33E+17
		5/7/2015	20 micron nylon net	PUF	3000	2.00349	5.359	27121	7.69E+14	0.0054	1.42E+17
		5/19/2015	20 micron nylon net	PUF	3000	2.0035	5.355	6863	1.94E+14	0.0054	3.60E+16
		6/1/2015	20 micron nylon net	PUF	3000	2.0035	5.385	6859	1.96E+14	0.0054	3.63E+16
		6/26/2015	20 micron nylon net	PUF	2900	2.00347	5.469	26279	7.76E+14	0.0054	1.44E+17
		7/6/2015	20 micron nylon net	PUF	3200	2.00348	5.378	34978	9.98E+14	0.0054	1.85E+17
		7/24/2015	20 micron nylon net	PUF	3000	2.0033	5.23	25213	6.81E+14	0.0054	1.26E+17
		7/27/2015	20 micron nylon net	PUF	3000	2.00356	5.244	36726	9.97E+14	0.0054	1.85E+17
		8/7/2015	20 micron nylon net	PUF	3400	2.035	5.233	35562	9.61E+14	0.0054	1.78E+17
		8/21/2015	20 micron nylon net	PUF	3200	2.00347	5.278	32573	8.95E+14	0.0054	1.66E+17
		9/1/2015	20 micron nylon net	PUF	2300	2.00355	5.355	27125	7.68E+14	0.0054	1.42E+17
20	4/15/2015	4/24/2015	NA-raw dust	NA-raw dust	2700	2.0032	5.036	12742	3.19E+14	0.0071	4.49E+16
		5/7/2015	NA-raw dust	NA-raw dust	3000	2.0033	5.758	18521	6.06E+14	0.0071	8.53E+16
		5/19/2015	NA-raw dust	NA-raw dust	3400	2.0032	5.468	6391	1.89E+14	0.0071	2.66E+16
		6/1/2015	NA-raw dust	NA-raw dust	3600	2.00342	5.29	5705	1.58E+14	0.0071	2.22E+16
		6/26/2015	NA-raw dust	NA-raw dust	2900	2.00334	5.975	18241	6.43E+14	0.0071	9.05E+16
		7/6/2015	NA-raw dust	NA-raw dust	2900	2.00322	5.883	18150	6.20E+14	0.0071	8.73E+16
		7/24/2015	NA-raw dust	NA-raw dust	3200	2.00301	5.541	20641	6.25E+14	0.0071	8.81E+16
21	5/11/2015	5/19/2015	20 micron nylon net	PUF	3400	2.00418	7.119	17689	8.85E+14	0.0068	1.30E+17
		6/1/2015	20 micron nylon net	PUF	3200	2.00411	7.089	20279	1.01E+15	0.0068	1.48E+17
		6/2/2015	20 micron nylon net	PUF	3400	2.00427	7.184	19436	9.90E+14	0.0068	1.46E+17
		6/26/2015	20 micron nylon net	PUF	3400	2.00418	7.163	31416	1.59E+15	0.0068	2.34E+17
		7/6/2015	20 micron nylon net	PUF	3400	2.00416	7.029	35687	1.74E+15	0.0068	2.56E+17
		7/24/2015	20 micron nylon net	PUF	3000	2.00425	7.238	28989	1.50E+15	0.0068	2.20E+17
		8/7/2015	20 micron nylon net	PUF	3200	2.00412	7.489	41317	2.29E+15	0.0068	3.36E+17

		8/21/2015	20 micron nylon net	PUF	3200	2..0428	7.29	43067	2.26E+15	0.0068	3.32E+17
		9/1/2015	20 micron nylon net	PUF	2100	2.0042	7.802	31980	1.92E+15	0.0068	2.83E+17
21b	5/11/2015	6/2/2015	NA	NA	3200	2.00422	9.612	2853	2.60E+14	0.017	1.53E+16
		7/24/2015	NA	NA	3000	2.0042	8.483	1592	1.13E+14	0.017	6.65E+15
22	1/13/2015	5/19/2015	20 micron nylon net	PUF	3200	NA	NA	NA	NA	0.006	NA
		6/1/2015	20 micron nylon net	PUF	3200	NA	NA	NA	NA	0.006	NA
23	5/22/2015	5/28/2015	NA	NA	2900	2.00314	7.71	5672	3.33E+14	0.0313	1.06E+16
		6/1/2015	NA	NA	3000	2.00325	7.703	56170	3.29E+15	0.0313	1.05E+17
		6/26/2015	NA	NA	2900	2.00306	8.083	72519	4.68E+15	0.0313	1.49E+17
		7/6/2015	NA	NA	2200	2.00304	8.137	65337	4.27E+15	0.0313	1.36E+17
		7/24/2015	NA	NA	2400	2.00343	7.558	168448	9.50E+15	0.0313	3.03E+17
		7/27/2015	NA	NA	2500	2.00317	7.248	191074	9.91E+15	0.0313	3.16E+17
		8/21/2015	NA	NA	2900	2.00329	7.615	59729	3.42E+15	0.0313	1.09E+17
		8/31/2015	NA	NA	2700	2.00349	7.222	12614	6.49E+14	0.0313	2.07E+16
		10/6/2015	NA	NA	2300	2.00356	6.675	56427	2.48E+15	0.0313	7.93E+16
24	6/30/2015	7/6/2015	20 micron nylon net	PUF	3400	2.0033	4.304	3411	6.24E+13	0.0015	4.16E+16
25	7/21/2015	7/27/2015	20 micron nylon net	PUF	2900	2.00371	6.185	43587	1.65E+15	0.004	4.11E+17
		8/7/2015	20 micron nylon net	PUF	3200	2.0037	6.137	33484	1.24E+15	0.004	3.11E+17
		8/13/2015	20 micron nylon net	PUF	3000	2.00373	6.312	29925	1.18E+15	0.004	2.94E+17
		8/21/2015	20 micron nylon net	PUF	3400	2.00365	6.335	31098	1.23E+15	0.004	3.08E+17
		8/31/2015	20 micron nylon net	PUF	2900	2.00354	5.682	31798	1.01E+15	0.004	2.53E+17
		10/6/2015	20 micron nylon net	PUF	2900	2.0036	5.572	26438	8.10E+14	0.004	2.03E+17
26	7/21/2015	7/27/2015	40 micron	PUF	3000	2.00384	6.532	71631	3.02E+15	0.0068	4.44E+17
		8/7/2015	40 micron	PUF	3200	2.00377	6.479	58058	2.41E+15	0.0068	3.54E+17
		8/13/2015	40 micron	PUF	3400	2.00377	6.413	56397	2.29E+15	0.0068	3.37E+17
		8/21/2015	40 micron	PUF	3200	2.00386	6.211	55743	2.12E+15	0.0068	3.12E+17
		8/31/2015	40 micron	PUF	3400	2.0037	6.16	54633	2.05E+15	0.0068	3.01E+17
		10/6/2015	40 micron	PUF	2900	2.00378	6.198	50990	1.93E+15	0.0068	2.84E+17
27	8/29/2015	9/15/2015	11 micron	PUF	3400	2.00387	6.949	6742	3.21E+14	0.0026	1.24E+17
		9/22/2015	11 micron	PUF	3200	2.0036	7.454	4303	2.36E+14	0.001	2.36E+17
		10/6/2015	11 micron	PUF	3200	2.0039	7.54	2374	1.33E+14	0.001	1.33E+17
28	8/29/2015	9/15/2015	40 micron	PUF	3600	2.00386	7.585	4621	2.62E+14	0.003	8.75E+16
		9/22/2015	40 micron	PUF	3600	2.00352	7.894	4510	2.77E+14	0.0012	2.31E+17
		10/6/2015	40 micron	PUF	3400	2.033	7.171	2527	1.28238E+14	0.0012	1.07E+17

APPENDIX 5: All Sample Data and Yields

Sample Number	Source Location	Location Number	Physical Location	Date Collected	Date Filtered	Date particles removed	Bulk Sample, type	Filtration time	Apparatus	Re-suspension method	Pre-filter	Sample Removal	sample attained?	Sample weight (mg)
1	Attic	1	Baton Rouge, LA	6/25/2014	6/25/2014	6/26/2014	No	20 mins	A	None	8 micron	Dry	yes-used prefilter	5
2	Outdoor Porch	2	Baton Rouge, LA	7/24/2014	7/24/2014	7/28/2014	No	6 mins	A	None	8 micron	Dry	yes-used prefilter	10
3	Attic	5	Baton Rouge, LA	8/15/2014	8/15/2014	NA	No	10 mins	A	None	8 micron	Dry	no	0
4	Attic	5	Baton Rouge, LA	8/31/2014	8/31/2014	NA	No	10 mins	A	Brush	8 micron	Dry	no	0
5	Outdoor Porch	2	Baton Rouge, LA	9/9/2014	9/9/2014	9/10/2014	Yes, Brush and jar	5 mins	B	Brush	40 micron	Wet	yes-used prefilter and filtered	21, 1.1
6	Window Unit Filter	5	Baton Rouge, LA	9/19/2014	9/19/2014	9/29/2014	Yes, Brush and jar	15 mins	B	Brush	40 micron	Wet	yes-used prefilter and filtered	17, 2.7
7	Vacuum Canister	1	Baton Rouge, LA	10/5/2014	10/13/2014	10/13/2014	Yes, Vacuum Canister	21 mins	B	Jar agitation	40 micron	Wet	yes	8.1
8	Vacuum Canister	1	Baton Rouge, LA	10/5/2014	11/2/2014	11/7/2014	Yes, Vacuum Canister	27 mins	A	Jar agitation	8 micron	Wet	yes	17
9	Vacuum Canister	1	Baton Rouge, LA	10/5/2014	11/18/2014	12/4/2014	Yes, Vacuum Canister	30 mins	A	Jar agitation	2.7 micron	Wet	yes	8
10	Attic	Not on map	Prarieville, LA	1/13/2015	1/14/2015	1/26/2015	Yes, Brush and jar	30 mins	A	Jar agitation	2.7 micon	Wet	no	NA
11	Vacuum Canister	1	Baton Rouge, LA	10/5/2014	2/2/2015	2/4/2015	Yes, Vacuum Canister	36 mins	C	Jar agitation	8 micron	Wet	yes	1.3
12	Vacuum Canister	1	Baton Rouge, LA	10/5/2014	2/9/2015	2/10/2015	Yes, Vacuum Canister	40 mins	C	Jar agitation	2.7 Micron	Wet	Yes-not measurable	0
13	Vacuum Canister	5	Baton Rouge, LA	2/3/2015	3/5/2015	3/5/2015	Yes, Vacuum Canister	24 mins	B	Jar agitation	40 Micron	Wet	Yes	23.5
14	Vacuum Canister	Not on map	Kenner, LA	3/15/2015	3/18/2015	3/19/2015	Yes, Vacuum Canister	30 mins	C	Jar agitation-with vortex	20 micron	Wet	Yes	6
15	Vacuum Canister	Not on map	Kenner, LA	3/15/2015	3/18/2015	3/19/2015	Yes, Vacuum Canister	30 mins	C	Jar agitation-with vortex	11 micron	Wet	Yes	1.4
16	Home surfaces	Not on map	Douglas, TX	NA	NA	NA	Yes, Brush and jar	NA	NA	NA	NA	NA	Yes	15
17	Vacuum Canister	1	Baton Rouge, LA	10/5/2014	3/30/2015	3/31/2015	Yes, Vacuum Canister	35	C	Jar agitation-with vortex	20 micron	Wet	yes	3.9
17b	Vacuum Canister	1	Baton Rouge, LA	10/5/2014	NA	NA	Yes, Vacuum Canister	NA	NA	NA	NA	NA	yes	26.3
18	Attic	1	Baton Rouge, LA	4/15/2015	4/20/2015	4/21/2015	Yes, Stinger vacuum	40	C	Jar agitation-with vortex	11 micron	Wet	yes	9
19	Attic	1	Baton Rouge, LA	4/15/2015	4/20/2015	4/21/2015	Yes, Stinger vacuum	40	C	Jar agitation-with vortex	20 micron	Wet	yes	16.5
20	Attic	1	Baton Rouge, LA	4/15/2015	NA	NA	Yes, Stinger vacuum	NA	C	NA	NA	NA	yes	7.1
21	Attic	4	Baton Rouge, LA	5/11/2015	5/13/2015	5/13/2015	Yes, stinger modified collection filter bag	40	C	Jar agitation-with vortex	20 micron	Wet	yes	13.8
21b	Attic	4	Baton Rouge, LA	5/11/2015	NA	NA	Yes, stinger modified collection filter bag	NA	NA	NA	NA	NA	yes	17
22	Outdoor Porch	2	Baton Rouge, LA	1/13/2015	5/14/2015	5/14/2015	Yes, Brush and jar	40	C	Jar agitation-with vortex	20 micron	Wet	yes	6
23	HVAC Filter	4	Baton Rouge, LA	5/22/2015	NA	NA	NA	NA	NA	NA	NA	NA	yes	31.3
24	Attic	4	Baton Rouge, LA	6/30/2015	7/3/2015	7/3/2015	Yes, Hand-held vacuum	40	C	Jar agitation-with vortex	20 micron	Wet	yes	1.3
25	Attic	4	Baton Rouge, LA	7/21/2015	7/21/2015	7/21/2015	Yes, Hand-held vacuum	40	C	Jar agitation-with vortex	20 micron	Wet	yes	13.2 mg
26	Attic	4	Baton Rouge, LA	7/21/2015	7/21/2015	7/21/2015	Yes, Hand-held vacuum	40	B	Jar agitation-with vortex	40 micron	Wet	yes	143.1
27	Attic	3	Baton Rouge, LA	8/29/2015	8/31/2015	9/1/2015	Yes, Hand-held vacuum	40	C	Jar agitation-with vortex	11 micron	Wet	yes	29
28	Attic	3	Baton Rouge, LA	8/29/2015	8/31/2015	9/1/2015	Yes, Hand-held vacuum	25	B	Jar agitation-with vortex	40 micron	Wet	yes	179.6
29	Attic	3	Baton Rouge, LA	8/29/2015	NA	NA	Yes, Hand-held vacuum	NA	NA	NA	NA	NA	yes	142.6

VITA

John Scott Tweedy Young was born in 1985 in Indianapolis, Indiana to Richard and Kim Young. John attended and graduated from North Central High School in 2004. After high school, John attended the College of Charleston in South Carolina. John graduated in 2008 with a Bachelor of Arts in English and a Bachelor of Arts in Biology. He worked for a small newspaper and as a freelance journalist before working as a grant administrator in Austin, Texas, for 3 years. In 2013 John was accepted to LSU and began a Masters of Science Degree in Plant, Environmental and Soil Sciences at Louisiana State University.